

# Diamond-like carbon binding peptides – evolutionary selection, characterization, and engineering

Bartosz Gabryelczyk



# **Diamond-like carbon binding peptides – evolutionary selection, characterization, and engineering**

---

Bartosz Gabryelczyk

*Academic disseration to be presented for public examination with premission of the Faculty of Biological and Environmental Sciences of the University of Helsinki in the B-building, lecture hall 5, Latokartanonkaari 7, Helsinki, on the 6th of March, 2015, at 12 o'clock.*



ISBN 978-951-38-8216-7 (Soft back ed.)

ISBN 978-951-38-8217-4 (URL: <http://www.vtt.fi/publications/index.jsp>)

VTT Science 77

ISSN-L 2242-119X

ISSN 2242-119X (Print)

ISSN 2242-1203 (Online)

Copyright © VTT 2015

JULKAISIJA – UTGIVARE – PUBLISHER

Teknologian tutkimuskeskus VTT Oy

PL 1000 (Tekniikantie 4 A, Espoo)

02044 VTT

Puh. 020 722 111, faksi 020 722 7001

Teknologiska forskningscentralen VTT Ab

PB 1000 (Teknikvägen 4 A, Esbo)

FI-02044 VTT

Tfn +358 20 722 111, telefax +358 20 722 7001

VTT Technical Research Centre of Finland Ltd

P.O. Box 1000 (Tekniikantie 4 A, Espoo)

FI-02044 VTT, Finland

Tel. +358 20 722 111, fax +358 20 722 7001

## Preface

This study was carried out at VTT Technical Research Centre of Finland during the years 2010–2014. I warmly thank current and former technology managers Dr. Kirsi-Marja Oksman-Caldentey, Dr. Raija Lantto, and Dr. Niklas von Weymarn for providing excellent working facilities. VTT Graduate School and Academy of Finland are acknowledged for funding of the research work. In addition, HYBER Centre of Excellence at Aalto University is thanked for the financial support during last year of my studies.

I am especially grateful to my supervisor Prof. Markus Linder. I was very lucky to have such a cool boss with great passion in science. I have to admit that this thesis project was very challenging for me. I have encountered many failures and had moments of frustration, however, Prof. Markus always found a way to motivate me, guide, and set on the right track. I greatly appreciate our regular meetings, the time, and guidance he has given to me. Thanks to Prof. Markus, I learnt how to deal with many scientific problems. I realised that a scientist always has to be very suspicious, take nothing for granted, and not celebrate when results of experiments “look good”... All these would never happen without his always easy-going and friendly approach which made me to feel that he was not my supervisor but rather a mentor and friend.

I am also grateful for the scientific guidance given by my thesis committee Prof. Kari Keinänen and Prof. Maija Tenkanen. I additionally thank to Prof. Kari for supervising my studies and guiding me through bureaucracy at University of Helsinki. I appreciate the smooth cooperation that we always had. I thank the pre-examiners of this thesis Dr. Peter Mattjus and Prof. Henrik Stålbrand for valuable feedback and comments. Moreover, I acknowledge The National Doctoral Programme in Informational and Structural Biology (ISB) for providing me the opportunity to participate in many interesting courses and meetings, and express recognition to VTT Graduate School coordinator Dr. Kristiina Poppius-Levlin for her contribution in the school as well as for organizing scientific events and seminars.

I would like to thank all the co-authors and co-operators that help me to conduct these multidisciplinary studies. This thesis would have not been accomplished if you had not shared with me your knowledge and expertise. I especially show my appreciation to Dr. Geza Szilvay for valuable comments, suggestions, and advices in the lab, as well as for help in preparation of the manuscripts. Members of Protein Dis-

covery and Engineering and former Nanobiomaterials teams are acknowledged for support and friendly atmosphere, technicians, in particular, Riitta Suihkonen, Päivi Matikainen and Arja Kiema for patience, help, and technical assistance in carrying out experiments, Anne Ala-Pöntiö for introducing me into the VTT labs at the beginning of my employment.

Colleagues at VTT and Aalto University, thanks for your kindness, all the discussions (not always scientific) during coffee breaks, and for time spent together at work and outside. It was very nice to be surrounded by so many interesting and intelligent people. Friends in Finland and Poland, thanks for your support in difficult moments.

Finally, I would like to thank my family and my lovely wife Natalia. Thank you parents that you always warmly welcomed me at home, thanks for delicious food that you every time provided, and sorry that I have been complaining so much how hard is to complete this PhD 😊. Natalia, there are no words that would express how to thank for your love, patience and support. I always felt that you have been close to me even though for most of my stay here there was a distance of more than 1000 km between us. Thank you for everything and sharing your life with me.

Espoo, January 2015

Bartek

## Academic dissertation

Supervisor Professor Markus Linder  
Department of Biotechnology and Chemical Technology  
Aalto University, Espoo, Finland

VTT Technical Research Centre of Finland  
Espoo, Finland

Pre-examiners Doctor Peter Mattjus  
Department of Biosciences,  
Åbo Akademi University, Turku, Finland

Professor Henrik Stålbrand  
Department of Biochemistry and Structural Biology  
Lund University, Sweden

Opponent Associate Professor Marc R. Knecht  
Department of Chemistry  
University of Miami, USA

Custos Professor Kari Keinänen  
Department of Biosciences  
Division of Biochemistry and Biotechnology  
University of Helsinki, Finland

## List of publications

This thesis is based on the following original publications which are referred to in the text as I–III. The publications are reproduced with kind permission from the publishers.

- I Bartosz Gabryelczyk, Géza R. Szilvay, Mikko Salomäki, Päivi Laaksonen, Markus B. Linder, 2013. Selection and Characterization of Peptides Binding to Diamond-like Carbon. *Colloids and Surfaces B, Biointerfaces* 110C: 66–73. doi:10.1016/j.colsurfb.2013.04.002.
- II Bartosz Gabryelczyk, Géza R. Szilvay, Markus B. Linder, 2014. The Structural Basis for Function in Diamond-like Carbon Binding Peptides. *Langmuir* 30 (29): 8798–8802. doi:10.1021/la502396p.
- III Bartosz Gabryelczyk, Géza R. Szilvay, Vivek K. Singh, Joonas Mikkilä, Mauri A. Kostianen, Jari Koskinen, Markus B. Linder, 2014. Engineering of the Function of Diamond-like Carbon Binding Peptides through Structural Design. *Biomacromolecules*, In PRESS. doi:10.1021/bm501522j.

## **Author's contributions**

### **Publication I**

The author planned the work together with Prof. Markus Linder and carried out the laboratory work. Ellipsometry measurements were performed at Turku University under supervision of Dr. Mikko Salomäki and Prof. Päivi Laaksonen. The author interpreted the data and had main responsibility in writing of the publication with Dr. Géza Szilvay, under the supervision of Prof. Markus Linder.

### **Publication II**

The author planned the work together with co-authors and carried out all the experimental work. The author interpreted the results and wrote the publication with Dr. Géza Szilvay, under the supervision of Prof. Markus Linder.

### **Publication III**

The author planned the work together with Prof. Mauri Kostianen, Prof. Jari Koskinen, Dr. Géza Szilvay, and Prof. Markus Linder. The co-authors: Dr. Vivek Singh and Joonas Mikkilä contributed in synthesis and analysis of part of the materials used in the experimental work (DLC flakes – Vivek Singh, PEG(6)-bis-maleimide – Joonas Mikkilä). The author carried out the laboratory work, interpreted the data, and wrote the publication with Dr. Géza Szilvay, under the supervision of Prof. Markus Linder.



# Contents

<b>Preface</b> .....	<b>3</b>
<b>Academic dissertation</b> .....	<b>5</b>
<b>List of publications</b> .....	<b>6</b>
<b>Author's contributions</b> .....	<b>7</b>
<b>List of abbreviations</b> .....	<b>10</b>
<b>1. Introduction</b> .....	<b>12</b>
1.1 Protein-solid interactions found in Nature as an inspiration for material designers .....	12
1.2 Approaches to investigate solid-binding proteins.....	15
1.3 Advantages of directed evolution approaches for selecting material-specific peptides .....	16
1.4 Applications of material-specific peptides.....	16
1.5 Selection of solid-binding peptides from combinatorial peptide display libraries .....	18
1.5.1 Selecting “true” binders from a library.....	19
1.5.2 Problem of target unrelated peptides.....	20
1.6 Analysis of features of peptides selected in a biopanning experiment .....	23
1.7 Analysis of peptide-target binding.....	24
1.7.1 Binding analysis using phages .....	25
1.7.2 Binding analysis using fusion proteins .....	25
1.8 Investigation of structural biases of peptide function.....	27
1.9 Post-selection engineering of material binding peptides .....	30
1.10 Experimental methods to study peptide binding to solid materials.....	31
<b>2. Aims of the study</b> .....	<b>34</b>
<b>3. Materials and methods</b> .....	<b>35</b>
3.1 DLC general information .....	35
3.1.1 Information about DLC coating used in this work (publication I–III) .....	36
3.2 Phage display.....	37
3.2.1 Biopanning against DLC surface (publication I).....	37
3.3 Phage particle binding studies (publication I) .....	38

3.3.1	Phage titer analysis (plaque assay).....	38
3.3.2	Phage ELISA.....	38
3.4	Fusion proteins of DLC binding peptides and alkaline phosphatase (publications I–III) .....	38
3.4.1	General information .....	38
3.4.2	Construction, expression and purification of the fusion proteins.....	38
3.4.3	Quantification of surface binding of peptide-AP fusion proteins (AP enzymatic assay) (publication I) .....	40
3.4.4	Simultaneous competition assay (publication II and III) .....	40
3.4.5	Sequential displacement competition assay (publication III) .....	40
3.5	Synthetic peptides .....	41
3.6	Synthesis of multivalent peptides (publication III) .....	41
3.7	Preparation of colloidal form of DLC (DLC flakes) (publication III).....	41
3.8	Zeta ( $\zeta$ ) potential measurements (publication III) .....	42
<b>4.</b>	<b>Results and discussion.....</b>	<b>43</b>
4.1	Selection of peptides from the PhD-12 phage library (publication I).....	43
4.2	Features and analysis of sequences of selected peptides (publication I) ..	46
4.3	Phage binding analysis by titer and ELISA (publication I) .....	49
4.4	Peptide binding analysis with AP fusion proteins (publication I) .....	50
4.5	Analysis of basic binding properties of DLCBP11(L)-AP (publication I).....	51
4.6	Analysis of DLCBP11(L) peptide variants (unpublished results).....	52
4.7	Analysis of basis of function of pep_L peptide by simulations competition assay (publication II) .....	54
4.7.1	Influence of chemical composition changes in the pep_L sequence	55
4.7.2	Influence of structural changes in the pep_L sequence .....	58
4.8	Engineering of the pep_L peptide to multivalent forms (publication III) .....	60
4.8.1	Construction of multivalent peptides (publication III).....	61
4.8.2	Influence of MPs structural design for affinity (publication III).....	63
4.8.3	Influence of MPs structural design for sequential competition and kinetics (publication III) .....	64
4.9	Utilization of DLC binding peptides in stabilization of colloidal DLC (publication III).....	66
<b>5.</b>	<b>Conclusions .....</b>	<b>68</b>
	<b>References.....</b>	<b>71</b>

## Appendices

Publications I–III

## List of abbreviations

AFM	atomic force microscopy
AP	alkaline phosphatase
ATR-FTIR	attenuated total reflection Fourier transform infrared spectroscopy
BSA	bovine serum albumin
CD	circular dichroism
CNTB	carbon nanotube binding peptide
CVD	chemical vapor deposition
DLC	diamond-like carbon
ELISA	enzyme-linked immunosorbent assay
GFP	green fluorescence protein
GRAVY	grand average of hydropathicity
hypPPV	hyperbranched poly(phenylene vinylene)
HRP	horse radish peroxidase
IMAC	immobilized-metal affinity chromatography
IPTG	isopropyl $\beta$ -D-1-thiogalactopyranoside
LDH	L-lactate dehydrogenase
MBP	maltose binding protein
MP	multivalent peptides
NMR	nuclear magnetic resonance
PACVD	plasma-assisted chemical vapor deposition
PEG	polyethylene glycol
PMMA	poly(methyl methacrylate)

PVD	physical vapor deposition
QCM	quartz crystal microbalance
SAM	self-assembled monolayer
SPR	surface plasmon resonance
SWNT	single-walled carbon nanotubes
TOF-SIMS	time-of-flight secondary ion mass spectroscopy
TUP	target unrelated peptide
UPLC	ultra-performance liquid chromatography
XPS	X-ray photoelectron spectroscopy

# 1. Introduction

## 1.1 Protein-solid interactions found in Nature as an inspiration for material designers

Over millions years of evolution, Nature has developed and diversified a number of proteins that display a wide variety of biological functions involved in almost every process in a living organisms. Proteins are versatile biomolecules that act, for example, as catalysts of biochemical reactions (enzymes), and serve as structural or transporter molecules. The common feature of all these proteins is that they have been formed through evolutionary pathways and operate at molecular level based on specific recognition. The mechanism of molecular recognition rely on structural fitting between protein and target molecule by the combination of numerous weak noncovalent interactions (electrostatic, hydrogen bonds, van der Waals, and hydrophobic). Proteins are able to specifically interact with different bio- and inorganic molecules, and these molecular interactions play an important role in sustaining of biological systems. For example, in antigen-antibody and receptor-ligand interactions, self-assembly of viruses, binding to inorganic materials and many others processes (Kessel & Ben-Tal 2010).

Proteins that interact with surfaces of inorganic materials (solid-binding proteins) are a particularly interesting group because many of their properties can potentially be utilized in materials science and nanotechnological applications (Sarıkaya et al. 2003, Briggs & Knecht 2012). Such solid-binding proteins are multifunctional entities that recognize, bind, and self-assembly at material surfaces (having various chemical composition and structure). Some of them also possess the ability to promote nucleation of an inorganic phase and control of crystal growth and morphology, thus, play a major role in formation of biological inorganic structures (biomineralization) (Baeuerlein 2007).

Inorganic surface specific proteins have been identified in different types of organisms ranging from proteo-bacteria to humans, and exhibit various biological functions which can be useful from a technological point of view. For instance, in some magnetotactic bacteria mediate formation of iron oxide nanocrystals that function for sensing and orientation in natural magnetic fields (Komeili 2007). Proteins binding surfaces of inorganic materials also work as adhesives enabling marine mussels binding to a wide variety of inorganic substrates in seawater

(Stewart et al. 2011). Other bind ice crystals and help organisms such as fish, insects, plants and soil bacteria to survive at low temperatures (Jia & Davies 2002). Still others bind and self-assemble at materials surfaces changing their chemical properties, for example, hydrophobins produced by filamentous fungi (Linder 2009) (Figure 1). Moreover, solid-binding proteins can mediate nucleation, growth, and assembly of a variety of biological materials with precise control of their composition and hierarchical architecture from nano to macroscale. This relation can be noticed, for example, in biological composites (such as nacre, bone, and tooth) in which specific structural arrangements between biomolecules and inorganic components create materials with extraordinary properties (light-weight, stiff and tough) (Meyers et al. 2008).

The examples from Nature show that proteins through mechanisms of molecular recognition and specific interactions at the interfaces can control material systems, providing them unique and often very sophisticated biological properties (Dickerson et al. 2008b). Thus, detailed understanding of the structural principles for the function of natural solid-binding proteins would enable us to tailor specific protein-surface interactions, design, and create novel proteins with desired functions for various practical applications (Sarikaya et al. 2003). Unfortunately, our knowledge about solid-binding proteins is still very limited and it is extremely difficult to control their interactions with materials, mimic principles of material molecular design found in Nature, and create artificial systems with similar properties from the bottom-up with hierarchical levels of organization. For instance, it is very challenging to achieve the combinations of properties found in biological composites within one synthetic material. Controlled biomineralization, self-assembly, adhesion, and tailoring of material interfaces and properties are also far from being understood. Therefore, many biological systems and materials have been extensively studied at the molecular level focusing especially at the interactions between proteins and their target molecules.

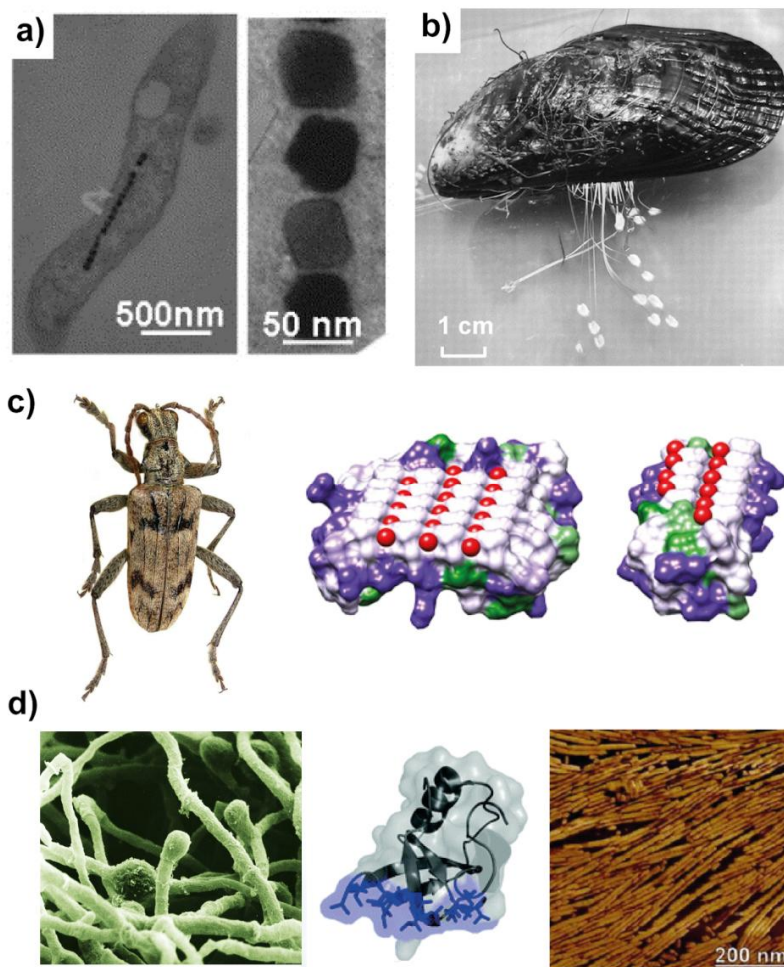


**Figure 1.** Examples of biological functions of solid-binding proteins in different organisms, (a) formation of iron oxide nanocrystals in magnetotactic bacteria, e.g. *Aquaspirillum magnetotacticum*, (b) adhesion to various materials in marine organism, e.g. blue mussel (*Mytilus edulis*) attached to glass surface, (c) binding of ice crystals, e.g. anti-freeze proteins from longhorn beetle *Rhagium inquisitor*, center and right picture showing crystal structure of RiAFP protein, water molecules indicated in red, (d) self-assemble at interfaces, e.g. hydrophobin from filamentous fungus *Trichoderma reesei*, crystal structure shows amphiphilic properties of the hydrophobin molecule (hydrophobic patch – blue, hydrophilic part – gray), atomic force microscopy image of characteristic self-assembly pattern. Sources of images: a (Tamerler & Sarikaya 2007), b (Holten-Andersen & Waite 2008), c (Hakim et al. 2013), d – left panel <http://www.ecoconnect.org.uk/>, center and right panel (Linder 2009).

## 1.2 Approaches to investigate solid-binding proteins

There are several approaches to obtain the inorganic surface-specific proteins and to investigate their interactions with materials. The traditional methods are based on the identification and isolation of natural solid-binding proteins from hard tissues using molecular biology techniques. Next step involves determination of their amino acid sequences and to define domains, peptide motifs, or critical amino acid residues associated with target recognition and binding. This approach was successfully used to identify and study, for example, ice-binding proteins (Garnham et al. 2011), amelogenin (a major protein in enamel) (Fan et al. 2009), and silicatein (extracted from skeletons of diatoms) (Shimizu et al. 1998). However, it frequently involves time consuming procedures, including isolation, purification, and sequence-structure analysis. In addition, technological utilization of isolated natural solid-binding proteins is often limited because of their large size (usually more than 100 amino acids long), requirement of specific physiological conditions, and often presence other proteins or factors enabling their proper biological function (for example, during biomineralization processes) (Tamerler & Sarikaya 2009).

Another approach (often supporting traditional techniques) utilizes knowledge of existing and previously investigated solid-binding proteins to design and create recombinant proteins with tailored functions for particular applications. Attempts to achieve this goal have been carried out by rationally designing novel proteins or engineering existing functional protein domains using computational methods (Höcker 2014, Damborsky & Brezovsky 2014). However, these approaches are often hampered due to the lack of detailed information on the molecular complementarity between a protein molecular architecture and the structure of the solid surface. Modelling of atomic lattices tends to be oversimplified and differ from real conditions, and thus, our ability to design rationally or predict a protein with specific function is still very limited (Tamerler & Sarikaya 2009).

In Nature, structure, function, and consequently other properties of proteins have been developed via successive cycles of mutation and selection that optimized them for a given set of conditions to perform their particular role. Therefore, in the absence of knowledge about structural details of given proteins, material surfaces, and mechanism of molecular interactions at the biomolecule-solid interface, a more rational approach to develop surface specific proteins would be to mimic the biological molecular evolution processes. These natural phenomena can be emulated in the laboratory scale with the use of directed evolution methods based on random or site-directed mutagenesis of existing proteins, or else the genetic selection of polypeptide motifs from combinatorial libraries. The latter approach, originally established and used in drug and antibody development for screening and characterization of novel high affinity ligands interacting with antibodies, receptors, enzymes, and other proteins (Kehoe & Kay 2005, Smith & Petrenko 1997), has also been adapted in material science (Brown 1997). In the past decades it has been successfully used for identifying numerous peptide sequences with affinity to various solid materials, for example, metals, semiconduc-



tors, oxides, minerals, polymers, and carbon based nanomaterials (Shiba 2010, Sarikaya et al. 2003, Briggs & Knecht 2012).

### **1.3 Advantages of directed evolution approaches for selecting material-specific peptides**

The greatest advantage of evolutionary selection protocols is that they can be utilized to identify peptides binding to virtually any kind of inorganic surface including also artificial, non-natural materials. Peptides bind their inorganic targets non-covalently and can form stable coatings on material surfaces that provide new surface characteristics without changing the materials bulk structure. Evolutionarily selected peptides are usually short and rather simple biomolecules (compare to proteins), thus, they can serve as very useful model systems for detailed investigations of the nature of peptide-solid interactions. Moreover, short functional peptides can be further engineered using recombinant DNA technology or chemical approaches to create mutations, recombinations, and repeats (multimers). The modifications can improve binding properties of selected peptides and tailor their function for desired applications that require specific control of interactions at biomolecule-solid interfaces.

### **1.4 Applications of material-specific peptides**

There are numerous examples of how the functionality of short material specific peptides can be utilized in practice. One of them is surface modification. Peptides, through selective binding and self-assembly properties, provide new functionality to material surfaces, and at the same time, they overcome many drawbacks of other widely used immobilization techniques, such as covalent modifications (Wong et al. 2009) or self-assembled monolayers (SAMs) (Schreiber 2000). Chemical approaches permanently modify the surface of the substrates because of the covalent immobilization of functional molecules, while SAMs can be only applied for limited number of materials. In addition, both techniques are rather cost- and time-consuming, and involve need of use harsh conditions that are usually not bio-compatible (Rusmini et al. 2007). Material specific peptides, on the other hand, can be easily used under environmental-friendly conditions, making them also suitable for biomedical applications. They have been widely applied to modify surfaces of many biomedical and implant materials such as glass, gold, platinum, and titanium (Khatayevich et al. 2010). Furthermore, material specific peptides can be also easily conjugated with different bioactive molecules, for example, non-fouling agents, antimicrobial peptides, or integrin receptor binding motif (RGD). Hence, they can be exploit, for instance, to create non-fouling coatings preventing protein adsorption and bacterial colonization onto implants as it was demonstrated for titanium binding peptide conjugated with PEG (Khoo et al. 2009), or as inducers of cell adhesion as it was shown for another titanium binding peptide functionalized with the integrin ligand that caused induction of adhesion

and increased viability of fibroblasts (Khatayevich et al. 2010). Solid-binding peptides have been also broadly used to functionalize technologically important materials. For example, self-assembled graphite binding peptides were applied to control its chemistry and wettability (Khatayevich et al. 2012), peptides binding to semiconductor surface (GaAs) modulated its electronic properties (electron affinity and surface potential) (Matmor & Ashkenasy 2012), while peptides binding to conductive synthetic polymer (chlorine-doped polypyrrole, PPyCl) were used to modify surfaces for biosensor applications (Sanghvi et al. 2005).

Material specific peptides can be also utilized as molecular anchors for directed surface immobilization of proteins. Genetic engineering or chemical coupling methods allow creating peptide-fusion proteins that exhibit material specificity (via peptide tags) and other functions, for instance enzymatic activity (discussed in more details in paragraph 1.7.2). Peptide linkers provide controlled adsorption of the fusion proteins with maintained native conformation and retained biological activity in contrast to other existing protein immobilization methods that often result in random protein immobilization and decrease or loss of biological activity. Specific peptide tags were applied for addressable immobilization of functional proteins on various surfaces, for example, gold binding peptides were used for directed display of enzymes, such as alkaline phosphatase and lactate dehydrogenase, that were able to catalyze enzymatic reactions on a variety of gold substrates, such as micropatterned gold surface, nanoparticles, electrodes (Cetinel et al. 2013, T. Kacar et al. 2009). Sapphire binding peptide fused to maltose binding protein was successfully immobilized on a sapphire ( $\alpha\text{-Al}_2\text{O}_3$ ) surface (Krauland et al. 2007) and silver specific peptide fused to multifunctional green fluorescence-maltose binding protein was bound to silver nanoparticles (Hnilova et al. 2012a). Both peptide-fusion proteins were used for developing protein biosensor applications.

Targeted assembly of nanoparticles on solid substrates represents another application of material specific peptides. In this case, peptides have been engineered to bi-functional forms able to bind simultaneously substrate and nano-objects. For instance, combining gold and silica binding sequences together resulted in a bi-functional peptide that was used for direct immobilization of gold nanoparticles onto a silica surface (Hnilova et al. 2012c). Another type of bi-functional peptide was constructed by biotinylation of a silica binding sequence that was applied for spatially selective self-assembly of streptavidin-functionalized quantum dot light emitters on micro-patterned chips used for development of LED devices (Demir et al. 2011). In addition to site directed deposition of nanoparticles on surfaces, engineered peptides have been shown to be useful for stabilization of their colloidal suspensions in aqueous environment as it was demonstrated for platinum nanocrystals (Li et al. 2009), carbon nanotubes (Sheikholeslam et al. 2012), gadolinium oxide nanoparticles (Schwemmer & Baumgartner 2012), or DLC flakes (publication III).

Material specific peptides are also useful in the synthesis of inorganic nanoparticles. Peptides can initiate nucleation, control crystal growth, and produce nanostructures with precise size and morphology. This control over crystal charac-

teristics often determines the properties of the synthesized material. Furthermore, peptide mediated production of materials can be carried out under mild reaction conditions (aqueous solutions, at or near room temperature, and close to neutral pH) in contrast to techniques used in traditional material-processing (Briggs & Knecht 2012). It has been shown that peptides can control synthesis of nanostructures of different materials, such as palladium (Pacardo et al. 2009) platinum (Li et al. 2009), gold (Kim et al. 2010, Li et al. 2014), silver (Naik et al. 2002), hydroxyapatite (Gungormus et al. 2008), silica (Sano et al. 2005b), and metal oxides (Oh et al. 2014). Peptides producing inorganic materials have been applied to advanced nanotechnological applications, for example, the Belcher group has demonstrated the use of such peptides incorporated in genetically engineered M13 viruses that were exploited as a scaffold for the fabrication and assembly of materials for various device applications, including high power batteries (Oh et al. 2013), catalysts (Nam et al. 2010), biosensors (Bardhan et al. 2014), photovoltaics (Dang et al. 2011), and tools for cancer imaging and detection (Ghosh et al. 2012, Ghosh et al. 2014). The Sarikaya group showed utilization of hydroxyapatite binding peptides that regulate calcium phosphate formation in tissue engineering for potential applications in restoration and regeneration of hard tissues, such as bone, cartilage, and teeth (Gungormus et al. 2010, Gungormus et al. 2012).

## **1.5 Selection of solid-binding peptides from combinatorial peptide display libraries**

Directed evolution methods used to identify material specific peptides are based on screening of combinatorial peptide libraries displayed, for example, on the surface of filamentous phages (phage display) (Smith & Petrenko 1997) or bacterial cells (cell surface display) (Lu et al. 1995). Combinatorial peptide libraries have usually a complexity in the order of  $10^9$  independent clones and are composed of peptides of equal length (most often 7 or 12 residues) but with randomized amino acid sequences. The libraries are generated by inserting random oligonucleotides encoding short peptide variants into genes encoding proteins that are present on the surface of bacteriophages or bacterial cells (*Escherichia coli*). The genetic fusion creates a physical link between the genotype (DNA sequence encoding peptide) and the phenotype (peptide sequence) and results in each phage or cell displaying a different and random peptide sequence (Figure 2). Many different systems utilizing various coat proteins of M13, fd, and f1 bacteriophages (Kehoe & Kay 2005), or outer membrane proteins, fimbria, and flagellar proteins of *E. coli* (Löfblom 2011) have been created to display combinatorial peptide libraries. However, the most common system that has been used for finding material binding peptides is based on pentavalent M13 phage display (developed by New England Biolabs). Thus, many examples presented in this thesis will refer to that system (New England Biolabs Manual, Version 1.2, 2014).

The typical *in vitro* screening process (biopanning) is based on affinity selection of peptides that bind to a given target (an inorganic surface). It is carried out by

exposing a library of phage or cell clones displaying a pool of randomized peptide variants onto a target surface. Several washing cycles of the phages or the cells eliminate non-specific binders to the substrate. Specifically bound fractions are then eluted from the surface by chemical or physical method and amplified for next biopanning round. The cycle (binding, washing, elution, and amplification) is repeated (usually 3–4 times) to enrich the pool of clones having high affinity to the target. After the last biopanning round, individual clones are selected and characterized by DNA sequencing to obtain the amino acid sequence of the polypeptides binding to the target substrate material (Figure 2).

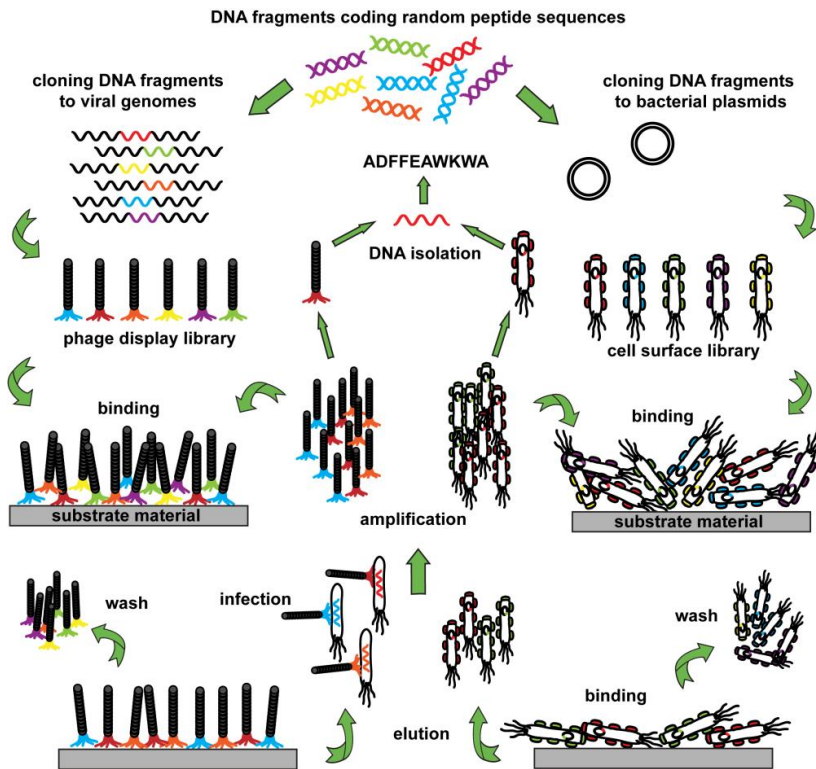


**Figure 2.** Phage display and cell-surface display. Principles of combinatorial libraries generation and biopanning process used for selecting peptide sequences binding to a given inorganic substrate material. Figure adapted from (Sarıkaya et al. 2003).

### 1.5.1 Selecting “true” binders from a library

The ideal outcome of the biopanning experiment is the selection of specific, high affinity binders to the target material. However, in order to achieve this goal sever-

al issues have to be considered. First, the biopanning protocols must be optimized to minimize any unspecific phage or cell binding. This can be accomplished by careful choice of panning buffer parameters, such as pH and ionic strength, and addition of agents that limit unspecific binding, for example, BSA or detergents (the most common is Tween-20).

Attention should also be paid to the solid material used as a target. Solid materials, unlike the protein targets, might be prone to surface modifications during cleaning or exposition to screening buffers, what can result in the recovery of peptides that bind to a surface or morphology different from the one that was originally intended. Thus, optimal buffers and proper cleaning protocols must be used to ensure that quality of the material will stay the same in each panning round (Sarıkaya et al. 2003, Seker & Demir 2011).

Another important issue is the elution process that recovers strong binders remaining adsorbed on the surface after the washing steps during panning. The most typical elution protocol (in phage display system) is based on using harsh chemical conditions such as low pH and high ionic strength. Studies showed that for some targets, chemical elution was insufficient and a considerable fraction of tight binders remained bound to a substrate (Sarıkaya et al. 2003). Moreover, for chemically reactive materials harsh chemical conditions may alter its surface properties and change the nature of the target-peptide interactions. Alternative solutions to chemical elution can be the use of the mechanical energy of ultrasonic waves (physical elution) (Donatan et al. 2009), the amplification of bound phages in the presence of the target by adding a bacterial host (elution by infection – phages detach from the target and infect bacterial cells) (Smith & Petrenko 1997), or lysing phages bound to the target followed by extraction of its DNA (Naik et al. 2004).

### **1.5.2 Problem of target unrelated peptides**

Despite the fact that many panning experiments have been design carefully (taking into consideration all the factors discussed above), it happens that some peptides are selected from phage display libraries, not as a result of affinity to the target. These peptides (termed target unrelated peptides, TUPs) are displayed on the phage clones binding to other surfaces than the target itself, such as components of the screening system (selection-related TUPs) (Vodnik et al. 2011, Thomas et al. 2010), or having accelerated propagation properties (propagation-related TUPs) (Nguyen et al. 2014). The selection-related TUPs have been identified as binders to various components of the screening system, such as polystyrene (e.g. tubes, pipette tips, microtiter wells), streptavidin (the capturing agent for biotinylated targets), blocking agents (BSA, milk), bivalent metal ions, such as  $\text{Co}^{2+}$ ,  $\text{Zn}^{2+}$ ,  $\text{Cu}^{2+}$  and  $\text{Ni}^{2+}$  (used for target immobilization in some phage display experiments), or certain small chemicals (salts, detergents, buffering agents) (Menendez & Scott 2005, Vodnik et al. 2011). For instance, the “plastic binders” are typically rich in aromatic residues (Phe, Tyr, Trp, His), such as FHWTWYW (Anni et al. 2001), FKFWLYEHVIRG (Feng et al. 2009), or contain the WXXW

motif as in case of VDWVGWASW sequence (Gebhardt et al. 1996). The HPQ motif is characteristic for peptides binding to streptavidin (Giebel et al. 1995), while histidine rich sequences for binders to bivalent metal ions, for example,  $\text{Co}^{2+}$  (KLSLRHDHIIHHH) (Berger et al. 2007) or  $\text{Cu}^{2+}$  (GRVHHHSLDY) (Park et al. 2006). Several peptides have been also described as binders to BSA but no consensus motif sequence has been found (Desjobert et al. 2004).

On the other hand, propagation-related TUPs are peptides displayed on phage clones containing advantageous mutations in their genome that allow them to propagate faster than the rest of the library. During the amplification steps carried out in bacterial cells (Figure 2) between biopanning rounds the concentration of faster propagation phages increases more rapidly than the normal phages found in a library. Thus, in the last round of the selection, peptides displayed on faster propagating phages may dominate the pool of selected sequences even though they do not possess high affinity to the target under study (Nguyen et al. 2014). A well-known example of such mutant with the accelerated propagation properties is the phage clone displaying the HAIYPRH sequence that contains a single mutation ( $\text{G} \rightarrow \text{A}$ ) in the 5'-untranslated region (5'-UTR, ribosome binding-site) of gene II (Brammer et al. 2008). Recently 24 other peptides displayed by mutated phage clones in the broadly used commercial libraries Ph.D.-7 and Ph.D.-12 (developed by New England Biolabs) have been also identified. Studies showed that phages displaying those sequences contained 14 different mutations, either in the 5'-UTR of gene II, or in close proximity of it (Nguyen et al. 2014).

The TUPs (selection- or propagation-related) are a serious drawback of the evolutionary selection methods. They may appear and be enriched already in first panning round and potentially dominate in the selection process. Thus, their identification is a very important step in analyzing biopanning results. Unfortunately, many researchers have not been aware of the problem and in numerous studies TUP were not recognized and discarded from true positive clones, and been a source of false positive results leading to incorrect conclusions. For instance, the propagation-related HAIYPRH sequence (described above) has been identified in at least 30 independent biopanning experiments (Huang et al. 2011; Vodnik et al. 2011) and described as a putative binder to various targets, for example, isotactic poly(methyl methacrylate) (Serizawa et al. 2007b), surface of hepatocellular carcinoma cells (Jia et al. 2014), and silica nanoparticles (Puddu & Perry 2012). Another good example is the sequence KLSLRHDHIIHHH which was confirmed as selection-related TUP binding to bivalent metal ions (Park et al. 2006). However, it has been also described in literature as suspected binder for at least 13 different substrates for instance silica nanoparticles (Patwardhan et al. 2012), titanium dioxide (Dickerson et al. 2008a), and anti-RPV-H monoclonal antibody (Buczowski et al. 2012). More examples of commonly selected target unrelated peptides are pretested in the Table 1.

**Table 1.** Examples of frequently isolated target unrelated peptides. Suspected TUPs have been found by many labs using completely different (unrelated) targets.

Peptide sequence/ type of TUP/ *	Examples of targets	References
SVSVGMPKPSRP/ suspected propaga- tion-related/>50	Concanavalin-A	(Pashov et al. 2005)
	Single-crystal hydroxyapatite	(Chung et al. 2011)
	Crystalline surface of GaSb(100)	(Estephan et al. 2009)
	DNA	(Wölcke & Weinhold 2001)
	Glycine receptor subunit alpha-1	(Tipps et al. 2010)
HAIYPRH/ propaga- tion-related/>30	Isotactic poly(methyl methacrylate), st-PMMA	(Serizawa et al. 2007b)
	Hepatocellular carcinoma cell line (HCCLM3)	(Jia et al. 2014)
	Colonic adenomas	(Miller et al. 2012)
	Silica nanoparticles	(Puddu & Perry 2012)
	Titanium nitrile	unpublished (VTT)
KLSLRHDHIIHHH/ selection-related/>13	Ferromagnetic L10 phase of FePt	(Reiss et al. 2004)
	Titania (TiO <sub>2</sub> ) nanoparticles	(Dickerson et al. 2008a)
	Hepatoma cell line (SMMC-7721)	(Jiang et al. 2006)
	Anti-RPV-H monoclonal antibody	(Buczowski et al. 2012)
LPLTPLP/ suspected propagation- related/>18	Polarized human umbilical vein endo- thelial cells	(Maruta et al. 2003)
	HMG box 2 domain of high mobility group protein B1	(Dintilhac & Bernués 2002)
	Transforming growth factor beta-1 (TGF-beta-1)	(Zong et al. 2011)
	Interleukin-6	(Mizuguchi et al. 2000)
SILPYYP/ suspected TUP for binding to various targets/10	Quinoprotein glucose dehydrogenase	(Yoshida et al. 2003)
	Neural stem cells, NSC	(Caprini et al. 2013)
	Small molecular ink	(Cui et al. 2010)
	Titanium nitrile	unpublished (VTT)
HWGMWSY/ suspect- ed plastic binder/6	Anti-E. coli K1 monoclonal antibody	(Shin et al. 2001)
	Bovine serum albumin (BSA)	(Desjobert et al. 2004)
	Anti-NE2 monclonal antibody (8H3)	(Gu et al. 2004)
TMGFTAPRFPHY/ suspected TUP for binding to various targets/9	Polycrystalline hydroxyapatite	(Chung et al. 2011)
	Germanium oxide	(Dickerson et al. 2004)
	Glycine receptor subunit alpha-1	(Tipps et al. 2010)

\* The number of independent biopanning experiments that identified the peptide.

In order to minimize the problem of analyzing TUP as “true” binders, and before drawing conclusions about the consensus sequence binding to the target material under study, all selected peptides should always be carefully examined. First and already very informative step in identifying potential TUP from biopanning results can be just simple screening of selected sequences using common internet seekers, for example, Google ([www.google.com](http://www.google.com)). If a query sequence has been described before (found by a seeker) it is very likely that it is TUP because the possibility of obtaining identical peptide sequence from a library with the complexity of order  $10^9$  of independent clones against different target in two independent panning experiments is extremely small. More advanced tools to scan and exclude possible target-unrelated peptides are provided by web platforms and databases such as SAROTUP “Scanner And Reporter Of Target-Unrelated Peptides” (Huang et al. 2011) (<http://i.uestc.edu.cn/sarotup/index.html>) or PepBank (Shtatland et al. 2007) (<http://pepbank.mgh.harvard.edu/>) that store information about the sequences that have been previously reported in other studies or identified as TUPs.

## **1.6 Analysis of features of peptides selected in a biopanning experiment**

The next step of analyzing biopanning results (after finding and excluding possible TUP) involves the investigation of overall features of selected novel sequences, i.e., searching for particular amino acid residues or common chemical properties that were enriched during biopanning, and identification of common sequence motifs that could indicate the potential consensus binding sequence. This kind of analysis can give first insights on the nature of possible interactions between selected peptides and the target substrate. For instance, it has been shown that for some targets there was an enrichment of specific amino acids or a consensus motif was identified implying that enriched residues might be involved in the binding mechanism to the substrate, for example, basic residues were enriched in the biopanning against single-crystalline sapphire (Krauland et al. 2007) or aromatic ones when poly(phenylene vinylene) (PPV) (Ejima et al. 2010) was used as a target, or else consensus binding sequences showing a motif rich in histidine and tryptophan at specific locations was identified in the panning against single-walled carbon nanotubes (SWNT) (Wang et al. 2003). On the other hand, in panning experiments against substrates, such as titanium (Sano & Shiba 2003), titanium oxide (Gronewold et al. 2009), calcium carbonate (Gaskin et al. 2000), palladium (Heinz et al. 2009), and many others, neither amino acid enrichment nor consensus binding patterns were found. Moreover, in some cases different peptides (with various chemical properties) binding to the same target have been discovered in independent panning experiments (by different research groups). For example, sequences, such as MHGKTQATSGTIQS (Brown 1997), VSGSSPDS (Huang et al. 2005), LKAHLPPSRLPS (Nam et al. 2006), WAGAKRLVLRRE (Hnilova et al. 2008), TGTSVLIATPYV (Kim et al. 2010), TLLVIRGLPGAC (Causa et al. 2013), all have been found to bind gold.



In general, the lack of enriched residues, consensus motifs, or existence of various sequences with distinct chemical properties binding to the same target suggest that the affinity of peptides cannot be explained simply by its chemical composition, but also other factors such as peptide three-dimensional conformation or properties and structure of a substrate material are potentially important (Walsh 2014). Furthermore, it should be noted that inorganic materials can often be found in many different forms, and even having exactly the same chemical composition and crystal structure they can vary in surface properties, e.g., charge, topography, roughness in each panning experiment. What is more, the panning as a selection process is unique evolution event, and although it is conducted in the controlled laboratory environment, it cannot be performed in the same way because it involves stochastic processes (analogues evolution in Nature) so the outcome of each biopanning section is expected to be different. Therefore, studies of chemical properties of selected peptides in biopanning experiment are not sufficient to explain the nature of peptide-target interactions. They should be followed by functional analysis validating and quantifying peptide binding to the target.

## 1.7 Analysis of peptide-target binding

The binding of selected peptides from a combinatorial library in a biopanning experiment can be analyzed in different molecular “contexts”, meaning that the function of peptides can be investigated when they are displayed on a phage but also when are released from the virus or cell and are linked to another molecular scaffold, for example a protein, or existing in a free soluble form (Figure 3). This kind of context depended function analysis is usually carried out using independent experimental methods, thus, it can verify the biopanning results (eliminating the possibility of analyzing false positive results) and help in obtaining more information about the peptide-target binding affinity and nature of the interactions (Chen et al. 2009).

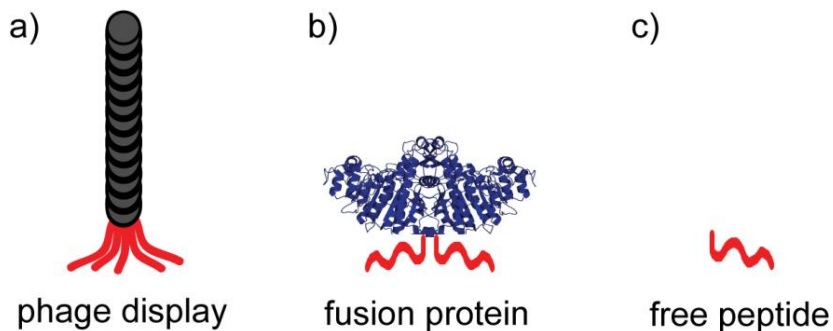


**Figure 3.** Different ways of analyzing peptide binding. Peptides (a) displayed on phage surface (b) forming fusion protein (c) in soluble free form.

### **1.7.1 Binding analysis using phages**

Peptide sequences obtained from biopanning experiments with phage display systems can be easily analyzed by comparing the adsorption properties of single phage clones displaying selected sequences (each single phage clone display one of selected peptides). The advantage of using phages is that peptides remain in the same molecular binding environment as during biopanning, i.e., fused with a phage coat protein, and are present in the identical number of copies, for instance, fused to the pIII phage protein using GGGS linker and present in 5 peptide copies as in the New England Biolabs phage display systems.

The most common techniques to analyze phage binding include titer analysis, ELISA, and microscopy. The titration allows for measuring of the number of phages bound to a substrate. However, it relies on their biological function, thus, before analyzing the phage titer, bound viruses need to be eluted from the substrate's surface and used to infect bacteria, therefore there is a possibility that some fraction of strong binding phages might not been harvested (eluted). On the other hand, in ELISA bound phage particles are detected directly on the surface using phage specific antibodies conjugated with a reporter enzyme without the need of elution step. Thus, in ELISA even very strongly bound phages can be detected but the necessity of using antibodies may cause problems of high background signals (due to their unspecific binding to an inorganic substrate material), which may lead to underestimation of the amount of adsorbed phages.

Phages bound to an inorganic surface can be also analyzed and imaged by the atomic force microscopy (AFM) or fluorescence microscopy (previously labeled with a fluorescent reporter). Both methods, similarly as ELISA, allow detecting phages bound directly on the substrate but the comparison of the binding of different phage clones is very challenging because the obtained binding-data have semi-quantitative character.

In general, all the techniques for phage binding analysis allow for only indirect estimation of the attached phage concentration and their relative binding strength. Thus, to evaluate phage binding thoroughly is important to use combination of different independent analyses.

### **1.7.2 Binding analysis using fusion proteins**

The fusion protein approach is usually applied when the binding of selected peptides in the biopanning process has been already verified. It allows evaluating if the selected peptides can retain their function when they are released from a host surface and are present in lower copy number or as individual binding units, as well as for more detailed studies of peptide-target interactions with analytical methods that are difficult to adapt for peptide display systems. The concentration of the peptide-fusion proteins can be accurately measured and controlled; hence, they can be utilized to determinate peptide binding affinities that are very difficult to measure when peptides are displayed on phages or cells. The possibility to engineer a peptide sequence linked to a protein allows for investigation of its bind-

ing mechanism, while attachment of more than one peptide copy to create and study multivalent display systems.

Peptide-fusion proteins can be created using genetic engineering or chemical methods. When recombinant DNA technologies are used, a synthetic gene encoding peptide is combined together with a protein gene and expressed in a production host (often, *E. coli* or yeast). The produced fusion protein is then purified. Peptides are often added as extra tags to the N- or C-terminus of proteins, or sometimes inserted within their permissive site (Karaca et al. 2014). Genetic engineering additionally allows for easy modifications of peptide sequences and tailoring of binding properties (more detailed information in paragraph 1.9). The challenge of creating fusion proteins using genetic engineering is that cloning, expression, and purification protocols may be time-consuming, and some peptide sequences might be difficult to produce in microorganisms.

In chemical methods peptides can be attached to proteins using crosslinking agents that react with both peptide and protein (Hermanson 2008b) or by direct reaction with protein (require chemical activation of peptide, for example, attachment of maleimide groups that react with thiol group of cysteine residues). Chemical methods allow for creation of different types of fusion proteins (Hermanson 2008a), however, the genetic engineering methods are usually more robust in production of large number of peptide-protein variants, and overcome problems with size limitation or poor solubility of synthetic peptides, as well as do not require chemical activation during synthesis (which sometimes may affect the overall properties of the fusion proteins).

In the literature there are many examples of studies where peptide-fusion proteins were used. For instance, many peptide sequences have been fused to enzymes, such as alkaline phosphatase (AP) (T. Kacar et al. 2009) or L-lactate dehydrogenase (LDH) (Cetinel et al. 2013), which were used as reporters to quantify the binding of the peptide-fusion protein to the target surface by measuring its enzymatic activity. Green fluorescence protein (GFP) was applied to monitor and visualize fusion proteins binding to specific locations on material surface (Yuca et al. 2011; Park et al. 2006). Maltose binding protein (MBP), which is a good model protein (due to high expression levels in *E. coli* and easy purification protocol), has often been utilized to study peptide adsorption parameters using biophysical techniques, such as surface plasmon resonance (SPR) (Hnilova et al. 2012b) or quartz crystal microbalance (QCM) (Sengupta et al. 2008), because measuring adsorption of the peptide-fusion proteins is more robust than free soluble peptides. Proteins forming multimers, AP or ferritin, were used to produce multivalent display systems and to investigate the influence of avidity effect on peptide binding (Sano et al. 2005a; T. Kacar et al. 2009).

In general, a fusion protein approach allows for thorough binding analysis and characterization of adsorption parameters of peptides with a variety of different analytical methods that are very difficult to apply using phages or free peptides. In addition, due to the possibility of genetic modifications of peptide sequences, fusion proteins can be used to study binding mechanisms and structure-function relationship in peptides.

## 1.8 Investigation of structural biases of peptide function

Given that peptides show an affinity for the interfaces under study, their function can be understood from two different views. Firstly, the amino acid composition of the sequence that defines certain specific peptide chemical characteristics (i.e., charge, hydrophobicity, solubility) may direct interactions favoring surface adhesion. Secondly, besides the chemical composition, the specific arrangement of amino acid residues in the primary sequence, and additionally, the three-dimensional structure of a peptide may also have a significant role and contributing effect.

The relation between the structure and function in material binding peptides has been extensively investigated using rational and random mutagenesis approaches. Useful insights provided by studies of point mutations of binding sequences that have been used to map important functional residues. For example, alanine scanning based on point mutations to alanine of each amino acid in the sequence (one at a time) was performed on the titanium dioxide binding peptide (LNAAVPFTMAGS) isolated by phage display. The study showed that each mutated peptide highly decreased its affinity for the substrate, thus, authors concluded that all amino acids, either hydrophobic or hydrophilic, of the original peptide are important for its function and the affinity to the target is driven by electrostatic and hydrophobic interactions (Vreuls et al. 2010). In another example, alanine scanning was used to identify functional residues in the sequence HTDWRLGTWHHS that was found as a binder to hyperbranched poly(phenylene vinylene) (hypPPV). The experiment revealed (similarly as in the case of the titanium dioxide binding peptide) that a substitution by alanine at any position of the hypPPV binding peptide significantly decreased its affinity to the target, suggesting that all amino acids are essential for the strong interaction. However, it was also found that the degree of decrease in affinity differed depending on the residue in the sequence which was mutated (Trp9>Trp4>Arg5>Leu6>Gly7>His10>His1>Thr8>Thr2>Asp3>His11>Ser12). Consequently, it was concluded that tryptophan residues (W) at the positions (4) and (9) in the sequence are the key residues for the affinity, which is therefore based on hydrophobic interactions between the aromatic groups of W side chains and the aromatic groups present in target (Ejima et al. 2010). On the other hand, alanine scanning of the ELWRPTR sequence binding to synthetic polymer poly(methyl methacrylate) (PMMA) revealed that not all residues are critical for the function. The study showed that the most critical residue was proline (P5) while the least ones were leucine (L2) and tryptophan (W3). Moreover, it was demonstrated that essential amino acids for the affinity are located in the C-terminal part of the peptide. The shorter 4-mer peptide comprising the C-terminal RPTR sequence in the original peptide, retained strong target specificity, in contrast to the N-terminal 4-mer peptide GLWR. It was also shown that the P5 residue was responsible for structural features important for the binding (Serizawa et al. 2007c). In another example, substitution of amino acids in the graphite binding peptide (IMVTESSDYSSY) probed the critical residues for its affinity and self-assembly properties on the surface. The study showed that the

mutant containing two tyrosine (Y) residues at the positions (9) and (12) replaced with alanine (A) completely lost its ability to bind to its target, while other mutants having the same residues substituted with either tryptophan (W) or phenylalanine (F) (two other natural amino acids containing aromatic moieties) resulted in retained binding affinity. Thus, it was concluded that the original peptide binds to graphite by its aromatic domain (YSSY) through a coupling of  $\pi$ -electrons. To examine the self-assembly characteristics of the peptide three residues (IMV) at the N-terminus were mutated by modifying its hydrophobic nature. For this purpose, two mutants containing either negative or positive sequence knockouts were prepared. In the design of the mutant having the negative knockout, the sequence IMV was replaced with three similarly sized hydrophilic amino acids: threonine (T), glutamine (Q), and serine (S) resulting of a mutant with hydrophilic character. A second mutant sequence was designed to restore hydrophobic characteristics of the domain, by replacing IMV sequence with three other aliphatic amino acids: leucine (L), isoleucine (I), and alanine (A). Functional studies (by atomic force microscopy) showed that hydrophobic mutant bound strongly to the substrate and maintained ordering pattern similar to that by WT peptide, while hydrophilic mutant formed highly porous and disordered structures, hence, it was concluded that the hydrophobic nature of the N-terminal domain of the peptide is responsible for its self-assembly on the surface (So et al. 2012).

Sequence shuffling and inversions represent other examples of mutational studies that have been applied to investigate if changes in the specific order of the connection between amino acid residues in the primary peptide sequence have influence on its function. Studies revealed that this kind of modifications had different functional effects; for instance, shuffling the sequence of platinum binding peptide showed that the order of residues in the sequence was not important. The mutated peptide retained almost in 100% its specificity for formation of platinum nanocrystals of certain shape and only one phenylalanine residue was identified to be the critical for this function (Ruan et al. 2013). A similar result was obtained in a study on a conducting polymer (chlorine-doped polypyrrole) where the effect of inverting the peptide sequence was small, suggesting that its binding to the target is composition specific but not conformation specific (Sanghvi et al. 2005). On the other hand, in a study on the peptides binding semiconductor surfaces random scrambling the sequence AQNPSDNNTHTH, which binds with high affinity to gallium arsenide, GaAs (100), but with low affinity to silica, Si (100), resulted in a loss of its binding selectivity (the scrambled peptide adsorbed to both materials with similar binding strengths), thereby demonstrating that the specificity the sequence is determined by both chemical composition and spatial conformation (Goede et al. 2004). The importance of the specific order of residues in the primary sequence was also shown in a study on peptides binding to gadolinium oxide (GdO). The authors demonstrated that the scrambled peptide lost its affinity to GdO and concluded (similarly as in the previous case) that peptide adsorption behavior depends strongly on both its amino acid sequence and three-dimensional structure (Schwemmer & Baumgartner 2012).

Valuable information about the role of molecular conformations of material binding peptides was provided also by comparing the functionality of the cyclic and linear versions of their sequences. The cyclic form of a peptide is produced by introducing two cysteine residues at its C- and N- terminus that form constrained "loop" of the sequence through disulfide bridge. For example, in comparing the two forms of platinum binding peptide, it was shown that the cyclic form displays equilibrium and adsorption rate constants significantly larger than those obtained for the linear form. It was concluded that this kind of adsorption behavior is a consequence of the presence of the covalent Cys-Cys loop in constrained version, resulting in a molecular architecture that is more rigid, in contrast to the linear form that lacks of such structural constraints and it is more flexible with a high degree of freedom in its conformation. The authors suggested that the compact structure of the cyclic peptide favors its binding dynamics and the adsorption kinetics, contrary to the linear form, which because of its high degree of flexibility, is more floppy and, therefore, has lower affinity to the surface (Ozgur et al. 2007). On the other hand, in similar studies on a peptide binding to titanium and silicon oxide, it was demonstrated that its linear form had better affinity to both targets. In this case, the authors claimed that the higher structural flexibility of the polypeptide chain allowed it to form a wider range of conformations to maximize its interaction with the targets (Chen et al. 2009). In another example, a study on two different gold-binding peptides (AuBP1 and AuBP2) showed that only one of them (AuBP1) retained the same adsorption behavior in both circular and linear forms while the second analyzed sequence (AuBP2) lost its high gold binding affinity in the linear form. This difference was explained due to observed (based on CD spectroscopy and modelling) structural change in the molecular conformations between the cyclic and linear versions, however, the details on molecular biases of the peptide function were not revealed (Hnilova et al. 2008).

The presented examples show that peptides function in very complicated fashion and frequently mutations in their sequence lead to unpredictable results that may additionally be modulated by the binding environment at the material interface. As a general conclusion, many structure-function mutagenesis studies identify a limited number of amino acids as critical, suggesting that chemical composition of the peptide is sufficient for its function. However, some studies assume also that the critical residues directly bind the material surface, while neighboring locally modulate the binding environment, and peptide affinity to a target is not only driven by strongly binding residues but also by peptide molecular conformation. Moreover, short peptides, unlike natural proteins, do not generally fold into well-defined three-dimensional structures and can often adopt multiple structural conformations in solution due to high polypeptide chain flexibility. This might result in peptides with identical chemical composition having many different "active" structural conformations (Tamerler et al. 2010). Thus, there is no general rule that could explain the principles of the function of material binding peptides. Each system is unique and has to be studied individually.

## 1.9 Post-selection engineering of material binding peptides

Although biopanning techniques have been proved to be successful for selection of peptides that bind specifically to inorganic materials, the identified sequences might not be fully optimal for their function. It should be noted that the size of the combinatorial libraries is usually not sufficient to cover all the potential variants what may theoretically limit possibility of selection of the best binding sequences. Thus peptides selected in biopanning can be considered as “first generation peptides” that can be introduced to subsequent evolution cycles and further engineered to “next generation peptides” with improved function.

One possible way to achieve this goal is using knowledge-based approaches such as site-directed mutagenesis or de novo design utilizing bioinformatics tools (Oren et al. 2007, Schrier et al. 2011). However, planning of successful engineering and optimization strategies with these methods requires detailed understanding of the molecular mechanism of the peptide-target surface interaction, structural data about peptides at the interface, and molecular architecture of the substrate at atomic scale. In many cases this information is not available. Therefore, knowledge-based approaches are still rather seldom applied and there are only few examples of studies describing their successful use (Masica et al. 2010, Oren et al. 2007, Schrier et al. 2011).

Another approach for improving affinities of solid-binding peptides is the multimerization of binding units. This strategy has been observed in many natural solid-binding proteins, for instance, anti-freeze proteins (Jia & Davies 2002), silaffins (Kröger et al. 2002), collagens (Shoulders & Raines 2009), lustrin (Shen et al. 1997). Studies revealed that these proteins contained multiple repeats of the same peptides, which functioned in a cooperative way and increased the strength of interactions with their targets due to the avidity effect (Mammen et al. 1998). The same concept has been also applied in material science to design artificial multivalent peptide systems. Such systems can be created by arranging binding units into tandem repeats (Seker et al. 2009) or by displaying them separately in many copies on molecular scaffolds that can provide multivalency, for example, multimeric proteins (Sano et al. 2005a), phage mimicking structures (Terskikh et al. 1997), and dendrimers (Helms et al. 2009). Both types of multivalent peptides can be created by fusing them to proteins using genetic engineering, by chemical synthesis, or by crosslinking together individual peptide units.

In the literature there are many examples of studies investigating interactions of multivalent peptide systems with solid materials that show positive correlation between peptide's binding affinity and number of peptide repeats. Such an effect was observed, for instance, when a titanium binding peptide was engineered to a tetravalent form with its binding affinity increasing 10 times compared to the monovalent form (Khoo et al. 2010) or when a collagen binding peptide was displayed in five copies using a dendrimer scaffold (100-fold better affinity was achieved) (Helms et al. 2009). An exceptionally large increase in binding affinity (4 orders of magnitude) was measured for another titanium binding sequence (minTBP-1) displayed on ferritin in 24 copies (Sano et al. 2005a). On the other hand, in some

studies, increasing the number of repeats did not enhance binding, as it was observed, for example, for 3-repeat tandem silica or platinum binding peptides. The authors suggested that one of possible explanations of this behavior were conformational changes between single and multiple repeat polypeptides that are unfavorable for adhesion (Seker et al. 2009). It was also found that for some peptides there is an optimum for the number of binding units in linear tandem repeats, for instance,  $n=5$  for gold binding peptide, and that further multimerization leads to decrease in binding (T. Kacar et al. 2009).

The examples of different functioning of some multivalent peptide systems suggest that simply increasing the number of the binding units does not always enhance the affinity. The affinity of a multimer might be affected by many structural factors, such as its overall three-dimensional structure, the way of connecting individual binding units, or by various parameters of the binding environment at the material interface. Thus, detailed understanding of the structure-function relationship of mono- and multivalent peptides systems is essential for successful engineering of their function.

## **1.10 Experimental methods to study peptide binding to solid materials**

Because of the great significance of inorganic-binding peptides in potential novel nanotechnological applications, a much effort has been put on the development of experimental techniques and models that enable the investigation of peptide-surface interaction phenomena. More specifically, to measure peptide adsorption, binding affinity, surface coverage, and kinetic parameters of peptide-surface interaction, as well as to predict and understand the peptide conformation at the interface (Gray 2004).

The simplest methods to measure peptide adsorption to inorganic surfaces include assays based on enzyme-linked immunosorbent assay (ELISA) and fluorescence. Both techniques are suitable for binding investigations of peptides displayed on phages, fused to a protein or other molecular scaffolds, or existing in a free form (discussed in more details, paragraph 1.7). In ELISA peptide binding is quantified by the enzymatic activity of a reporter enzyme that is usually conjugated with specific antibody recognizing a protein fused with the peptide (for example, one of phage coat proteins in case of peptides displayed on phages). The reporter enzyme can be also linked directly to the peptide, and the binding of the fusion molecule can be detected without using antibodies. Additionally, the peptide-fusion proteins can be used together with synthetic peptides in competition ELISA assays which are robust methods to investigate the effects of structural changes in the peptide sequence.

Fluorescence assays and microscopy, similarly as ELISA, require labeling of peptides with a reporter, in this case with a fluorescent probe or a protein (for example GFP), and allow for measurement of adsorbed labeled molecules directly on the surface of a substrate. Fluorescence microscopy can additionally provide



useful information about specific location of bound peptides on the substrate what might be especially important when surfaces composed from many different materials are used, for instance micropatterned surfaces (B. T. Kacar et al. 2009).

More detailed information about the process of peptide adsorption on solids can be obtained by label-free techniques, such as quartz crystal microbalance (QCM) (Höök et al. 1998) and surface plasmon resonance (SPR) spectroscopy (Bakhtiar 2012). The QCM monitors a decrease in resonance frequency of a quartz crystal coated with a target material upon biomolecules adsorption and provides quantitative information about the mass of adsorbed biomolecules (including bound water molecules). Additionally QCM can be also used to analyze viscoelastic properties of adsorbed biomolecule films (by monitoring a parameter called the dissipation factor). SPR, on the other hand, quantifies the amount of mass adsorbed to a surface based on changes in refractive index. It allows for in situ following of biomolecule adsorption, and can be utilized for determination of peptide binding kinetic parameters, however since the measurement is based on monitoring of adsorption and desorption rates it does not take into account possible rebinding of biomolecules to the surface. QCM and SPR are suitable for analysis of the binding under various experimental conditions (peptide concentration, pH, and ionic strength), but they can be only be applied for studies with a limited number of materials, for example, gold and silver in case of SPR. The use of other materials is possible but it requires coating of the quartz crystals (QCM) or chip surfaces (SPR) with the substrate which may be very challenging (especially obtaining ultra-thin coating layer for the SPR surfaces).

Problems with obtaining the correct coating in measurement devices with a substrate material can be overcome with the use of ellipsometry (Tompkins & Irene 2005) or atomic force microscopy (AFM) (West 2006). Ellipsometry is an optical technique that measures the change of polarization of a light beam upon reflection off a sample (protein or peptide), correlates it to the sample's thickness and refractive index, and provides information about the mass (dry mass without water molecules) of adsorbed biomolecules on the substrate surface. The method is especially useful for verifying the binding data obtained with biochemical techniques or QCM. AFM provides also comprehensive information about a peptide binding on a substrate. Although it is not suitable for quantitative analysis, it allows for imaging (also in liquid environment) of biomolecules adsorbed on a surface and monitoring their assembly processes (Yu et al. 2008). AFM can be also applied for the measurements of the interaction force between peptide and a target surface (it can resolve the interaction of a single molecule with a substrate) with pico-Newton resolution (Krysiak et al. 2014).

Other surface analytical techniques, such as X-ray photoelectron spectroscopy (XPS) (Yin et al. 2012) and time-of-flight secondary ion mass spectroscopy (TOF-SIMS) (Suzuki et al. 2007), have also been used to probe adsorbed biomolecules, but the analysis with these methods must be done in the dried state in an ultrahigh vacuum environment what often changes the structure of adsorbed biomolecules.

Investigation of the binding mechanism and structure-function relationship of material binding peptides, besides information about peptide adsorption param-

ters, require also knowledge of their three-dimensional structures in solution and when adsorbed on the surface (more details, paragraph 1.8). However, polypeptide chains tend to be flexible and adopt many different conformations (often depending on the molecular environment at the interface), therefore, obtaining structural information is usually challenging mainly due to insufficient experimental techniques that are not able to follow in detail the molecular events at the interface, and lack of data about material's surface properties at atomic scale. Nevertheless, some valuable information about the secondary structure of peptides in solution can be obtained with the using circular dichroism (CD) spectroscopy (Kelly & Price 2000), and adsorbed at interface by attenuated total reflection Fourier transform infrared spectroscopy (ATR-FTIR) (Haris & Chapman 1995). More quantitative information on molecular conformations of peptides can be obtained by solid and liquid-state nuclear magnetic resonance (NMR) spectroscopy (Mirau et al. 2011), but the technique is often difficult to apply because of high background signals from the solid material.

As mentioned above, the existing experimental techniques are usually not sufficient for the complete investigation of the peptide-solid interactions, thus, experimental observations are often supported by computer modeling based on molecular dynamics and mechanics (Senn & Thiel 2009). The computational studies have been especially helpful to test the peptide's conformational changes, as well as the effects of mutations, and to simulate the molecular interaction mechanisms at the peptide solid material interface. Modelling studies have been applied, for example, in the investigation of peptide binding to materials such as quartz (Oren et al. 2010), titanium (Schneider & Ciacchi 2012), carbon nanotubes (Su et al. 2007), and gold (Tang et al. 2013). However, in many cases modeling simulations are carried out in simplified environments, and only for defined (crystalline) substrates that might not represent fully the real situations. Furthermore, the results of modeling are not always confirmed by experimental data; thus, often remain speculative (Ramakrishnan et al. 2014).

## 2. Aims of the study

The overall aim of this work was to apply molecular biomimetic approaches based on directed evolution to find and study biomolecules that recognize and interact specifically with surfaces of inorganic materials. The studies focused on understanding fundamental aspects of specific peptides-solid materials interactions, as well as on how these interactions can be controlled and tailored. Finally, it was investigated how engineered material-binding biomolecules can be utilized for practical nanotechnological applications. More precisely, the aims were:

- To select from a combinatorial peptide phage display library, peptides that specifically bind to diamond-like carbon (DLC), and to characterize in detail their binding properties in different display contexts i.e. using phages and fusion proteins (publication I)
- To gain a basic understanding what factors define affinity of selected diamond-like carbon binding peptides and what is the relation between the peptide primary sequence (chemical composition), three-dimensional structure and function (publication I and II)
- To study if the affinity of the DLC binding peptides can be increased by their multimerization, and investigate how structural design of multimeric peptides affect their adsorption properties and kinetic effects during the binding (publication III)
- Finally, to utilize the developed peptides in nanotechnological applications for functionalization of the DLC surface and for controlling properties of a colloidal form of DLC (publication III).

## 3. Materials and methods

### 3.1 DLC general information

Diamond-like carbon (DLC) is a common term describing hard carbon coatings having similar mechanical, optical, electrical, and chemical properties to diamond but different dominant crystalline structure. DLC compared to crystalline diamond composed of tetrahedral (sp-3 bonded) carbon atoms is amorphous material consisting of a mixture of carbon atoms connected with sp-2 and sp-3 types of bonds. DLC coatings can be doped with other elements, for example, hydrogen. DLC films are divided according to their hydrogen content to non-hydrogenated amorphous carbon (a-C) and amorphous hydrogenated carbon (a-C:H) coatings. Non-hydrogenated DLC coatings containing high amount of diamond bonds (sp-3 fraction up to 85%) are called tetrahedral amorphous carbon coatings (ta-C) (Hauert 2004).

DLC coatings have excellent optical, electrical, and tribological properties, high hardness, corrosion resistance, chemical inertness, and biocompatibility. Combination of such outstanding properties in one material is rather uncommon, thus, DLC has been used in a wide range of multifunctional industrial applications including razor blades, engine parts exposed to high friction and wear, scratch-resistance glass, magnetic hard discs, low friction aerospace coatings (Erdemir & Donnet 2006), and biomedical applications, for example, as a coating on implants (Roy & Lee 2007). Although DLC films have excellent material characteristics development of many industrial and biomedical applications such as biomedical implants, sensors, and lubrication require also understanding and controlling its surface properties. Functionalization of DLC coatings through biomolecules such as peptides developed in directed evolution process that are able to recognize DLC and bind to it specifically with high affinity is one of the approaches to achieve this goal.

DLC films are produced by various methods based on chemical vapor deposition (CVD) or physical vapor deposition (PVD). The structure (ratio between sp-2 and sp-3 bonds of carbon atoms), hydrogen content, and physico-chemical properties of DLC may be adjusted and controlled depending on the deposition tech-

nique, parameters, and carbon source applied, thus allowing tailoring the film properties for particular applications. For example films with a high proportion of sp<sup>2</sup>-bonded carbon atoms tend to be relatively soft (resemble graphite in mechanical tests) while films with more sp<sup>3</sup>-bonded carbons are more diamond-like, therefore they are super hard and possess superior mechanical properties. Hydrogenated DLC films have similar hardness to a-C DLC but they exhibit very low friction and wear coefficient (Erdemir & Donnet 2006).

### 3.1.1 Information about DLC coating used in this work (publication I–III)

The DLC coating (brand name: BALINIT DLC) used in the experimental work described in this thesis was obtained from a commercial supplier (Oerlikon Balzers). BALINIT DLC is an amorphous hydrogen containing (a-C:H, hydrogen content 15–20%) carbon coating prepared by plasma-assisted chemical vapor deposition (PACVD) process. The coating was applied on blocks made of stainless steel (martensitic AISI440B quenched) with the thickness around 2  $\mu\text{m}$ . Blocks containing wells were used for panning experiment and phage binding analysis (Figure 4a), pins for binding studies with the peptide-AP fusion proteins (Figure 4b), big disc for ellipsometry (Figure 4c), small discs for binding and competition studies between synthetic peptides or multivalent DLC binding peptides with pep\_L-AP fusion protein (Figure 4d). All DLC surfaces were cleaned before each experiment with 2% Hellmanex II (Hellma GmbH & Co. KG, Germany), rinsed with MilliQ water and ethanol, and finally dried under nitrogen.

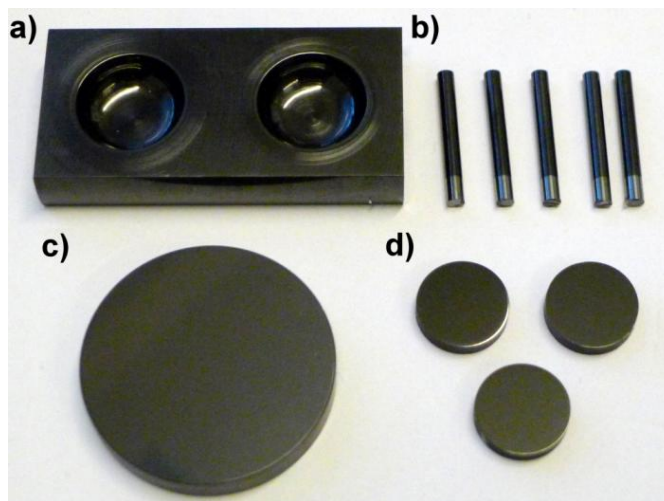


**Figure 4.** DLC surfaces used in the binding studies with DLC binding peptides: (a) panning experiment and phage binding analysis, (b) peptide-AP fusion proteins, (c) ellipsometry, (d), competition studies with synthetic peptides/multimers and pep\_L-AP fusion protein.

## 3.2 Phage display

Phage display is a selection technique in which a library of peptide variants is expressed on the surface of bacteriophage particles (general information about the technique, described in introduction paragraph 1.5). Most of the phage display systems are based on the engineered M13 bacteriophage. Wild type M13 phage is a filament (65 Å in diameter and 9300 Å in length) (Figure 5). The virus consists of a circular single stranded DNA (6407-base) genome coated with about 2700 copies of a major coat protein, pVIII, and five copies of each of the four minor coat proteins (pVII and pIX located on one end, and pIII and pVI on the other end of the virus particle). The most common approach to utilize phage for display purposes is to fuse peptide sequences (up to 50 amino acids) to the amino terminus of pIII protein. The system based on pIII protein allows for pentavalent display and is generally utilized for discovery of high affinity binders in contrast to the major coat protein systems (pVIII) in which each phage displays multiple copies of peptides. The multiple display often causes an avidity effect (cooperative binding of individual peptide units) which limits the possibility of selection of high-affinity binders (Kehoe & Kay 2005).

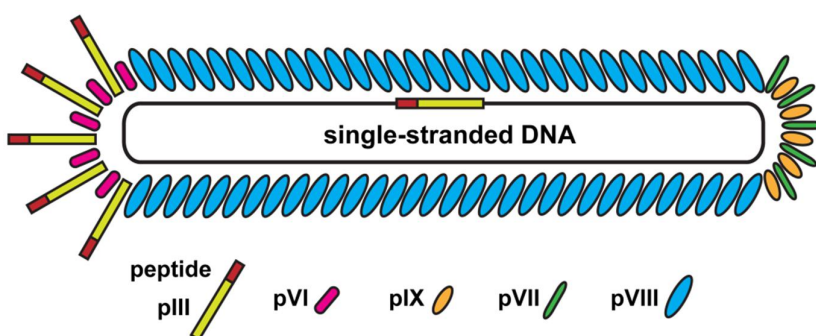


**Figure 5.** Schematic of the M13 phage. The minor coat protein (pIII, indicated in yellow) is used to display peptides (red). The gene encoding pIII fusion protein is indicated with the same color marking.

### 3.2.1 Biopanning against DLC surface (publication I)

Peptides binding to DLC surfaces were selected from a commercial M13 bacteriophage library (Ph.D-12 phage display library), obtained from New England Biolabs. The library contains phages displaying random 12-mer peptides fused to the pIII protein and have a complexity on the order of  $10^9$  independent clones (New England Biolabs Manual, Version 1.2, 2014). The biopanning process was performed according to instructions provided by the supplier. Three selection cycles were carried out and after the last round the peptide sequences of randomly picked phage clones were determined by DNA sequencing.

### **3.3 Phage particle binding studies (publication I)**

#### **3.3.1 Phage titer analysis (plaque assay)**

Titer analysis of selected phages binding to DLC was performed using  $2 \times 10^{11}$  pfu of amplified single phage clones and the same DLC surfaces as used in the biopanning. Wild type phages (without displayed peptides) were used as negative controls. Phage titer was determined based on the number of plaque forming units (pfu) in the monolayer bacterial culture grown on an agar plate.

#### **3.3.2 Phage ELISA**

The ELISA assay of selected phages binding to DLC was performed using  $10^{12}$  pfu of amplified single phage clones and the same DLC surfaces as used in the biopanning. Phage clones bound to the DLC surface were detected using an anti-M13 monoclonal antibody conjugated to horse radish peroxidase (HRP) (GE Healthcare). The binding of phages was quantified based on the amount of the product of HPR enzymatic reaction recorded by measuring absorbance at 405 nm. The wild type phage (without displayed peptides) was used as a negative control.

### **3.4 Fusion proteins of DLC binding peptides and alkaline phosphatase (publications I–III)**

#### **3.4.1 General information**

Alkaline phosphatase (EC 3.1.3.1) is a dimeric enzyme (hydrolase) that is widely used as a reporter in immunoassays for removing inorganic phosphate groups from various types of molecules. AP can be easily fused to other molecules without changing its enzymatic activity; hence it was combined together with DLC binding peptides and used as a reporter to study their adsorption properties, and to compare their binding affinities (publication I). Peptide-AP fusion proteins were also utilized to investigate functional effects of sequence and structural changes (publication II), and multivalency (publication III).

#### **3.4.2 Construction, expression and purification of the fusion proteins**

The constructs for expression of peptide-AP proteins were prepared by recombinant DNA technology. The sequence encoding a DLC binding peptide was fused to N-terminus of bacterial alkaline phosphatase and a 6xHis tag was added to its C-terminus (for affinity purification). The sequence encoding the flexible linker (GGGPTSGGG) was inserted between peptide and AP in order to separate two components. DNA constructs containing the sequence of 12-mer peptides and linker were assembled using sense and antisense synthetic oligonucleotides (Sigma-Aldrich), the inserts encoding the longer peptides, and the bacterial AP

gene from were obtained as synthetic genes (GeneArt, Germany). Both DNA constructs were assembled together and inserted to an expression vector (pGBtacLacZ) using the “golden gate” cloning method (Engler et al. 2008). A negative control for the peptide-AP fusion was prepared using an identical construct which only lacked the inserted peptide sequence. The expression vector (Figure 6) contained the tac promoter (induced by isopropyl  $\beta$ -D-1-thiogalactopyranoside, IPTG), pelB signal sequence (for export to periplasmic space) lacIq repressor, and ampicillin resistance gene. The fusion protein gene was expressed in *E. coli* RV308 production strain. The periplasmic fraction containing produced protein was isolated by freeze/thaw cycles. The protein purification was carried out by Immobilized-Metal Affinity Chromatography (IMAC) using a Ni-column (GE Healthcare) and a BioLogic DuoFlow chromatography system (Bio-Rad Laboratories). Purified proteins were analyzed for size and purity by SDS-PAGE (Bio-Rad Laboratories) and immunoblotting using anti-AP (Invitrogen) and anti-HIS tag (Abcam) antibodies.

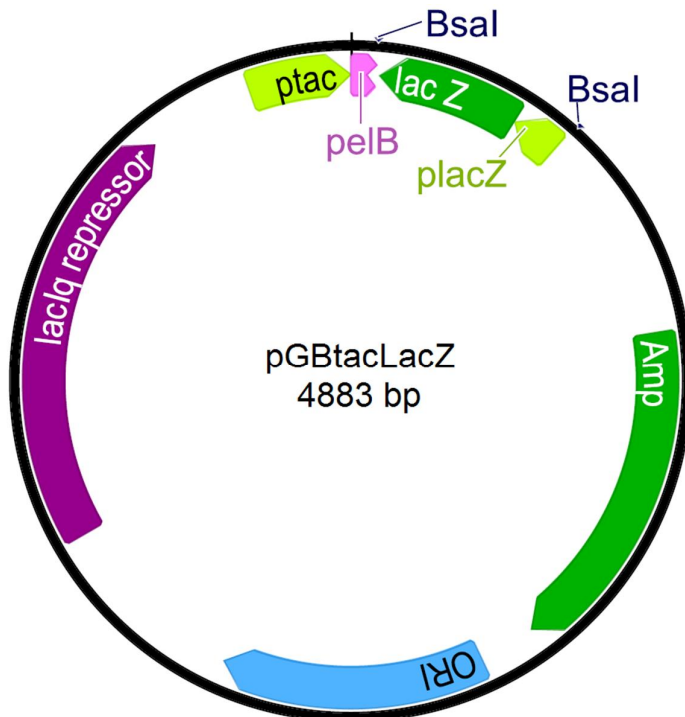


**Figure 6.** Map of pGBtacLacZ expression vector. During “golden gate” cloning (Engler et al. 2008) lacZ gene (for blue/white colony screening) and Bsal sites are removed and replaced with the insert containing peptide-AP synthetic gene. Positive clones (possessing plasmid with the insert) grow in white colonies.



### **3.4.3 Quantification of surface binding of peptide-AP fusion proteins (AP enzymatic assay) (publication I)**

The AP enzymatic assay was used to compare the binding to DLC surface of different peptide-AP fusion proteins. During the binding experiment the fusion proteins were first incubated on the DLC surface, loosely bound molecules were discarded through washing and the amount of the fusion protein bound to the DLC was quantified by measuring the enzymatic activity of AP. The enzymatic assay was carried out by incubating the AP substrate, p-nitrophenyl phosphate (pNPP) (Sigma-Aldrich), diluted in diethanolamine-MgCl<sub>2</sub> buffer (Reagena, Finland) on the DLC surface. The solution containing product of the enzymatic reaction, p-nitrophenol (pNP), was transferred to microtiter plate and quantified by measuring absorbance at 405 nm. The amount of protein adsorbed to the DLC surface was determined using a standard curve of AP activity prepared for each fusion protein.

### **3.4.4 Simultaneous competition assay (publication II and III)**

The simultaneous competition assay was developed to investigate how mutations (publication II) and multimerization (publication III) of the binding sequence (pep\_L) affect on its function (binding affinity). During the competition experiment synthetic peptides (described in paragraph 3.5) (containing mutations of the pep\_L) and pep\_L-AP (reporter protein) competed simultaneously for the adsorption to DLC surface. The concentration of the fusion protein was kept constant while the amount of the synthetic peptides was gradually increased. The competition efficiency of synthetic peptides was quantified by measuring the amount of the fusion protein that remained bound on the surface using AP enzymatic assay (described in paragraph 3.4.3).

### **3.4.5 Sequential displacement competition assay (publication III)**

The sequential displacement experiments were designed to investigate the potential role of kinetic effects in the binding of multivalent DLC binding peptides. During the assays solutions of pep\_L or multivalent peptides (MP) and the pep\_L-AP reporter were applied on the DLC surface sequentially i.e. the DLC surface was first incubated either with peptide or fusion protein solution and then protein was applied on the surface coated previously with peptides, and peptides were applied on the surfaces coated previously with the fusion proteins respectively. The displacement efficiency was evaluated by quantifying the amount of the reporter protein that remained bound on the surface after the competition based on the AP enzymatic assay (described in paragraph 3.4.3).

### 3.5 Synthetic peptides

Synthetic peptides (purity >95%) used in the competition assays (paragraph 4.7) and for the synthesis of multivalent forms of DLC binding peptides (described in paragraph 3.6) were purchased from a commercial supplier (GenScript). Stock solutions were made and their concentrations were determined by amino acid analysis (Amino Acid Analysis Center, University of Uppsala, Sweden). UPLC was then used to make standard curves and concentration determinations using an ACQUITY UPLC (Waters) system, and a C18 (1.7  $\mu\text{m}$ ) column (2.1 x 50 mm) (Waters) with a water/acetonitrile mobile phase with 0.1% trifluoroacetic acid.

### 3.6 Synthesis of multivalent peptides (publication III)

Multivalent peptides used in competition experiments (paragraph 4.8) and for stabilization of the DLC flakes (paragraph 4.9) were produced by chemical conjugation of maleimide-functionalized crosslinkers with the sulfhydryl group of the C-terminal cysteine of peptide pep\_L-Cys (detailed information about synthesis is found in the supporting information of publication III).

Synthesized peptide conjugates were purified using reversed-phase HPLC, on a semi-preparative Vydac C4 column (1 x 25 cm). The purity of peptide samples was analyzed by UPLC (as above) while their molecular masses by MALDI-TOF Autoflex II (Bruker Daltonics, Germany).

### 3.7 Preparation of colloidal form of DLC (DLC flakes) (publication III)

DLC flakes were prepared by depositing an about 100 nm thick DLC film on a layer of NaCl crystals supported on a glass surface. The salt was dissolved in water which led to a spontaneous delamination and cracking of the DLC film into a powder consisting of flake-like particles of approximately 10–100  $\mu\text{m}$  size (Figure 7a). DLC flakes were collected by centrifugation, washed to remove traces of salt, and resuspended in water. The size of the flakes was reduced (to below 5  $\mu\text{m}$ , Figure 7b–c) by the application of mechanical energy by ultrasonication using tip sonicator.

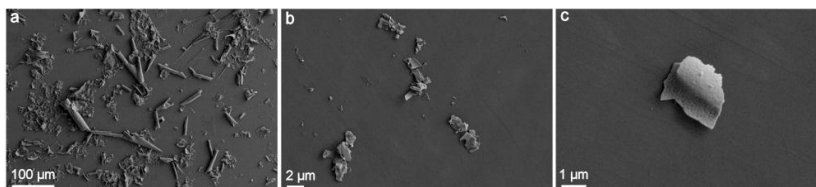


**Figure 7.** Scanning electron microscopy image of DLC powder: (a) flakes after delamination from salt crystals and (b) after sonication, (c) individual DLC flake.

### **3.8 Zeta ( $\zeta$ ) potential measurements (publication III)**

Zeta potential measurements of the DLC flakes (and the DLC flakes modified with peptides) were carried out using Nano ZS Zetasizer (Malvern Instruments) and the disposable capillary cells at 25 °C. Fresh samples were prepared before each measurement.

## **4. Results and discussion**

### **4.1 Selection of peptides from the PhD-12 phage library (publication I)**

28 phage clones were randomly chosen after the third round of the panning of the Ph.D-12 phage display library on DLC and their peptide encoding DNA, was sequenced. In the pool of sequenced clones 18 peptides were novel (named DLCBP1-18, Table 2). Interestingly, 8 out of the 18 novel sequences were longer (indicated by the suffix "L" in their names) than the 12 amino acids expected in the PhD-12 library. The remaining 10 of selected peptides were identified as target unrelated (named DLCBP(TUP)1-10, Table 3) because they have been already described in other panning studies as binders to various targets unrelated to DLC (more information about TUP described in paragraph 1.5.2).

**Table 2.** Sequences and chemical properties of peptides selected from the Ph.D.-12 library in biopanning against DLC surfaces (publication I).

Name	Amino acid sequence	Length <sup>a</sup>	GRAVY <sup>b</sup>	Net charge <sup>c</sup>	pI <sup>d</sup>
DLCBP1	YLTQKSPPYQG	12	-1.367	+1	8.50
DLCBP2	KHYWPSTPLT	12	-0.592	+1	8.60
DLCBP3	WTCQKAPCVARV	12	0.158	+2	8.96
DLCBP4	FKMPQTMVMRTK	12	-0.508	+3	11.17
DLCBP5	GFNSAYKQMRD	12	-1.375	+1	8.59
DLCBP6	LPYPQHPGSLGR	12	-0.942	+1	8.75
DLCBP7	FPPSWLAASNRP	12	-0.425	+1	9.75
DLCBP8	LPPQHPW/DNSKH	12	-1.958	0	6.92
DLCBP9	HSPVLKTPSTHA	12	-0.558	+1	8.76
DLCBP10	YSWHTDPKTLKR	12	-1.767	+2	9.70
DLCBP(L)11	HFYPGANRSTTQGGGSANLHQTAASAKNSAPQKSENKRVPFYSHSRTRENNRSIYTA	57	-1.260	+6	10.61
DLCBP(L)12	FHLNSNPQLQRSGGGPNLHHAAATASYSSTPKSENKRVPFYSHSPPRPSGVIGKTQP	56	-0.930	+5	10.55

DLCBP(L)13	KYTTDLPNRSRWVEVRPNLHQKANQTTVTSEPOSENKRVPFYSHSKLGGKKGCSDSQ	57	-1.321	+5	9.63
DLCBP(L)14	GNLHHQSKYATNHSQPKSENKRVPFYSHSAPRADKKPKDKKG	42	-1.833	+6	10.09
DLCBP(L)15	TDQLRPNLHHATSNASSSSASKSENKRVPFYSHSRHQITPPSITYR	46	-1.172	+4	10.42
DLCBP(L)16	VPLPPPPLTSVQGGGSHSTSKYYNPPAKKSENKRVPFYSHSRSPNMIRSLAYM	53	-0.925	+6	10.21
DLCBP(L)17	AGWSLHNINSRPGGGSANLHHYTSYKESAEYKSENKRVPFYSHSRQTTAASPTKSR	57	-1.282	+4	9.77
DLCBP(L)18	EDATARIDRRFGEVRPNLHHYQHQQKPEYAAKSENKRVPFYSHSAIPMINTSKNVSL	57	-1.340	+2	9.31
CNTB	LLADTTTHRPWT	12	-0.800	0	6.92

<sup>a</sup> amino acids, <sup>b</sup> GRAVY – grand average of hydropathicity, calculated based on (Kyte & Doolittle 1982); <sup>c</sup> net charge at pH 7, <sup>d</sup> pI, isoelectric point. GRAVY and pI value were calculated using Protparam program <http://web.expasy.org/protparam/>

## **4.2 Features and analysis of sequences of selected peptides (publication I)**

Sequences of selected the 12-mer (DLCBP1-10) and long peptides (DLCBP(L)11-18) were positively charged (except DLCBP8 and CNTB) at neutral pH (Table 2), had pI values between 6.92 and 11.17, and hydrophilic character based on their GRAVY index (Kyte & Doolittle 1982). Sequence alignment of selected 12-mer clones did not show any consensus sequence.

An unexpected result of the panning experiment was the selection of phages displaying long (42–57-mer) peptides. According to the supplier the long sequences are present in the Ph.D-12 library in small percentage (< 1%) due to errors in a cloning step (ligation) during library preparation. The DNA of those clones contain more than one copy of the insert encoding the random peptide, the short linker connecting peptide with pIII phage protein, and a part of the leader pIII protease sequence combined together in forward and reversed orientation (Figure 8). Incorporation of such an insert in the phage genome results in peptide sequences longer than 12 amino acids are displayed on the phage (details about putative mechanism of the generation of the long peptides in the library were described in publication I). Although long peptides can be considered as by-products in the library, they were selected in the panning experiment designed to identify DLC binding peptides. What is more, the long sequences were enriched to about 30% of all selected clones (to 44% excluding DLCBP(TUPs)). Therefore, their selection was considered as significant and they were further studied along with the standard 12-mer peptides.

There are many potential reasons why longer peptides were selected as binders to DLC. For example, they can have better possibilities for attaining optimal structural conformation for favorable interactions with the target. Another reason may be that longer peptides possess more “binding sites” to the target which leads to multivalent and cooperative binding. Moreover sequences analysis of selected peptides (short and long) showed that almost all of them had positive charge (at pH 7) and that the long peptides had generally more of positively charged residues than the short peptides. This observation may indicate that positive charge could be one of the factors involved in the binding mechanism of peptides to DLC.

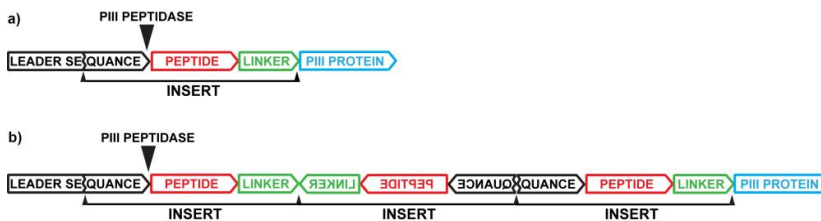


**Figure 8.** Schematics of the cloning of DNA sequence encoding random peptide to the phage genome. (a) Normal case (phage displaying 12-mer peptide), the DNA insert containing: the C-terminal part of the pIII leader sequence (black), a random peptide (red), and linker (green) is incorporated between N-terminal part of the pIII leader sequence and the sequence coding N-terminal part of the pIII minor coat protein (blue). (b) When a long peptide sequence is displayed on the phage; several DNA parts containing the 12-mer insert (as in case “a”) in forward and reversed orientation are combined together and whole fragment is fused with the phage genome in the same places as in the normal case.

The sequences identified as TUPs (Table 3) were examined using the SAROTUP tool (Huang et al. 2011) and Google internet seeker ([www.google.com](http://www.google.com)). Analyzing of the number of results in Google when a TUP sequence was used as a query indicated how frequently the sequences have been mentioned before in other studies. The analysis showed that selected TUPs have been described as binders to various targets (organic and inorganic) unrelated to DLC (Table 3). However, one of the target unrelated peptides has been previously described (among other targets) as a carbon nanotube binding peptide (CNTB) (Su et al. 2006). Since carbon nanotubes and DLC are structurally related materials, the peptide was chosen for further analysis, and the remaining TUPs were neglected.



**Table 3.** Sequences and analysis of target unrelated peptides selected in biopanning against DLC surface (publication I, supplementary information)

Name	Sequence	Examples of targets found in MIMO DB database	NR <sup>a</sup>
DLCBP(TUP)1	AAPLGTHPSMHP	Anti-DENV2-NS1 polyclonal antibody immunoglobulin G	6
DLCBP(TUP)2	ATWSHHLSSAGL	Anti-IL-2 monoclonal antibody 3B3	58
DLCBP(TUP)3	TMGFTAPRFPHY	TIMREX SLP30 primary synthetic potato - shape graphite Glycine receptor subunit alpha-1 Protein tonB Polycrystalline hydroxyapatite Germanium oxide Troponin I, cardiac muscle Interleukin 2	775
DLCBP(TUP)4	TPTDNSVFAAS	IGF1R protein	0*
DLCBP(TUP)5	HYSRYNPGPHPL	Polymethylmethacrylate (PMMA)	7
DLCBP(TUP)6	MPAVMSSAQVPR	Polyethylene	114
DLCBP(TUP)7	SHALPLTWSTAA	Wound-healing matrix (Integra®) Zinc-terminated sides of single-crystalline ZnO (0001)	92
DLCBP(TUP)8	GTPPMSPLVSRV	Periplasmic binding protein BtuF	2
DLCBP(TUP)9	SVVPSKATWGFA	Porcine aminopeptidase N (pAPN)	7
DLCBP(TUP)10 (CNTB)	LLADTTHRPWT	Anti-MUC1 monoclonal antibody (PR81) Hydroxyapatite Protein tonB Anti-EGFR monoclonal antibody (12H23) Umbilical endothelial cells Titania (TiO <sub>2</sub> ) nanoparticles Semiconductor crystalline surface ZnSe(100) Single-walled carbon nanotubes	1160

<sup>a</sup> NR – number of results found using Google seeker when peptide sequence was used as a query

\* – the sequence was not found by Google but reported in the PhD thesis (Wirtz 2009)

### 4.3 Phage binding analysis by titer and ELISA (publication I)

Panning results were verified by analyzing binding of single phage clones using two independent methods – phage titer analysis and phage ELISA. In the titer analyses, phage bound to DLC were eluted from the surface, and then their amount was analyzed based on the plaque assay (material and methods, paragraph 3.3.1) while in ELISA bound phages were detected directly on the surface using the anti-M13 antibody conjugated to horse radish peroxidase (HRP), without the need of phage elution (material and methods, paragraph 3.3.2).

Both methods demonstrated that phages displaying the long peptides (DLCBP11(L)–14(L)) showed orders of magnitude better binding to DLC compare to phage displaying 12-mer peptides (DLCBP1–8 and CNTB) and control wild type (WT) phage (without peptide). The performance of all 12-mer peptides in the titer assay was similar to the WT control and CNTB whereas in ELISA DCLBP3, DLCBP7 and CNTB showed approximately 3 times higher binding than the wild type phage (Figure 9).

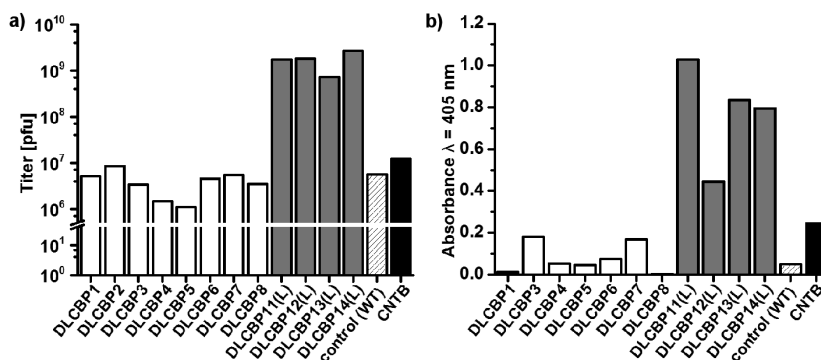


**Figure 9.** Phage binding to DLC determined by (a) titer and (b) ELISA (publication I).

The results of the binding studies using single phage clones indicated that the selection of high affinity DLC binding peptides was successful. However it should be noted that peptides connected to phage are displayed in 5 copies and as a consequence of multivalent display the affinity of phage might be higher compare to a single peptide due to cooperative peptide binding (avidity effect) (Mammen et al. 1998). Moreover the function of a peptide (affinity to the target) might be depended on the presence fusion partner i.e. pIII phage protein. In other words the peptide may lose its binding ability when not displayed on a phage.

#### 4.4 Peptide binding analysis with AP fusion proteins (publication I)

A fusion protein approach was used to study the adsorption properties of selected peptides in a different context compared to the phage binding environment. Based on the phage binding analysis four peptides were chosen: DLCBP11(L), DLCBP14(L), DLCBP3, and CNTB. These were fused to bacterial (*E. coli*) alkaline phosphatase (AP) via a peptide spacer (GGGPTSGGG) using genetic engineering. In the resulting bi-functional fusion protein, the peptide was responsible for binding to DLC, the AP functioned as a reporter enzyme to monitor the amount of fusion protein adsorbed on the DLC surface while the linker provided flexible connection and proper separation between two domains. AP is a dimeric protein, thus the fusion protein in its active form allowed for divalent display of the DLC binding peptide (Figure 10a–b).

Binding experiments demonstrated that only DLCBP11(L) retained its binding affinity to DLC as a fusion partner of the AP (Figure 10c). Based on the binding curve the adsorption parameters of the DLCBP11(L)-AP fusion were calculated according to the Langmuir isotherm model (Langmuir 1918) and the binding constant ( $K_d$ ) of  $63 \pm 14$  nM was obtained. The results were additionally verified with ellipsometry, an optical technique, which is independent of enzymatic activity (publication I). Other peptides that performed well when displayed on phage (DLCBP14(L), DLCBP3, and CNTB), when fused to AP, showed only a binding that was comparable with the background binding of the control AP without fused peptide (Figure 10d). As mentioned before, this context-dependent binding behavior, observed also in other studies for various material binding peptides (Sano et al. 2005a, Bastings et al. 2011, Terskikh et al. 1997), might be related to avidity effect of pentavalent peptide display on phage particles, hence reducing number of peptide copies from five (phage) to two for the dimeric peptide-AP fusion proteins can lead to weaker binding affinity. What is more, when comparing the measured affinity of the peptide-AP fusion protein with other systems it should be noted that the affinity of the dimer is likely to be higher than the individual peptide due to the possibility of cooperative binding. However, the binding affinity determined for DLCBP11(L)-AP was in the nanomolar range that is considered to be very high and is similar to other high affinity binding solid material binding peptides (Hnilova et al. 2012b, Gronewold et al. 2009, Tamerler et al. 2006, Chen et al. 2009).

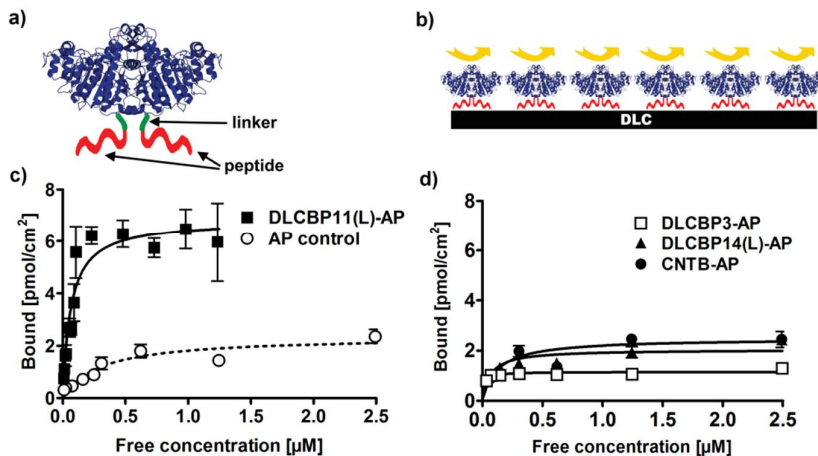


**Figure 10.** Peptide binding analysis using fusion proteins. (a) Schematic of a bi-functional peptide-AP fusion protein, with DLC binding peptide (red), linker (green), and AP protein (blue). (b) When fusion proteins are bound to the DLC surface, the enzymatic activity of AP allows for quantification of adsorbed proteins. (c) The adsorption of the best binding peptide-AP fusion, DLCBP11(L)-AP (filled squares), compared with the AP control (open circles). (d) The adsorption of peptides DLCBP3-AP (open squares), DLCBP14(L)-AP (filled triangles), and CNTB-AP (filled circles). The Langmuir isotherm model was fitted to the DLCBP11(L)-AP adsorption data. Data are presented as mean values and showing standard deviation ( $N = 3$ ), (data presented in the panel c and d – publication I).

#### 4.5 Analysis of basic binding properties of DLCBP11(L)-AP (publication I)

The basic features of interactions of the DLCBP11(L) peptide with the target surface were investigated by measuring influence of the ionic strength (NaCl concentration) and pH on the affinity of DLCBP11(L)-AP fusion protein to DLC. Experiments showed that increasing the ionic strength led to a gradual decrease of the binding of DLCBP11(L)-AP but did not significantly affect the binding of the AP-control (Figure 11a) whereas increasing the pH from 7 to 9 reduced binding of both proteins (Figure 11b). Therefore, it was concluded that the binding of the DLCBP11(L) peptide to DLC surface is dependent of both factors. However, the nature of the interaction with the target cannot be explained, based only on this observation. Moreover, the DLCBP11(L) peptide does not reveal any overall feature (except the presence of positive charge and slightly hydrophilic character) that could be identified based on its amino acid composition (Table 2) and aid in understanding mechanism of the interactions. Furthermore in many studies, additional, important information about driving forces of the binding of material specific peptides were obtained by investigating or modeling of the structural features of a

target material at molecular level (Vallee et al. 2010, Slocik & Naik 2010). In case of the DLC (due to its amorphous structure) this approach remains a significant challenge in contrast to well-defined surfaces of crystalline materials.

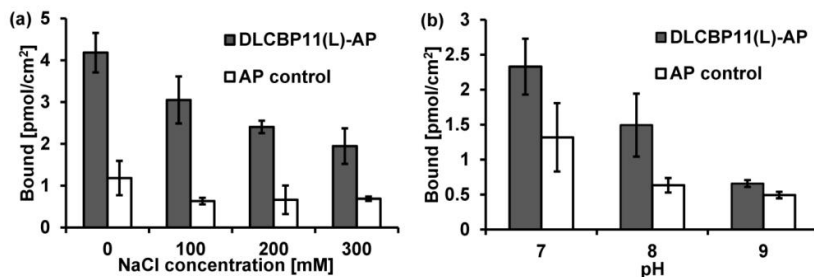


**Figure 11.** Effect of ionic strength (a) and pH (b) on DLCBP11(L)-AP (gray) and AP (white) binding to DLC. The amount of bound protein was determined by the enzymatic activity of the AP. The results are mean values, error bars indicate standard deviations (N = 3), (publication I).

#### 4.6 Analysis of DLCBP11(L) peptide variants (unpublished results)

Next, a mutagenesis approach was used in order to conduct a more detailed study on what factors define the affinity of the DLCBP11(L) peptide to the target surface. Due to significant length of DLCBP11(L) peptide sequence, first, it was tested if its full length is required for the binding. For that reason, the sequence of the peptide was divided into three segments (marked with numbers 1–3, Figure 12a). Peptide variants composed of one of each segment, as well as containing different combinations of the segments (DLCBP11(L)\_1+2, an example of the variant, Figure 12b) were designed as fusion proteins with the AP enzyme and expressed in *E. coli* as described before (paragraph 3.4.2). However, it was observed that the fusion proteins containing the peptide segments did undergo proteolytic cleavage during production. The cleavage was likely due to improper processing of the pelB signal sequence that was attached to AP proteins for their exporting to periplasmic space. It should be noted that the AP enzyme in *E. coli* is first expressed in a non-active form (as a monomer) in the bacterial cytoplasm, and then, it is exported to periplasmic space where the mature (dimeric) active form is assembled. Enzyme monomers are targeted to the periplasmic space by the signal sequence which is cleaved off during transport through the cell membrane (Chang et al. 1980). The signal peptidase that is responsible for the proteolytic cleavage most probably cut also parts of the fused peptides. As the result of this process, a pool of AP monomers containing partially processed peptides was formed which then assembled into active dimers.

The purified AP-fusion proteins containing partially trimmed peptides were analyzed by MALDI-TOF mass spectrometry and obtained information about the molecular mass of the processed monomers was utilized to map the putative cleavage sites in the peptide sequences (marked with A and B, Figure 12b). Subsequently, site directed mutagenesis was used to modify identified cleavage sites. The introduction of a modification (substitution of serine (S) with glutamine (Q)) of two amino acid residues adjacent to the putative cleavage site A reduced the degree of peptide proteolysis to less than 5% while mutating site B was unsuccessful in preventing the cleavage (Figure 12c). The homogeneity of the fusion protein containing mutated peptide (named pep\_L-AP) was confirmed by SDS-PAGE (Figure 12d) and MALDI-TOF mass spectrometry (Figure 12e). The binding of the pep\_L-AP fusion protein (containing only the trimmed part of segment 2 of the original DLCBP11(L) sequence, Figure 12c) was analyzed using the AP binding assay and compared with the binding of the DLCBP11(L)-AP (containing full length of the binding sequence, Figure 12a). Unexpectedly the performance of the two proteins was almost identical and the comparison of their binding isotherms showed that their affinities were very similar (Figure 12f) thus the pep\_L sequence was used for further studies.

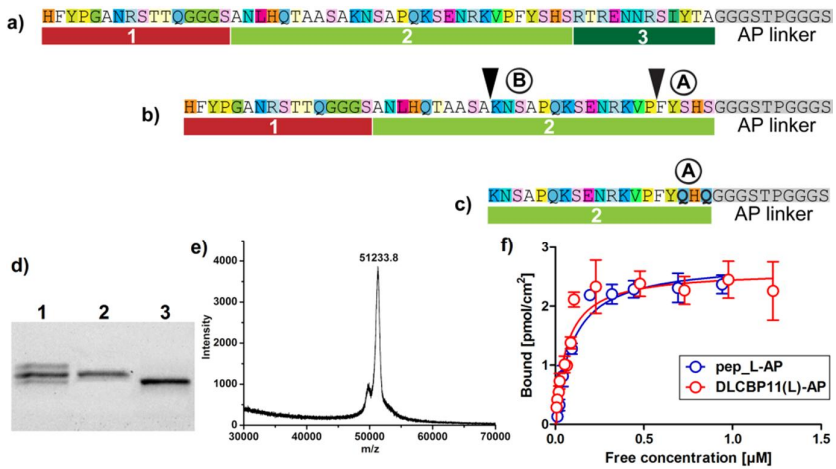


**Figure 12.** Analysis of DLCBP11(L) peptide variants. (a) The amino acid sequence the original peptide divided into three segments. (b) An example of one of the investigated variants (DLCBP11(L)\_1+2), with putative proteolysis sites indicated. (c) The amino acid sequence of the variant with mutated cleavage site A (pep\_L). (d) Analysis of the homogeneity of purified pep\_L-AP fusion protein by SDS-PAGE showing: line 1 – DLCBP11(L)\_1+2-AP (not mutated), line 2 – pep\_L-AP fusion protein, line 3 – control AP without fused peptide. (e) Mass spectrum of pep\_L-AP showing a well-defined peak (f) Comparison of binding curves of DLCBP11(L)-AP (red) and pep\_L-AP (blue), (panel f, publication II, supporting information).

#### **4.7 Analysis of basis of function of pep\_L peptide by simulations competition assay (publication II)**

A competition assay (paragraph 3.4.4) was designed to overcome problems arising from the proteolytic processing during expression of fusion proteins and to obtain a robust method of comparison of peptides carrying various mutations. The assay was based on the simultaneous competition for binding to the DLC surface between the pep\_L-AP fusion proteins and synthetic peptide variants of the original pep\_L sequence (Table 4, and Table 5) existing in a free, soluble form (not fused to the reporter protein). It allowed comparing the ability of different synthetic peptides to reduce the binding of the pep\_L-AP fusion protein to DLC surface. During the competition experiment a mixture of pep-L-AP fusion protein and synthetic peptides was applied and incubated on the DLC surface. Subsequently the surface was rinsed, and the fusion protein that remained bound to the surface was detected by its enzymatic activity (Figure 13a).

First, the competition assay was used to evaluate how the original pep\_L peptide competed for binding with the pep\_L-AP fusion protein. The competition curve (Figure 13b) was obtained by keeping the concentration of pep\_L-AP constant and adding increasing amounts of free peptide. As expected, by increasing molar ratio of free pep\_L to pep-L-AP less fusion protein remained bound to the surface. However, the 50% level of reduction in binding did not occur at 1/1 ratio, but around 17-fold excess of the peptide (the value was calculated from the exponential decay model used for data fitting). The fact that higher than expected molar excess of peptide was needed to compete out the fusion protein can be explained due to its dimeric nature. Since AP exist in dimeric form, thus the two peptide units fused to it can function in cooperative way which can lead to increased affinity compare to the single free peptide (Mammen et al. 1998).

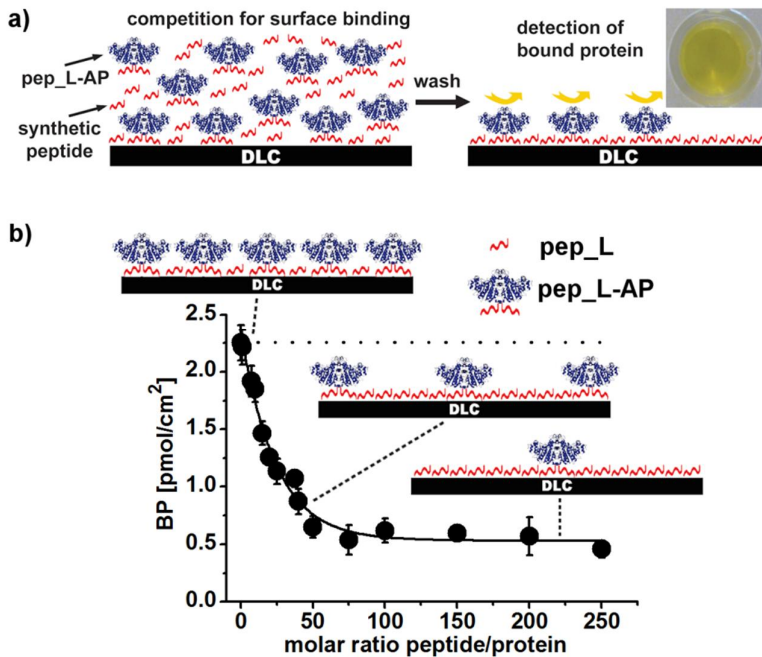


**Figure 13.** Simultaneous competition assay. (a) The experimental setup was designed to study the ability to compete for the binding to target surface (DLC) between fusion protein (pep\_L-AP) and synthetic peptides (variants of pep\_L sequence). The amount of bound protein was quantified based on the enzymatic activity of alkaline phosphatase (AP). (b) Competition curve of pep\_L and pep\_L-AP fusion protein showing that increasing the molar ratio between peptide and fusion protein led to reduced binding of the fusion protein. A one-phase exponential decay model was used for the data fitting. The adsorption of pep\_L-AP at molar ratio =0 is the baseline signal (a dotted line is shown as a guide for the eye). Data are presented as mean values and showing standard deviation (N= 3). BP – bound protein.

#### 4.7.1 Influence of chemical composition changes in the pep\_L sequence

Next the competition experiment was used to study how composition changes (duplication, deletion, and point mutations) (Table 4) of the pep\_L sequence affected its binding to the target surface.

In the dimeric peptide pep\_L\_pep two of the initial binding units were connected with the GGGSTPGGS linker as tandem repeats. This construct was designed to verify the effect of enhanced binding affinity of a dimer. The doubling of the peptide segment led to significantly better capability to compete with the pep\_L-AP-fusion protein. The dimeric peptide showed a 50% level of reduction in binding at the peptide/fusion protein molar ratio approximately 4 (Figure 14). This result



verified the assumption but demonstrated also that pep\_L-AP fusion protein had still higher affinity than dimeric peptide probably due to more favorable geometry for synergistic binding.

A peptide variant, named pep (Table 4) was used to investigate role of the linker sequence GGGSTPGGS that was originally designed to connect DLC binding peptide units with AP enzyme in the fusion protein. It was observed that removing of the linker sequence in the pep variant decreased its ability to compete out the AP fusion protein from the DLC surface (Figure 14). Therefore, it was concluded that role of the linker was not limited only to join two components in the fusion protein but also to contribute in proper functionality of the peptide (most probably to stabilize it and provide optimal orientation). Thus, the linker was considered as a part of the binding unit.

The effect of point mutations in the pep\_L sequence was investigated to get the structural understanding of its function. The most distinct feature of the primary structure of the peptide was that it possessed an unusually high number of residues with a positive charge. For that reason the variant (+/-)\_pep\_L in which the positively charged amino acids residues lysine (K) at position 1, and 7, and arginine (R) at positions 11 and 12 were changed to negatively charged aspartic acid (D), and the variant (+/0)\_pep\_L that contained the lysine (K) residues substituted to neutral asparagine (N) residues and the arginine (R) to glutamine (Q) were designed (Table 4). The competition experiments (Figure 14) showed that both peptides with mutations targeting the positively charged residues completely lost their capability to compete out the AP fusion protein from the DLC surface. The results provided also important information about structure-function understanding of the pep\_L peptide since indicated that the positively charged residues are essential for the binding and that Coulombic interactions are important driving forces for the affinity of the peptide. However, the experiments did not reveal the possible role of three-dimensional structure of the peptide and whether the mutations altered its conformation. An alternative explanation of the result may be that modification of charges of the peptide disrupted its structural features, which led to reduced affinity.

**Table 4.** Peptide sequences and their physicochemical properties, used for studying DLC binding specificity (publication II).

Name	Sequence	nt <sup>a</sup>	pI <sup>b</sup>
pep_L	KNSAPQKSEN RKVPFYQH Q <b>GGG</b> ST <b>PGGS</b>	+3	10
pep_L_pep	KNSAPQKSEN RKVPFYQH Q <b>GGG</b> ST <b>PGGS</b> - -KNSAPQKSEN RKVPFYQH Q	+6	10.2
pep	KNSAPQKSEN RKVPFYQH Q	+3	10
(+/-)_pep_L	<b>D</b> NSAP <b>Q</b> <b>D</b> SEN <b>DD</b> VPFYQH Q <b>GGG</b> ST <b>PGGS</b>	-5	3.7
(+/0)_pep_L	<b>N</b> NSAP <b>Q</b> <b>N</b> SEN <b>Q</b> <b>N</b> VPFYQH Q <b>GGG</b> ST <b>PGGS</b>	-1	5.2

[a] estimated net charge at pH 7.5, [b] isoelectric point. Mutated residues were marked in bold underlined, linker in bold italic. pI value was calculated using Protparam program (<http://web.expasy.org/protparam/>).

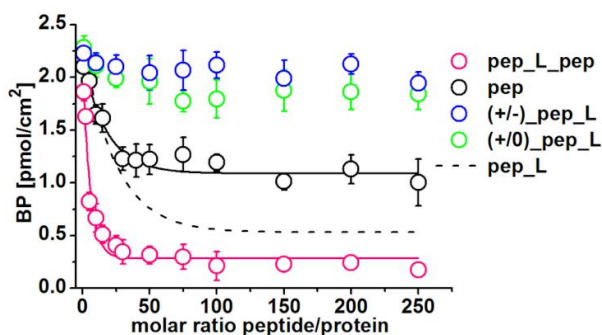


**Figure 14.** Influence of chemical composition changes in the pep\_L sequence on binding specificity to the target surface studied by a competition assay. The doubling of the peptide segment in pep\_L\_pep led to significantly better capability to compete with the pep\_L-AP-fusion protein, while removing the linker part in pep variant caused its partial reduction. Mutations of positively charged residues to negative in (+/-)\_pep\_L and to neutral in (+/0)\_pep\_L variants led to complete loss of the function. A one-phase exponential decay model was used for the data fitting. Data are presented as mean values and showing standard deviation (N = 3). BP – bound protein. Pep\_L data (from Figure 13) is shown as a reference curve (publication II).

#### 4.7.2 Influence of structural changes in the pep\_L sequence

Subsequently, to study if the defined chemical composition of the pep\_L peptide (i.e. charge, pI, hydrophobicity) is sufficient for its function, a variant R\_pep\_L in which the entire amino acids sequence had been reversed (Table 5) was analyzed. The reversed peptide had exactly the same chemical composition as the original peptide but different arrangement of amino acid residues in the primary sequence, thus as a consequence of the sequence reversal it did not retain the same overall conformational features. Remarkably, this peptide showed only a very low capability to compete for binding in the competition assay (Figure 15). Therefore, the result showed that not only the chemical composition of the peptide but also the three-dimensional structure determined by specific primary amino acid sequence contribute to its function.

Following experiments were designed to study if it would be possible to identify a location especially sensitive to structural variations. For this purpose, a set of peptides containing variants possessing 25%, 50% or 75% of their sequence reversed was constructed (Table 5). The performance of modified peptides was compared to the original pep\_L sequence and the fully reversed sequence R\_pep\_L.

The results of the competition experiment using peptides having inverted segments restricted to 25% (one segment out of four) are presented in Figure 15a. The peptide R\_pep\_L\_1/4 showed approximately half lower ability to compete out the fusion protein (reaching the 50% reduction of pep\_L-AP binding at about 40 molar excess of peptide to fusion protein), while peptides R\_pep\_L\_2/4, R\_pep\_L\_3/4, and R\_pep\_L\_4/4 showed almost the same performance as the original pep\_L peptide (Figure 15a).

The effect of 50% sequence inversion (two out of four segments simultaneously) was investigated by comparing performance of peptides R\_pep\_L\_1-2/4, R\_pep\_L\_3-4/4 having two adjacent segments inverted (Figure 15b) and peptides R\_pep\_L\_1,4/4, R\_pep\_L\_2-3/4, R\_pep\_L\_1,3/4, R\_pep\_L\_2,4/4 with two segments in different locations inverted (Figure 15c). All half reversed peptides did not show significant loss in their performance. Interestingly peptide R\_pep\_L\_2,4/4 was able to compete with the fusion protein as efficient as the pep\_L peptide (reaching 50% reduction in binding at a peptide to protein molar ratio of 17).

Finally the peptides with 75% inversion of their sequences (three segments out of four at the same time) were examined (Figure 15d). These modifications led to significant loss of the peptides ability to compete for binding with the fusion protein. Peptides R\_pep\_L\_2-4/4, R\_pep\_L\_1,3-4/4, and R\_pep\_L\_1-2,4/4 showed a loss in function comparable to the fully reversed sequence, R\_pep\_L. Only the peptide R\_pep\_L\_1-3/4 partially retained its competition ability reaching half efficiency at a peptide fusion protein ratio of about 78 which is approximately 4.5 times lower than for the original peptide.

**Table 5.** Peptide sequences used for studying the effect of sequence reversion (publication II).

Name	Sequence
pep_L	KNSAPQKSENKVPFYQH <b>GGG</b> STPGGG <b>S</b>
R_pep_L	<b><u>SGGGPTSGGGQHGYFPVKRNESKQPASNK</u></b>
R_pep_L_1/4	<b><u>SKQPASNK</u></b> ENRKVPFYQHGGGGSTPGGG <b>S</b>
R_pep_L_2/4	KNSAPQKS <b><u>FPVKRNE</u></b> YQHGGGGSTPGGG <b>S</b>
R_pep_L_3/4	KNSAPQKSENKVPFY <b><u>GGGQHGY</u></b> STPGGG <b>S</b>
R_pep_L_4/4	KNSAPQKSENKVPFYQHGGGG <b><u>SGGGPTS</u></b>
R_pep_L_1-2/4	<b><u>FPVKRNESKQPASNK</u></b> YQHGGGGSTPGGG <b>S</b>
R_pep_L_3-4/4	KNSAPQKSENKVPFY <b><u>SGGGPTSGGGQHGY</u></b>
R_pep_L_1,4/4	<b><u>SKQPASNK</u></b> ENRKVPFYQHGGGG <b><u>SGGGPTS</u></b>
R_pep_L_2-3/4	KNSAPQKS <b><u>FPVKRNEGGGQHGY</u></b> STPGGG <b>S</b>
R_pep_L_1,3/4	<b><u>SKQPASNK</u></b> ENRKVPFY <b><u>GGGQHGY</u></b> STPGGG <b>S</b>
R_pep_L_2,4/4	KNSAPQKS <b><u>FPVKRNE</u></b> YQHGGGG <b><u>SGGGPTS</u></b>
R_pep_L_2-4/4	KNSAPQKS <b><u>SGGGPTSGGGQHGYFPVKRNE</u></b>
R_pep_L_1,3-4/4	<b><u>SKQPASNK</u></b> ENRKVPFY <b><u>SGGGPTSGGGQHGY</u></b>
R_pep_L_1-2,4/4	<b><u>FPVKRNESKQPASNK</u></b> YQHGGGG <b><u>SGGGPTS</u></b>
R_pep_L_1-3/4	<b><u>GGGQHGYFPVKRNESKQPASNK</u></b> STPGGG <b>S</b>

Reversed residues were marked in bold italic underlined.

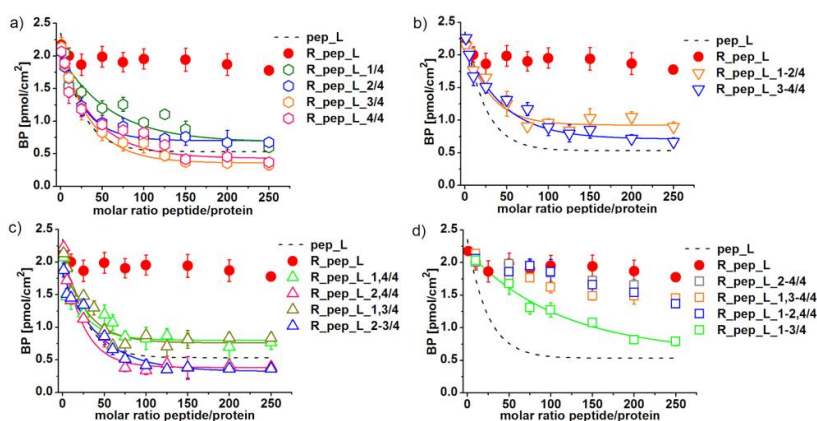


**Figure 15.** Influence of full or partial inversions (structural changes) of the pep\_L sequence on the performance in the competition assay. (a) 25% of sequence reversed compared to fully reversed initial sequence (b) 50% reversed (c) 50% reversed (d) 50% reversed

reversed in non-adjacent segments (d) 75% reversed. One-phase exponential decay model was used for the data fitting. Data are presented as mean values and showing standard deviation (N = 3). BP – bound protein. Pep\_L data (reused from Figure 13) serve as a reference curve.

Taken together, all the results obtained with the simultaneous competition experiments lead to the conclusion that the binding of pep\_L to DLC is a complex recognition event. Although it was demonstrated by point mutations that positively charged residues are important for the peptide function, the peptide-DLC interaction cannot be explained based on this result only. The collected sequence inversion data clearly show that the positive charges are necessary for the function but not alone sufficient, and the affinity of the peptide must also be dependent on its optimal three-dimensional structure(s). Despite the evidence for sequence dependency, the results show also that the recognition event allows a significant variation in configuration before it is critically affected. This configurational freedom might be related to the lack of defined secondary structures of the peptides in solution (analysis of measured CD-spectra revealed that all peptides had random coil conformation (publication II)) which allows for flexibility of their structures and do not restrict them to only one optimal conformation.

Comparing the results with other studies (detailed examples described in the introduction, paragraph 1.8) it can be concluded that researchers often used a mutagenesis approach to identify a limited number of amino acids as critical for the function and based on that tried to explain the mechanism of interaction at peptide-solid material interface (Vreuls et al. 2010, Ejima et al. 2010, So et al. 2012). Some studies also showed that only chemical composition of the peptide is important, not its overall configuration (Ruan et al. 2013, Sanghvi et al. 2005), others concluded that both factors have contributing effect and showed that mutations often led to altered peptide chain flexibility which caused loss of binding affinity to the target (Goede et al. 2004, Schwemmer & Baumgartner 2012). These studies showed that although the positively charged residues are important for binding they must also be in their right conformational environment provided by the peptide structure, which means that it may be unfruitful to try to exactly locate critical residues or parts (segments) of the sequence that could be involved in the function. Rather the interaction is a complex event in which regions of the peptide are functionally interconnected in a nonlinear way.

#### **4.8 Engineering of the pep\_L peptide to multivalent forms (publication III)**

Multimerization is one of the approaches used in engineering of material binding peptides in order to utilize them for nanotechnological applications. Since the binding studies with the simultaneous competition assay (Figure 14) showed better performance of the duplicated sequence (pep\_L\_pep) it was investigated if the use of repeated DLC binding domains could further increase its affinity and stability on the target surface. However, successful application of peptide multivalent

systems for practical use require also an understanding of their structure-function relationships, therefore the pep\_L peptide was engineered to di-, tri-, and tetravalent forms using different linkers and their functionality in relation to the molecular architecture was compared.

#### **4.8.1 Construction of multivalent peptides (publication III)**

Multivalent peptides (MPs) binding to the DLC surface were created by chemical conjugation to a series of maleimide-functionalized cross-linkers that reacted with sulfhydryl group of a cysteine residue that was introduced to the C-terminus of the pep\_L peptide. The resulting set of MPs consisted of three variants of divalent peptides with two identical pep\_L units connected by linkers of different length, as well as star-shaped tri-, and tetravalent peptides. Additionally, the tandem repeat double peptide pep\_L\_pep (synthesized as one long peptide chain having a duplicated DLC binding sequence following directly an initial one) was used for comparison (Figure 16).



#### 4.8.2 Influence of MPs structural design for affinity (publication III)

The effect of MPs structure for binding affinity to the target was analyzed using a competition assay in which MPs and the reporter protein (pep\_L-AP) competed simultaneously for DLC surface binding (the same assay was used to study the structural basis of function of pep\_L sequence, described in paragraph 4.7). The assay allowed measuring the ability of different peptide constructs to reduce the binding of the pep\_L-AP fusion protein to DLC surface, and ranking their relative affinity from the graph, (Figure 17) by comparing the competition curves and molar ratio value at which pep\_L-AP binding was reduced by 50%.

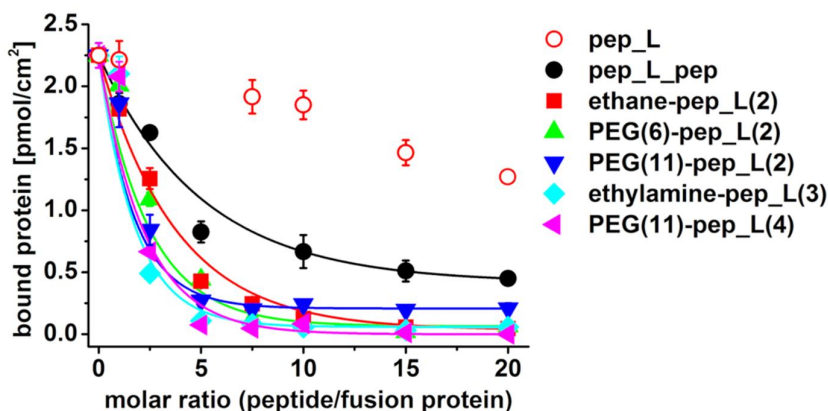


**Figure 17.** Competition curves for the peptides with increasing molar ratio of peptide to reporter. One-phase exponential decay model was used for the data fitting. Data are presented as mean values and showing standard deviation (N = 3) (publication III).

The results of the competition experiment (Figure 17) clearly show that all MPs efficiently competed out the reporter (as seen from the steeply decreasing curves) in contrast to the monovalent pep\_L peptide that reduced its binding only partially (even when 20x molar excess of peptide was applied). The affinity of chemically conjugated divalent peptides was correlated with the linker length, and improved by increasing the distance between the binding units from 8 Å to 52 Å (extended conformation). The increase in the affinity can be explained based on a cooperative binding effect i.e. when one of the peptide units binds, the effective concentration of its pair becomes high in proximity to the surface and therefore it binds with a higher probability (Mammen et al. 1998). The effect of the linker on the affinity of a multivalent molecule depends on how well the architecture of binding units in a multimer corresponds to the distance between binding sites on the surface. As the affinity increased with increasing linker length, the results suggest that binding sites on the surface are relatively far apart from each other, most probably due to



heterogeneity of DLC, as a consequence of its amorphous structure (Hauert 2004).

Increasing the number of peptide units in the MPs to three in ethylamine-pep\_L(3), and four in PEG(11)-pep\_L(4) led to the affinity enhancement. For instance, a 2.5 excess of a MP gave a 63% reduction in reporter (pep\_L-AP) binding for PEG(11)-pep\_L(2), a 78% reduction for ethylamine-pep\_L(3), and a 70% reduction for PEG(11)-pep\_L(4). Although at low concentrations trivalent, tetravalent, and divalent PEG(11)-pep\_L(2) peptide, show very similar behavior (competition curves), however at higher concentrations they differ in the level of reducing the pep\_L-AP binding (values at which the curves leveled out at high ratios). For example, at the highest applied concentration the PEG(11)-pep\_L(2) reduced the reporter adsorption to 11%, the trivalent MP to approximately to 1% while the tetravalent MP limited its binding completely.

The effect of the tandem repeat peptide pep\_L\_pep on reporter binding was the lowest among the divalent peptides (and all MPs under study). This construct was synthesized as a single peptide and contained a partly duplicated sequence in a head-to-tail arrangement (in contrast to the tail-to-tail arrangement in the chemically conjugated MPs). Therefore, the difference in function of pep\_L\_pep peptide might be related to different chemical nature of the linker (Figure 16), and the way of connecting of the binding units.

#### **4.8.3 Influence of MPs structural design for sequential competition and kinetics (publication III)**

The effect of structural design of multivalent DLC binding peptides and the potential role of kinetic effects in the binding were investigated using competition assays which allowed studying how the pep\_L-AP fusion protein and different peptides could compete out each other when one had already been bound to the surface. In the first assay the displacement of surface bound peptide by the reporter protein was measured (Figure 18a). During the experiment the substrate's surface was initially saturated with a peptide, rinsed with the buffer to remove any unbound molecules, incubated with pep\_L-AP or plain buffer (control), and finally the remaining pep\_L-AP was assayed. In the second assay (Figure 18b) the order of the peptide and protein additions was reversed, i.e. the ability of the peptides to displace surface bound reporter protein was determined.

Results of the displacement assays demonstrated that, in line with the simultaneous competition assay, the MPs were able to effectively reduce the reporter protein binding on DLC (Figure 18c). The monovalent peptide showed again the weakest performance, with 85% reporter binding after competition. Using the divalent peptide pep\_L\_pep the surface was still occupied by 75% (first assay) and 69% (second assay) of the bound reporter protein, respectively. The chemically conjugated divalent peptides showed similar functionality with only <22% bound reporter left on the surface. Again, increasing linker length had a positive effect on the peptide binding, especially in the assay measuring displacement of peptides by fusion protein (first assay).

Unexpectedly, the tri- and tetravalent MP showed a distinct behavior in the competition experiments, for example, ethylamine-pep\_L(3) showed better performance than PEG(11)-pep\_L(4) when it was used to compete out pep\_L-AP (second assay). The trivalent peptide displaced the reporter protein almost completely, limiting its adsorption to only 0.2%. On the other hand PEG(11)-pep\_L(4) demonstrated better resistance of being competed out by the pep\_L-AP. The tetravalent peptide restricted reporter binding to only 1% while the trivalent peptide to 16.5%.

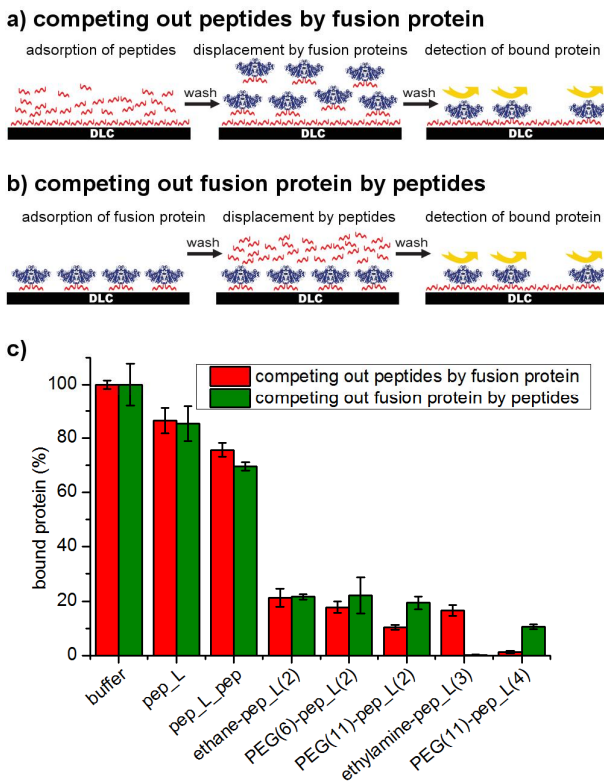


**Figure 18.** Sequential competition assays used to compare function and kinetics of MPs. Schematic presentations of the assays (a) peptide displacement by reporter and (b) reporter displacement by peptide. (c) Amount of bound the reporter protein after the competition. Data are presented as mean values with standard deviations (N = 3) (publication III).

Overall, the results of sequential displacement assays indicated that the dynamics of surface interactions of tri- and tetravalent peptide are distinctly different, and depend on order of the binding as well as the arrangement of the binding units in the multimer. The difference in performance between the MPs can be explained

by the dissimilarity of their size. The trivalent peptide due to the small size and star shape structure of the linker is more compact and less flexible than tetravalent peptide. This architecture is probably more optimal and helps the trivalent peptide for easier penetration through protein layer and displacement of adsorbed molecules in contrast to, large in size, and flexible tetravalent peptide. However, the flexibility of the linker arms in the tetravalent peptide may also have the beneficial function, i.e. it can cause difficulties for the fusion protein to penetrate through adsorbed peptides and reach the binding sites of the DLC surface.

#### **4.9 Utilization of DLC binding peptides in stabilization of colloidal DLC (publication III)**

The function of MPs at interfaces was investigated by studying their influence on the Zeta potential and colloidal stability of the dispersion of colloidal form of DLC (DLC flakes, preparation of the material was described in paragraph 3.7). The Zeta potential of unmodified DLC flakes was very negative at basic pHs and gradually became less charged as the pH was lowered (Figure 19a). The addition of DLC binding peptides to the suspension of the DLC flakes increased their Zeta potential across the whole pH range indicating that peptides modified surface properties of the DLC flakes. The mechanism of the interaction remained unknown, however it should be noted that the DLC binding peptides contain a high number of positively charged residues. In addition, it was also shown earlier (paragraph 4.7.1) that the positive charge is one of the factors influencing binding affinity of the monovalent peptide (pep\_L) to the DLC coating. Furthermore, the experiment with the weakly binding control peptides (+/-)\_pep\_L (pI 3.7) and (+/0)\_pep\_L (pI 5.2) (Table 4), showed only a small change in zeta potential of the DLC flakes, therefore it is very likely that the peptides interact with the DLC flakes based on electrostatic attraction.

The colloidal stability of unmodified and peptide-coated DLC flakes was evaluated by observation of the sedimentation rate of the suspensions at different pHs (Figure 19b). The unmodified DLC flakes, in line with zeta potential results, were stable at pH 6.5 and 11 (zeta potential -40 mV) for 12–24 h (at room temperature) while at pH 2 sedimented (zeta potential -6 mV). Modification of the DLC flakes with PEG(11)-pep\_L(4) (and all other peptides under study) reversed their stability pattern. The flakes sediment at pH 7 and 11 after 1h incubation (room temperature), and remained stable in solution at pH 2.5. The result showed that developed peptides can be used for the modification of colloidal DLC flakes, and to control their stability in solution.

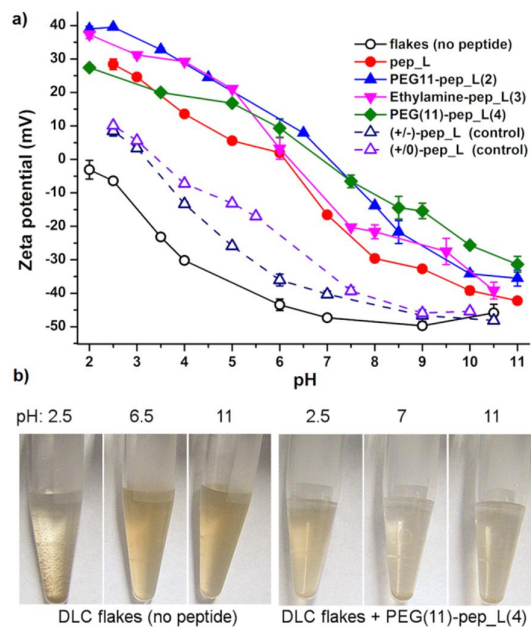


**Figure 19.** Surface modification of the DLC flakes by the DLC binding peptides. (a) Zeta potential of the DLC flakes coated with different peptide variants as a function of pH (N = 3). (b) Influence of peptides on the stability of colloidal dispersions of DLC. Flakes after 1 h with and without peptides and at different pH values (publication III).

## 5. Conclusions

In recent years directed evolution approaches using biopanning methods based on screening of combinatorial peptide libraries displayed on phage or bacterial cells have been used in numerous studies. The technique can be successfully utilized for finding high affinity binders, specific to target materials under study. However, several important issues should be taken into account when analyzing the results of the selection experiments. Firstly, the biopanning, especially using phage display, often leads to the selection of target unrelated peptides (TUPs), which can enrich together with specific (target related) binders and might dominate the pool of selected clones. The TUPs are either binders to other than target components of the screening system or then they are peptides displayed on the phage clones containing mutations in their genomes that enhance their propagation properties. Thus, they are false positives and, if not recognized and discarded from the pool of “true” (specific) binders, lead to incorrect conclusions. Numerous examples in the literature show that the problem of TUPs has often been unknown or neglected, and many described sequences are very likely target unrelated binders. Enrichment of TUPs can be limited by optimizing the biopanning conditions and reducing the number of the selection rounds. However, there is no guarantee that these approaches will prevent the selection of any TUPs. Therefore, it is essential that each sequence obtained from the biopanning experiment (or taken from the literature) is carefully examined by comparing it with the sequences that have been found previously in other studies. This can be easily done using internet seekers or online tools for screening databases that store information about reported TUPs.

Secondly, selected peptides in biopanning experiments require extensive binding characterization in order to confirm that they exhibit real affinity for the target. It is essential that the analysis are carried out using independent experimental methods (that limit the risk of obtaining false positive results) in different display contexts, i.e., when a peptide is displayed on the phage, linked to a protein or other molecular scaffold, or else exist in free soluble form. The context display analysis is especially important because it allows evaluating if the binding properties of selected peptides can be retained when they are released from a phage or bacterial cell surface, which is essential in order to utilize them for practical applications. Furthermore peptides displayed on a host are usually present in many

copies which can lead to enhancement of their affinity due to a cooperative binding effect.

Moreover, the development of peptides for practical applications requires knowledge of their binding affinity, and understanding of their structural basis of function. Phage/cell display systems allow only for measuring relative affinities with a very limited number of analytical methods. Thus, the detailed characterization of binding must be carried out using techniques that are suitable for accurately measuring their concentration, and quantitative analysis of adsorption on the surface. This can be achieved when peptides are present in free soluble form or linked to a protein or other molecular scaffold.

Despite the challenges, the results described in this thesis, and also many other examples from the literature, show that the biopanning method is a powerful tool for finding peptides binding with a high affinity to various materials. In the case of the DLC binding peptides, special attention has been put on a thorough characterization of the binding properties of the selected sequences. This finally resulted in the development of a peptide system that was fully functional in nanotechnological applications. The methods for quantification of adsorbed peptide-fusion proteins on the DLC surface by the enzymatic activity of alkaline phosphatase were very robust. Therefore, they could be used in measurement of binding parameters and in structure-function studies (the competition assays). Moreover, the methods overcome many drawbacks of other traditional approaches used for studying adsorption of biomolecules to solid materials such as QCM, SPR, and fluorescence. The traditional methods are either difficult to use, for example, due to problems of coating of the measurement devices with a substrate under study (in case of QCM or SPR) or they sometimes lead to underestimation of binding affinities, or even show results that might be incorrect. For instance, the HAIYPRH sequence was described as a putative binder to cellulose with the binding affinity constant  $5.18 \pm 0.80 \times 10^{-10}$  M (Serizawa et al. 2007a). However, it was also described as target unrelated peptide (confirmed as propagation related TUP) (Brammer et al. 2008).

The unexpected selection and enrichment of long sequences of the DLC binding peptides showed that for this target the size of the short peptides generally present in the library might have been insufficient. The result also indicated that long peptides may be a good strategy to functionalize targets having amorphous structure, such as DLC. This assumption is also supported by collected data on the function of multimeric DLC binding peptides. Multimerization turned out to be a successful strategy for enhancing the binding affinity of DLC peptides but it also showed that the function of a multimer depends of its specific design which might be related to presence of non-homogeneous binding sites on the amorphous DLC surface.

The work also demonstrated that the developed peptides can be used for practical applications such as self-assembled peptide coatings for surface functionalization or preventing protein adsorption, tags for immobilization of functional molecules on the DLC surface (for example enzymes), and also to modify the properties of the colloidal form of the material (DLC flakes). Functionalization of the DLC surface by peptides can be useful in development of biomedical applications. DLC

is it often used as a coating material for implants, thus DLC binding peptides can improve their biocompatibility serving, for example, as non-fouling coating preventing bacterial adsorption or molecular linkers for immobilizing bioactive molecules under ambient conditions, overcoming problems of covalent modifications that limit usefulness in some biomedical applications.

Colloidal DLC represents a new approach of utilizing diamond-like carbon in nanotechnology which has not been described before. The flakes possess the superior physico-chemical material properties of DLC, and interactions with DLC-specific peptides offer a possible route for their functionalization for various applications, for example, as self-assembling coatings, additives in lubricants, or biomimetic composite materials.

## References

- Anni, H., Nikolaeva, O. & Israel, Y., 2001. Selection of phage-display library peptides recognizing ethanol targets on proteins. *Alcohol*, 25, pp.201–209.
- Baeuerlein, E., 2007. *Handbook of Biomineralization, Biological Aspects and Structure Formation*. Wiley-VCH Verlag GmbH & Co. KGaA, Weinheim, Germany.
- Bakhtiar, R., 2012. Surface plasmon resonance spectroscopy: a versatile technique in a biochemist's toolbox. *Journal of Chemical Education*, 90 (2), pp.203–209.
- Bardhan, N.M., Ghosh, D. & Belcher, A.M., 2014. Carbon nanotubes as in vivo bacterial probes. *Nature Communication*, 5, 4918.
- Bastings, M.M.C. et al., 2011. From phage display to dendrimer display: insights into multivalent binding. *Journal of the American Chemical Society*, 133(17), pp.6636–6641.
- Berger, S., Bannantine, J.P. & Griffin, T., 2007. Autoreactive antibodies are present in sheep with Johne's disease and cross-react with *Mycobacterium avium* subsp. *paratuberculosis* antigens. *Microbes and Infection*, 9, pp.963–970.
- Brammer, L. a et al., 2008. A target-unrelated peptide in an M13 phage display library traced to an advantageous mutation in the gene II ribosome-binding site. *Analytical Biochemistry*, 373 (1), pp.88–98.
- Briggs, B. D. & Knecht M. R., 2012. Nanotechnology meets biology: peptide-based methods for the fabrication of functional materials. *The Journal of Physical Chemistry Letters* (3), pp.405–418.
- Brown, S., 1997. Metal-recognition by repeating polypeptides. *Nature Biotechnology*, 15 (3), pp.269–272.
- Buczowski, H. et al., 2012. A novel approach to generating morbillivirus vaccines: Negatively marking the rinderpest vaccine. *Vaccine*, 30, pp.1927–1935.
- Caprini, A. et al., 2013. A novel bioactive peptide: Assessing its activity over murine neural stem cells and its potential for neural tissue engineering. *New Biotechnology*, 30, pp.552–562.
- Causa, F. et al., 2013. Evolutionary screening and adsorption behavior of engineered M13 bacteriophage and derived dodecapeptide for selective dec-



- oration of gold interfaces. *Journal of Colloid and Interface Science*, 389 (1), pp.220–229.
- Cetinel, S. et al., 2013. Addressable self-immobilization of lactate dehydrogenase across multiple length scales. *Biotechnology Journal*, 8, pp.262–272.
- Chang, C.N.A.N. et al., 1980. Processing of alkaline phosphatase precursor to the mature enzyme by an *Escherichia coli* inner membrane preparation. *Journal of Bacteriology*, 142 (2), pp.726–728.
- Chen, H. et al., 2009. Context-dependent adsorption behavior of cyclic and linear peptides on metal oxide surfaces. *Langmuir*, 25, pp.1588-1593
- Chung, W. et al., 2011. Evolutionary screening of collagen-like peptides that nucleate hydroxyapatite crystals. *Langmuir*, 27, pp.7620–7628
- Cui, Y. et al., 2010. Recognition of patterned molecular ink with phage displayed peptides. *Journal of the American Chemical Society*, 132, pp.1204–1205.
- Damborsky, J. & Brezovsky, J., 2014. Computational tools for designing and engineering enzymes. *Current Opinion in Chemical Biology*, 19 (0), pp.8–16.
- Dang, X. et al., 2011. Virus-templated self-assembled single-walled carbon nanotubes for highly efficient electron collection in photovoltaic devices. *Nature Nanotechnology*, 6 (6), pp.377–384.
- Demir, H.V. et al., 2011. Spatially selective assembly of quantum dot light emitters in an LED using engineered peptides. *ACS Nano*, 5 (4), pp.2735–2741.
- Desjobert, C. et al., 2004. Identification by phage display selection of a short peptide able to inhibit only the strand transfer reaction catalyzed by human immunodeficiency virus type 1 integrase. *Biochemistry*, 43 (41), pp.13097–13105.
- Dickerson, M.B. et al., 2008a. Identification and design of peptides for the rapid, high-yield formation of nanoparticulate TiO<sub>2</sub> from aqueous solutions at room temperature. *Chemistry of Materials*, 20 (4), pp.1578–1584.
- Dickerson, M.B., Sandhage, K.H. & Naik, R.R., 2008b. Protein- and peptide-directed syntheses of inorganic materials. *Chemical Reviews*, 108, pp.4935–4978.
- Dickerson, M.B. et al., 2004. Identification of peptides that promote the rapid precipitation of germania nanoparticle networks via use of a peptide display library. *Chemical Communications*, (15), pp.1776–1777.

- Dintilhac, A. & Bernués, J., 2002. HMGB1 interacts with many apparently unrelated proteins by recognizing short amino acid sequences. *Journal of Biological Chemistry*, 277, pp.7021–7028.
- Donatan, S. et al., 2009. Physical elution in phage display selection of inorganic-binding peptides. *Materials Science and Engineering: C*, 29(1), pp.14–19.
- Ejima, H., Matsuno, H. & Serizawa, T., 2010. Biological identification of peptides that specifically bind to poly(phenylene vinylene) surfaces: recognition of the branched or linear structure of the conjugated polymer. *Langmuir*, 26 (22), pp.17278–17285.
- Engler, C., Kandzia, R. & Marillonnet, S., 2008. A one pot, one step, precision cloning method with high throughput capability. *PloS one*, 3 (11), p.e3647.
- Erdemir, A. & Donnet, C., 2006. Tribology of diamond-like carbon films: recent progress and future prospects. *Journal of Physics D: Applied Physics*, 39 (18), pp.R311–R327.
- Estephan, E. et al., 2009. Selection and mass spectrometry characterization of peptides targeting semiconductor surfaces. *Biotechnology and Bioengineering*, 104 (6), pp.1121–1131.
- Fan, Y., Sun, Z. & Moradian-Oldak, J., 2009. Controlled remineralization of enamel in the presence of amelogenin and fluoride. *Biomaterials*, 30, pp.478–483.
- Feng, B. et al., 2009. A novel affinity ligand for polystyrene surface from a phage display random library and its application in anti-HIV-1 ELISA system. *Biologicals*, 37, pp.48–54.
- Garnham, C.P., Campbell, R.L. & Davies, P.L., 2011. Anchored clathrate waters bind antifreeze proteins to ice. *Proceedings of the National Academy of Sciences U.S.A.*, 108 (18), pp.7363–7367.
- Gaskin, D.J.H., Starck, K. & Vulfson, E.N., 2000. Identification of inorganic crystal-specific sequences using phage display combinatorial library of short peptides: A feasibility study. *Biotechnology Letters*, 22, pp.1211–1216.
- Gebhardt, K., Lauvrak, V., Babaie, E., Eijsink, V. & Lindqvist, B.H., 1996. Adhesive peptides selected by phage display Characterization, applications and similarities with fibrinogen. *Peptide Research*, 9 (6), pp. 269–278

- Ghosh, D. et al., 2014. Deep, noninvasive imaging and surgical guidance of sub-millimeter tumors using targeted M13-stabilized single-walled carbon nanotubes. *Proceedings of the National Academy of Sciences U.S.A.*, 111 (38), pp.13948–13953.
- Ghosh, D. et al., 2012. M13-templated magnetic nanoparticles for targeted in vivo imaging of prostate cancer. *Nature Nanotechnology*, 7, pp.677–682.
- Giebel, L.B. et al., 1995. Screening of cyclic peptide phage libraries identifies ligands that bind streptavidin with high affinities. *Biochemistry*, 34, pp.15430–15435.
- Goede, K., Busch, P. & Grundmann, M., 2004. Binding Specificity of a Peptide on Semiconductor Surfaces. *Nano Letters*, 4 (11), pp.2115–2120.
- Gray, J.J., 2004. The interaction of proteins with solid surfaces. *Current Opinion in Structural Biology*, 14 (1), pp.110–115.
- Gronewold, T.M.A. et al., 2009. Selection process generating peptide aptamers and analysis of their binding to the TiO<sub>2</sub> surface of a surface acoustic wave sensor. *Acta Biomaterialia*, 5 (2), pp.794–800.
- Gu, Y. et al., 2004. Selection of a peptide mimicking neutralization epitope of hepatitis E virus with phage peptide display technology. *World Journal of Gastroenterology*, 10, pp.1583–1588.
- Gungormus, M. et al., 2012. Cementomimetics-constructing a cementum-like biomineralized microlayer via amelogenin-derived peptides. *International Journal of Oral Science*, 4 (2), pp.69–77.
- Gungormus, M. et al., 2010. Self assembled bi-functional peptide hydrogels with biomineralization-directing peptides. *Biomaterials*, 31 (28), pp.7266–74.
- Gungormus, M. et al., 2008. Regulation of in vitro calcium phosphate mineralization by combinatorially selected hydroxyapatite-binding peptides. *Biomacromolecules*, 9 (3), pp.966–973.
- Hakim, A. et al., 2013. Crystal structure of an insect antifreeze protein and its implications for ice binding. *Journal of Biological Chemistry*, 288, pp.12295–12304.
- Haris, P.I. & Chapman, D., 1995. The conformational analysis of peptides using Fourier transform IR spectroscopy. *Biopolymers*, 37, pp.251–263.
- Hauert, R.A., 2004. An overview on the tribological behavior of diamond-like carbon in technical and medical applications. *Tribology International*, 37, pp.991–1003.

- Heinz, H. et al., 2009. Nature of molecular interactions of peptides with gold, palladium, and Pd-Au bimetal surfaces in aqueous solution. *Journal of the American Chemical Society*, 131 (16), pp.9704–9714.
- Helms, B. a et al., 2009. High-affinity peptide-based collagen targeting using synthetic phage mimics: from phage display to dendrimer display. *Journal of the American Chemical Society*, 131 (33), pp.11683–11685.
- Hermanson, G.T., 2008a. Chapter 26 – Enzyme Modification and Conjugation. In G.T. Hermanson, ed. *Bioconjugate Techniques (Second Edition)*. New York: Academic Press, pp.961–968.
- Hermanson, G.T., 2008b. Chapter 4 – Homobifunctional Crosslinkers. In G.T. Hermanson, ed. *Bioconjugate Techniques (Second Edition)*. New York: Academic Press, pp.234–275.
- Hnilova, M. et al., 2012a. Multifunctional protein-enabled patterning on arrayed ferroelectric materials. *ACS Applied Materials & Interfaces*, 4 (4), pp.1865–1871.
- Hnilova, M., Karaca, B.T., et al., 2012b. Fabrication of hierarchical hybrid structures using bio-enabled layer-by-layer self-assembly. *Biotechnology and Bioengineering*, 109 (5), pp.1120–1130.
- Hnilova, M., Khatayevich, D., et al., 2012c. Single-step fabrication of patterned gold film array by an engineered multi-functional peptide. *Journal of Colloid And Interface Science*, 365 (1), pp.97–102.
- Hnilova, M. et al., 2008. Effect of molecular conformations on the adsorption behavior of gold-binding peptides. *Langmuir*, 24 (21), pp.12440–12445.
- Holten-Andersen, N. & Waite, J.H., 2008. Mussel-designed protective coatings for compliant substrates. *Journal of Dental Research*, 87, pp.701–709.
- Huang, J. et al., 2011. MimoDB 2.0: a mimotope database and beyond. *Nucleic Acids Research*, pp.1–7.
- Huang, Y. et al., 2005. Programmable assembly of nanoarchitectures using genetically engineered viruses. *Nano Letters*, 5, pp.1429–1434.
- Höcker, B., 2014. Design of proteins from smaller fragments-learning from evolution. *Current Opinion in Structural Biology*, 27, pp.56–62.
- Höök, F. et al., 1998. Energy dissipation kinetics for protein and antibody-antigen adsorption under shear oscillation on a quartz crystal microbalance. *Langmuir*, 14, pp.729–734

- Jia, W.-D. et al., 2014. A novel peptide that selectively binds highly metastatic hepatocellular carcinoma cell surface is related to invasion and metastasis. *Cancer Letters*, 247(2), pp.234–242.
- Jia, Z. & Davies, P.L., 2002. Antifreeze proteins: an unusual receptor-ligand interaction. *Trends in Biochemical Sciences*, 27 (2), pp.101–106.
- Jiang, Y.-Q. et al., 2006. Targeting of hepatoma cell and suppression of tumor growth by a novel 12mer peptide fused to superantigen TSST-1. *Molecular Medicine*, 12, pp.81–87.
- Kacar, B.T. et al., 2009. Quartz binding peptides as molecular linkers towards fabricating multifunctional micropatterned substrates. *Advanced Materials*, 21, pp.295–299.
- Kacar, T. et al., 2009. Directed self-immobilization of alkaline phosphatase on micro-patterned substrates via genetically fused metal-binding peptide. *Biotechnology and Bioengineering*, 103 (4), pp.696–705.
- Karaca, B., Hnilova, M. & Tamerler, C., 2014. Addressable biological functionalization of inorganics: Materials-selective fusion proteins in bio-nanotechnology. In M.R. Knecht & T.R. Walsh, eds. *Bio-Inspired Nanotechnology SE – 8*. Springer New York, pp.221–255.
- Kehoe, J.W. & Kay, B.K., 2005. Filamentous phage display in the new millennium. *Chemical Reviews*, 105 (11), pp.4056–4072.
- Kelly, S.M. & Price, N.C., 2000. The use of circular dichroism in the investigation of protein structure and function. *Current Protein & Peptide Science*, 1, pp.349–384.
- Kessel, A. & Ben-Tal, N., 2010. *Introduction to Proteins: Structure, Function, and Motion*, Chapman & Hall/CRC Mathematical and Computational Biology, CRC Press pp.1–65.
- Khatayevich, D. et al., 2012. Controlling the surface chemistry of graphite by engineered self-assembled peptides. *Langmuir*, 28 (23), pp.8589–8593.
- Khatayevich, D. et al., 2010. Biofunctionalization of materials for implants using engineered peptides. *Acta Biomaterialia*, 6 (12), pp.4634–4641.
- Khoo, X. et al., 2010. Staphylococcus aureus resistance on titanium coated with multivalent PEGylated-peptides. *Biomaterials*, 31 (35), pp.9285–9292.
- Khoo, X. et al., 2009. Directed assembly of PEGylated-peptide coatings for infection-resistant titanium metal. *Journal of the American Chemical Society*, 131 (31), pp.10992–10997.

- Kim, J. et al., 2010. Peptide-mediated shape- and size-tunable synthesis of gold nanostructures. *Acta Biomaterialia*, 6 (7), pp.2681–2689.
- Komeili, A., 2007. Molecular mechanisms of magnetosome formation. *Annual Review of Biochemistry*, 76, pp.351–366.
- Krauland, E.M. et al., 2007. Peptide tags for enhanced cellular and protein adhesion to single-crystalline sapphire. *Biotechnology and Bioengineering*, 97 (5), pp.1009–1020.
- Krysiak, S. et al., 2014. Peptide desorption kinetics from single molecule force spectroscopy studies. *Journal of the American Chemical Society*, 136 (2), pp.688–697
- Kröger, N. et al., 2002. Self-assembly of highly phosphorylated silaffins and their function in biosilica morphogenesis. *Science*, 298, pp.584–586.
- Kyte, J. & Doolittle, R.F., 1982. A simple method for displaying the hydropathic character of a protein. *Journal of Molecular Biology*, 157 (1), pp.105–132.
- Langmuir, I., 1918. The Adsorption of Gases on Plane Surface of Glass, Mica and Platinum. *Journal of the American Chemical Society* 40 (9), pp 1361–1403.
- Li, Y. et al., 2014. Peptide-mediated synthesis of gold nanoparticles: effects of peptide sequence and nature of binding on physicochemical properties. *Nanoscale*, 2014, 6, pp. 3165–3172.
- Li, Y., Whyburn, G.P. & Huang, Y., 2009. Specific peptide regulated synthesis of ultrasmall platinum nanocrystals. *Journal of the American Chemical Society*, 131 (44), pp.15998–15999.
- Linder, M.B., 2009. Hydrophobins: Proteins that self assemble at interfaces. *Current Opinion in Colloid & Interface Science*, 14(5), pp.356–363.
- Lu, Z. et al., 1995. Expression of thioredoxin random peptide libraries on the *Escherichia coli* cell surface as functional fusions to flagellin: a system designed for exploring protein-protein interactions. *Bio/technology*, 13, pp.366–372.
- Löfblom, J., 2011. Bacterial display in combinatorial protein engineering. *Biotechnology Journal*, 6 (9), pp.1115–1129.
- Mammen, M., Choi, S.-K. & Whitesides, G.M., 1998. Polyvalent interactions in biological systems: Implications for design and use of multivalent ligands and inhibitors. *Angewandte Chemie International Edition*, 37, pp.2754–2794.

- Maruta, F. et al., 2003. Use of a phage display library to identify oligopeptides binding to the luminal surface of polarized endothelium by ex vivo perfusion of human umbilical veins. *Journal of Drug Targeting*, 11, pp.53–59.
- Masica, D.L. et al., 2010. De novo design of peptide-calcite biomineralization systems. *Journal of the American Chemical Society*, 132, pp.12252–12262.
- Matmor, M. & Ashkenasy, N., 2012. Modulating semiconductor surface electronic properties by inorganic peptide-binders sequence design. *Journal of the American Chemical Society*, 134 (50), pp.20403–20411.
- Menendez, A. & Scott, J.K., 2005. The nature of target-unrelated peptides recovered in the screening of phage-displayed random peptide libraries with antibodies. *Analytical Biochemistry*, 336 (2), pp.145–157.
- Meyers, M.A. et al., 2008. Biological materials: Structure and mechanical properties. *Progress in Materials Science*, 53(1), pp.1–206.
- Miller, S.J. et al., 2012. Targeted detection of murine colonic dysplasia in vivo with flexible multispectral scanning fiber endoscopy. *Journal of Biomedical Optics*, 17, p.021103.
- Mirau, P.A., Naik, R.R. & Gehring, P., 2011. Structure of peptides on metal oxide surfaces probed by NMR. *Journal of the American Chemical Society*, 133 (45), pp.18243–18248.
- Mizuguchi, H. et al., 2000. Screening of an oligopeptide antagonist for interleukin-6 from a random phage library. *Biotechnology Letters*, 22 (12), pp.1015–1020.
- Naik, R.R. et al., 2004. Peptide templates for nanoparticle synthesis derived from polymerase chain reaction-driven phage display. *Advanced Functional Materials*, 14 (1), pp.25–30.
- Naik, R.R. et al., 2002. Biomimetic synthesis and patterning of silver nanoparticles. *Nature Materials*, 1 (3), pp.169–172.
- Nam, K.T. et al., 2006. Virus-enabled synthesis and assembly of nanowires for lithium ion battery electrodes. *Science*, 312, pp.885–888.
- Nam, Y.S. et al., 2010. Biologically templated photocatalytic nanostructures for sustained light-driven water oxidation. *Nature Nanotechnology*, 5 (5), pp.340–344.

- New England Biolabs, 2014. Ph.D. Phage Display Libraries. Instruction Manual, Version 1.2. Access online: <http://www.neb.com/nebecomm/ManualFiles/manualE8111.pdf>
- Nguyen, K.T.H. et al., 2014. Identification and characterization of mutant clones with enhanced propagation rates from phage-displayed peptide libraries. *Analytical Biochemistry*, 462, pp.35–43.
- Oh, D. et al., 2014. M13 virus-directed synthesis of nanostructured metal oxides for lithium-oxygen batteries. *Nano Letters*, 14 (8), pp.4837–4845.
- Oh, D. et al., 2013. Biologically enhanced cathode design for improved capacity and cycle life for lithium-oxygen batteries. *Nature communications*, 4, p.2756.
- Oren, E.E. et al., 2010. Probing the molecular mechanisms of quartz-binding peptides. *Langmuir*, 26 (13), pp.11003–11009.
- Oren, E.E. et al., 2007. A novel knowledge-based approach to design inorganic-binding peptides. *Bioinformatics*, 23 (21), pp.2816–2822
- Ozgur, U. et al., 2007. Adsorption behavior of linear and cyclic genetically engineered platinum binding peptides. *Langmuir*, 23 (19), 7895–7900
- Pacardo, D.B. et al., 2009. Biomimetic synthesis of Pd nanocatalysts for the stille coupling reaction. *ACS Nano*, 3 (5), pp.1288–1296
- Park, T.J. et al., 2006. Protein nanopatterns and biosensors using gold binding polypeptide as a fusion partner. *Analytical Chemistry*, 78 (20), pp.7197–7205.
- Pashov, A. et al., 2005. Targeting carbohydrate antigens in HIV vaccine development. *Vaccine*. pp. 2168–2175.
- Patwardhan, S. V et al., 2012. Chemistry of aqueous silica nanoparticle surfaces and the mechanism of selective peptide adsorption. *Journal of the American Chemical Society*, 134(14), pp.6244–6256.
- Puddu, V. & Perry, C.C., 2012. Peptide adsorption on silica nanoparticles: evidence of hydrophobic interactions. *ACS Nano*, 6 (7), pp.6356–6363.
- Ramakrishnan, S.K. et al., 2014. Molecular Mechanism of Selective Binding of Peptides to Silicon Surface. *Journal of Chemical Information and Modeling* 2014 54 (7), 2117-2126
- Reiss, B.D. et al., 2004. Biological routes to metal alloy ferromagnetic nanostructures. *Nano Letters*, 4, pp.1127–1132.



- Roy, R.K. & Lee, K.R., 2007. Biomedical applications of diamond-like carbon coatings: A review. *Journal of Biomedical Materials Research Part B Applied Biomaterials*, 83 (1), pp.72–84.
- Ruan, L. et al., 2013. Tailoring molecular specificity toward a crystal facet: a lesson from biorecognition toward Pt{111}. *Nano Letters*, 13, pp. 840–846
- Rusmini, F., Zhong, Z. & Feijen, J., 2007. Protein immobilization strategies for protein biochips. *Biomacromolecules*, 8 (6), pp.1775–1789.
- Sanghvi, A.B. et al., 2005. Biomaterials functionalization using a novel peptide that selectively binds to a conducting polymer. *Nature Materials*, 4 (6), pp.496–502.
- Sano, K.-I., Ajima, K., et al., 2005a. Endowing a ferritin-like cage protein with high affinity and selectivity for certain inorganic materials. *Small*, 1 (8-9), pp.826–832.
- Sano, K.-I., Sasaki, H. & Shiba, K., 2005b. Specificity and biomineralization activities of Ti-binding peptide-1 (TBP-1). *Langmuir*, 21 (7), pp.3090–3095.
- Sano, K.-I. & Shiba, K., 2003. A hexapeptide motif that electrostatically binds to the surface of titanium. *Journal of the American Chemical Society*, 125 (47), pp.14234–14235.
- Sarikaya, M. et al., 2003. Molecular biomimetics: Nanotechnology through biology. *Nature Materials*, 2 (9), pp.577–585.
- Schneider, J. & Ciacchi, L.C., 2012. Specific material recognition by small peptides mediated by the interfacial solvent structure. *Journal of the American Chemical Society*, 134 (4), pp.2407–2413.
- Schreiber, F., 2000. Structure and growth of self-assembling monolayers. *Progress in Surface Science*, 65 (5–8), pp.151–257.
- Schrier, S.B., Sayeg, M.K. & Gray, J.J., 2011. Prediction of calcite morphology from computational and experimental studies of mutations of a de novo-designed peptide. *Langmuir*, 27 (18), pp.11520–11527.
- Schwemmer, T. & Baumgartner, J., 2012. Peptide-mediated nanoengineering of inorganic particle surfaces: a general route toward surface functionalization via peptide adhesion domains. *Journal of the American Chemical Society*, 134, pp. 2385–2391.
- Seker, U.O.S. & Demir, H.V., 2011. Material binding peptides for nanotechnology. *Molecules*, 16 (2), pp.1426–1451.

- Seker, U.O.S. et al., 2009. Quantitative affinity of genetically engineered repeating polypeptides to inorganic surfaces. *Biomacromolecules*, 10 (2), pp.250–257.
- Sengupta, A. et al., 2008. A Genetic Approach for Controlling the Binding and Orientation of Proteins on Nanoparticles. *Langmuir*, 24 (14), pp.2000–2008.
- Senn, H.M. & Thiel, W., 2009. QM/MM methods for biomolecular systems. *Angewandte Chemie International Edition*, 48, pp.1198–1229.
- Serizawa, T. et al., 2007a. Cellulose-binding heptapeptides identified by phage display methods. *Chemistry Letters*, 36 (8), pp.988–989
- Serizawa, T., Sawada, T. & Kitayama, T., 2007b. Peptide motifs that recognize differences in polymer-film surfaces. *Angewandte Chemie International Edition*, 46 (5), pp.723–726.
- Serizawa, T., Sawada, T. & Matsuno, H., 2007c. Highly Specific Affinities of Short Peptides against Synthetic Polymers. *Langmuir*, 23 (22), pp.11127–11133
- Sheikholeslam, M., Pritzker, M. & Chen, P., 2012. Dispersion of multiwalled carbon nanotubes in water using ionic-complementary peptides. *Langmuir*, 28 (34), pp.12550–12556.
- Shen, X. et al., 1997. Molecular cloning and characterization of Lustrin A, a matrix protein from shell and pearl nacre of *Halotis rufescens*. *Journal of Biological Chemistry*, 272, pp.32472–32481.
- Shiba, K., 2010. Exploitation of peptide motif sequences and their use in nanobiotechnology. *Current Opinion in Biotechnology*, 21 (4), pp.412–425
- Shimizu, K. et al., 1998. Silicatein  $\alpha$ : Cathepsin L-like protein in sponge biosilica. *Proceedings of the National Academy of Sciences U.S.A.*, 95 (11), pp.6234–6238.
- Shin, J.S. et al., 2001. Monoclonal antibodies specific for *Neisseria meningitidis* group B polysaccharide and their peptide mimotopes. *Infection and Immunity*, 69, pp.3335–3342.
- Shoulders, M.D. & Raines, R.T., 2009. Collagen structure and stability. *Annual Review of Biochemistry*, 78, pp.929–958.
- Shtatland, T. et al., 2007. PepBank—a database of peptides based on sequence text mining and public peptide data sources. *BMC Bioinformatics*, 8, p.280.

- Slocik, J.M. & Naik, R.R., 2010. Probing peptide-nanomaterial interactions. *Chemical Society Reviews*, 39(9), pp.3454–3463.
- Smith, G. & Petrenko, V., 1997. Phage display. *Chemical Reviews*, 2665 (97), 391–410.
- So, C.R. et al., 2012. Controlling self-assembly of engineered peptides on graphite by rational mutation. *ACS Nano*, 6 (2), pp.1648–56.
- Stewart, R.J., Ransom, T.C. & Hlady, V., 2011. Natural underwater adhesives. *Journal of Polymer Science. Part B, Polymer Physics*, 49 (11), pp.757–771
- Su, Z. et al., 2007. Single-walled carbon nanotube binding peptides: probing tryptophan's importance by unnatural amino acid substitution. *The Journal of Physical Chemistry. B*, 111 (51), pp.14411–14417.
- Su, Z., Leung, T. & Honek, J.F., 2006. Conformational selectivity of peptides for single-walled carbon nanotubes. *The Journal of Physical Chemistry. B*, 110 (47), pp.23623–23627.
- Suzuki, N. et al., 2007. Adsorption of genetically engineered proteins studied by time-of-flight secondary ion mass spectrometry (TOF-SIMS). Part A: data acquisition and principal component analysis (PCA). *Interface*, pp.419–426.
- Tamerler, C. et al., 2010. Molecular biomimetics: GEPI-based biological routes to technology. *Biopolymers*, 94 (1), pp.78–94.
- Tamerler, C. et al., 2006. Adsorption kinetics of an engineered gold binding Peptide by surface plasmon resonance spectroscopy and a quartz crystal microbalance. *Langmuir*, 22 (18), pp.7712–7718.
- Tamerler, C. & Sarikaya, M., 2009. Genetically designed Peptide-based molecular materials. *ACS Nano*, 3 (7), pp.1606–1615.
- Tamerler, C. & Sarikaya, M., 2007. Molecular biomimetics: utilizing nature's molecular ways in practical engineering. *Acta Biomaterialia*, 3 (3), pp.289–299.
- Tang, Z. et al., 2013. Biomolecular Recognition Principles for Bionanocombinatorics: An Integrated Approach to Elucidate Enthalpic and Entropic Factors. *ACS Nano* 2013 7 (11), pp.9632–9646.
- Terskikh, A.V. et al., 1997. "Peptabody": a new type of high avidity binding protein. *Proceedings of the National Academy of Sciences U.S.A.*, 94 (5), pp.1663–1668.

- Thomas, W.D., Golomb, M. & Smith, G.P., 2010. Corruption of phage display libraries by target-unrelated clones: Diagnosis and countermeasures. *Analytical Biochemistry*, 407, pp.237–240.
- Tipps, M.E. et al., 2010. Identification of novel specific allosteric modulators of the glycine receptor using phage display. *The Journal of Biological Chemistry*, 285, pp.22840–22845.
- Tompkins, H.G. & Irene E.A., 2005. *Handbook of Ellipsometry*, William Andrew.
- Vallee, A., Humblot, V. & Pradier, C.-M., 2010. Peptide interactions with metal and oxide surfaces. *Accounts of Chemical Research*, 43 (10), pp.1297–306.
- Vodnik, M. et al., 2011. Phage display: selecting straws instead of a needle from a haystack. *Molecules*, 16 (1), pp.790–817
- Vreuls, C. et al., 2010. Inorganic-binding peptides as tools for surface quality control. *Journal of Inorganic Biochemistry*, 104 (10), pp.1013–1021.
- Walsh, T., 2014. Fundamentals of Peptide-Materials Interfaces. In M.R. Knecht & T.R. Walsh, eds. *Bio-Inspired Nanotechnology SE – 2*. Springer New York, pp.17–36.
- Wang, S. et al., 2003. Peptides with selective affinity for carbon nanotubes. *Nature Materials*, 2 (3), pp.196–200.
- West, P.E., 2006. *Introduction to Atomic Force Microscopy: Theory, Practice, Applications*. P. West.
- Wirtz, D.H., 2009. *Strukturbasierte Entwicklung von Kinaseinhibitoren*, Köln University, Germany.
- Wong, L.S., Khan, F. & Micklefield, J., 2009. Selective Covalent Protein Immobilization: Strategies and Applications. *Chemical Reviews*, 109 (9), pp.4025–4053.
- Wölcke, J. & Weinhold, E., 2001. A DNA-binding peptide from a phage display library. *Nucleosides, Nucleotides and Nucleic Acids*, 20 (4–7), pp.1239–1241.
- Yin, Y. et al., 2012. Comparison on protein adsorption properties of diamond-like carbon and nitrogen-containing plasma polymer surfaces. *Thin Solid Films*, 520 (7), pp.3021–3025.
- Yoshida, H. et al., 2003. Improved substrate specificity of water-soluble pyrroloquinoline quinone glucose dehydrogenase by a peptide ligand. *Biotechnology Letters*, 25, pp.301–305.

- Yu, L. et al., 2008. Protein HGFI from the edible mushroom *Grifola frondosa* is a novel 8 kDa class I hydrophobin that forms rodlets in compressed monolayers. *Microbiology*, 154, pp.1677–1685.
- Yuca, E. et al., 2011. In vitro labeling of hydroxyapatite minerals by an engineered protein. *Biotechnology and Bioengineering*, 108 (5), pp.1021–30.
- Zong, X.L. et al., 2011. Transforming growth factor-1 phage model peptides isolated from a phage display 7-mer peptide library can inhibit the activity of keloid fibroblasts. *Chinese Medical Journal*, 124, pp.429–435.

PUBLICATION I

## **Selection and characterization of peptides binding to diamond-like carbon**

Colloids and Surfaces: B, Biointerfaces 2013, 110C: 66–73.

Copyright 2013 Elsevier.

Reprinted with permission from the publisher.



## Selection and characterization of peptides binding to diamond-like carbon



Bartosz Gabryelczyk<sup>a</sup>, Géza R. Szilvay<sup>a</sup>, Mikko Salomäki<sup>b</sup>,  
Päivi Laaksonen<sup>a</sup>, Markus B. Linder<sup>a,c,\*</sup>

<sup>a</sup> VTT Technical Research Centre of Finland, P.O. Box 1000, FI-02044 VTT, Espoo, Finland

<sup>b</sup> Department of Chemistry, University of Turku, FI-20014, Finland

<sup>c</sup> Department of Biotechnology and Chemical Technology, Aalto University, P.O. Box 16100, FI-00076 Aalto, Finland

### ARTICLE INFO

#### Article history:

Received 11 January 2013

Received in revised form 5 April 2013

Accepted 8 April 2013

Available online xxx

#### Keywords:

Diamond-like carbon  
Inorganic binding peptides  
Alkaline phosphatase  
Phage display  
Ellipsometry  
Protein adsorption

### ABSTRACT

Phage display was used to find peptides specific for amorphous diamond-like carbon (DLC). A set of putative binders was analyzed in detail and one sequence was found that functioned both as a peptide fused to the pIII protein in M13 phage and as a peptide fused to the enzyme alkaline phosphatase (AP). The dissociation constant of the peptide–AP fusion on DLC was 63 nM and the maximum binding capacity was 6.8 pmol/cm<sup>2</sup>. Multiple ways of analysis, including phage titer, enzyme-linked immunosorbent assay, and ellipsometry were used to analyze binding and to exclude possible false positive results. DLC binding peptides can be useful for self-assembling coatings for modifying DLC in specific ways.

© 2013 Elsevier B.V. All rights reserved.

### 1. Introduction

Interactions between biomolecules and inorganic material surfaces are essential for the formation and properties of biological composite materials such as nacre, bone, and spiculi [1,2]. For example, proteins and peptides control the nucleation, growth, and assembly of the mineral phase via specific molecular recognition [2]. Although interactions of proteins and peptides with solid surfaces are very common in nature there is only limited knowledge of how proteins specifically recognize solid materials and how this process can be controlled.

Understanding material specific molecular binding is important for the engineering of new self-assembled systems that can be utilized for example in biomimetic materials, biomedical materials, and biosensors [3–5]. Selecting novel material specific peptides from combinatorial peptide libraries (such as phage display libraries) peptide–surface interaction factors can be identified [6–9]. Due to their relative simplicity, peptides serve as good model systems for the study of molecular recognition, surface binding,

and self-assembly at interfaces. Furthermore, the short, functional peptides offer many possibilities for the formation of hierarchical assemblies [10–13].

Material specific peptides can be identified through peptide display or directed evolution systems, thereby overcoming difficulties in rationally designing peptides with predicted functions [14]. In this approach, a combinatorial peptide library usually with equal length but randomized amino acid sequence is displayed for example on the surface of filamentous phages or bacterial cells. Surface displayed peptides with a desired function can be identified by selecting or screening for a particular binding function. Phage display and cell surface display have been used to select peptides that bind to various solid materials like metals [15–17], metal oxides [18], semiconductors [19], minerals [20], carbon materials [21–23], polymers [24]. The short functional peptides can be further engineered using recombinant DNA technology to create mutations, recombinations, and tandem repeats. The modifications can improve binding properties of the peptides and tailor their function for a particular application. Furthermore, engineered material specific peptides can be fused with other biomolecules thus creating multifunctional molecules [22,25].

In this study we focused on diamond like carbon (DLC) which is an amorphous carbon material that is used as an extremely wear-resistant coating material. DLC coatings are chemically stable, optically transparent and have good mechanical properties due to their hardness, low friction coefficient, high wear and corrosion

\* Corresponding author at: VTT Technical Research Centre of Finland, P.O. Box 1000, FI-02044 VTT, Espoo, Finland. Tel.: +358 40 097 1207.

E-mail addresses: bartosz.gabryelczyk@vtt.fi (B. Gabryelczyk), geza.szilvay@vtt.fi (G.R. Szilvay), mikko.salomaki@utu.fi (M. Salomäki), paiivi.laaksonen@vtt.fi (P. Laaksonen), markus.linder@vtt.fi (M.B. Linder).

resistance, and smoothness. Depending on the fabrication process, amorphous DLC can be formed with different carbon-sp<sup>3</sup>/carbon-sp<sup>2</sup> hybridization ratio, incorporated with hydrogen, or can be doped with other elements in order to tune its properties. All DLC types combine some of the superior properties of diamond [26].

DLC has been widely used as a coating material for many applications such as electronics, optics, and mechanical and biomedical devices [27,28]. Understanding and controlling the surface properties of DLC is a necessity for the use of DLC in applications such as biomedical implants, sensors, and lubrication [29–31]. Development of biomolecules that would be able to recognize DLC and bind to it strongly would enable targeted and well-defined modification and functionalization of DLC coatings for various applications. Moreover, surface modification through self-assembly of biomolecules can be advantageous compared to covalent modifications which have drawbacks such as the need to use harsh conditions, limited number of available protocols, cost and time consuming and low yield reactions. The reaction conditions in forming covalent linkages are often not biocompatible which limit usefulness in some biomedical applications [32]. The hydrogenated amorphous DLC (a-C:H) is well studied with respect to its biocompatibility properties [33], and several groups have studied adsorption of human blood proteins (HSA, fibrinogen) to DLC coatings [34–36]. However, a detailed view of the protein adsorption mechanism as well as binding affinities is still lacking. To our knowledge there are no previous studies on developing DLC binding peptides. These peptides could be used as simple model systems for understanding protein interactions with DLC and DLC biocompatibility in general.

In this paper we describe the development and characterization of peptides that bind to DLC (a-C:H) coating. Phage display was used to select DLC binding peptides from a 12-mer peptide library. The peptides were studied as fusion constructs where they were linked to either phage particles or alkaline phosphatase (AP) enzyme. Using DLC binding peptides that were genetically fused to an enzyme we could show the targeted functionalization of DLC surfaces.

## 2. Materials and methods

### 2.1. Preparation of DLC surface

DLC coating with the commercial name BALINIT<sup>®</sup> DLC (Oerlikon Balzers, Liechtenstein) was applied on blocks of stainless steel (martensitic AISI440B quenched). BALINIT<sup>®</sup> DLC is an amorphous hydrogen containing (a-C:H) type of DLC prepared by plasma-assisted chemical vapor deposition (PACVD) process. The hydrogen content of the coating was between 15 and 20% and its thickness around 2 μm. In biopanning and binding studies of selected phage clones, blocks having rounded depressions to contain the liquid (approx. 0.5 ml capacity) were used. In binding experiments with alkaline phosphatase fusion proteins, similarly coated steel rods with a diameter 3 mm, length 20 mm, and rounded edges were used as binding surfaces. For ellipsometry measurements flat blocks were used. All DLC surfaces were cleaned before the binding experiments with 2% Hellmanex<sup>®</sup> II (Hellma GmbH & Co. KG, Germany), rinsed with MilliQ – water and ethanol, and finally dried under nitrogen.

### 2.2. Biopanning with a phage display library

Peptides binding to DLC were selected from a M13 bacteriophage library displaying random 12-mer peptides (Ph.D.<sup>TM</sup>-12 phage display library, New England Biolabs, MA, USA) using the phage display method [37], and according to the suppliers

instructions. The phage library stock (reported complexity of 10<sup>9</sup> independent clones) was diluted in TBST-0.1% buffer (150 mM NaCl, 50 mM Tris-HCl, pH 7.5, 0.1% Tween 20) to a concentration of 2 × 10<sup>12</sup> pfu/ml of which 100 μl was used as the input library for the biopanning. The target surface was incubated with the phage library for 1 h at room temperature with gentle agitation, washed 10 times with TBST-0.1% buffer, and subsequently bound phage were eluted by incubating the substrate for 15 min with 0.2 M glycine-HCl buffer at pH 2.2 containing 1 mg/ml bovine serum albumin (BSA) (Sigma-Aldrich, UK). The eluate was then neutralized with 1 M Tris-HCl pH 9.5 buffer. An aliquot of eluted phage solution was used for titrating and the rest of the eluted phages were amplified by infecting *E. coli* (ER2738). Titering, amplification, and sequencing of amplified phage were performed according to instructions provided by the supplier. The amplified phage pool was then used for a subsequent round of biopanning. Three cycles of biopanning were done with increasing Tween 20 concentration in rounds two (0.25%) and three (0.5%). After the third round of biopanning the peptide sequences of randomly picked clones were determined by DNA sequencing using an automatic DNA sequencer (Applied Biosystems, CA, USA).

### 2.3. Quantification of phage particle binding by titering

Analysis of phage binding to DLC was performed using 2 × 10<sup>11</sup> pfu of amplified single phage clones in TBST-0.5% and placed in the wells coated with DLC film and incubated for 1 h at room temperature with gentle agitation. After washing 10 times with TBST-0.5% the bound phages were eluted, neutralized and titered as described above. Wild type phages (without displayed peptides) were used as negative controls.

### 2.4. Quantification of phage particle binding by ELISA

Amplified phage particles were diluted to a concentration of 1 × 10<sup>12</sup> pfu/ml in TBST-0.5% and incubated with the substrate (DLC coated wells) for 1 h. After washing the wells 10 times using TBST-0.5% a 5000-fold dilution of Anti-M13 Monoclonal antibody conjugated to horse radish peroxidase (HRP) (GE Healthcare, UK) in TBST-0.5% containing 5 mg/ml BSA, was incubated with the phage particles bound to the DLC for 1 h. Subsequently the substrate surface was washed 6 times with TBST-0.5% and an HRP substrate solution of 0.4 mM 2,2'-Azino-bis(3-ethylbenzothiazoline-6-sulfonic acid) diammonium salt (ABTS) (Sigma-Aldrich, UK) and 0.05% H<sub>2</sub>O<sub>2</sub> (Merck, Germany) in 50 mM sodium citrate was added. After 10 min the solution was transferred from the DLC coated well to a 96-well plate and the absorbance at λ = 405 nm was measured using the Varioskan Flash Multimode Reader (Thermo Scientific, MA, USA).

### 2.5. Construction of fusion proteins of peptides and alkaline phosphatase

For analyzing the binding properties of peptides outside of the phage particle context, fusion proteins were made in which selected peptides were linked to the enzyme alkaline phosphatase (AP) from *E. coli* by recombinant DNA techniques. The AP thus functioned as a reporter enzyme. Peptides were fused to the N-terminus of AP with a short linker segment (GGGPTSGGG) inserted in between. DNA constructs for fusing peptides with AP were prepared using the "Golden gate" cloning method [38] which is a one-step cloning reaction that allows the simultaneous insertion of several DNA fragments into a vector. The 12-mer peptide encoding constructs were assembled using sense and antisense synthetic oligonucleotides (Sigma-Aldrich, UK). The inserts encoding the longer peptides, and the bacterial AP gene [39] with a



6xHis tag at the C-terminus were obtained from a commercial supplier (GeneArt, Germany) as synthetic genes with suitable flanking Bsal restriction sites in entry vectors with kanamycin resistance marker gene. An expression vector pGBtacLacZ (Figure SM 1) was constructed from pKktac vector containing tac promoter (induced by isopropyl  $\beta$ -D-1-thiogalactopyranoside (IPTG)), lacIq repressor, and ampicillin resistance gene [40]. Downstream of a tac promoter and pelB signal sequence was a lacZ gene in reverse orientation for blue/white colony screening flanked by Bsal sites. An insertion between the Bsal sites removed the lacZ gene (resulting in white colonies) and Bsal sites. For the “Golden gate” reaction the oligonucleotides (phosphorylated) encoding a 12-mer peptide or entry vector containing insert of longer peptide, the entry vector containing AP, and the expression vector were combined to yield fusion constructs with pelB sequence (for periplasmic targeting) followed by the peptide encoding sequence and finally the AP gene with a hexahistidine tag. A negative control for the peptide–AP fusion was made by making an identical construct which only lacked the inserted peptide sequence.

## 2.6. Expression and purification of peptide–AP fusion proteins

Expression vectors containing the genes encoding the peptide–AP fusion proteins were transformed into the *E. coli* RV308 production strain. Cell cultures were grown in SB medium containing 100  $\mu$ g/ml ampicillin at 37 °C until OD<sub>600nm</sub> was 1. Expression of fusion proteins was induced with 1 mM IPTG (Promega, WI, USA) and carried out overnight at 30 °C. Subsequently cells were harvested by centrifugation and the periplasmic fraction was isolated by freeze/thaw cycles. Purification of peptide–AP fusion proteins was carried out by Immobilized-Metal Affinity Chromatography using a Ni-column (Pharmacia, Sweden) and a BioLogic DuoFlow chromatography system (Bio-Rad Laboratories, UK). Proteins were eluted from the column by a 5–500 mM linear imidazole (Sigma–Aldrich, UK) gradient. The fractions containing the desired proteins were pooled, concentrated using a 10 kDa MW cut-off ultrafiltration device (Amicon ultra-15, Millipore, MA, USA) and the sample buffer exchanged to TBS pH 7.5 using an Econo-Pac 10 DG column (Bio-Rad Laboratories, UK). The protein concentrations were determined from absorbance at 280 nm using a NanoDrop™ 2000c Spectrophotometer (Thermo Scientific, MA, USA). Purified proteins were analyzed for size and purity by sodium dodecyl sulfate polyacrylamide gel electrophoresis (SDS–PAGE) (Bio-Rad Laboratories, UK) and immunoblotting using anti-AP (Invitrogen, CA, USA) and anti-HIS tag (Abcam, UK) antibodies.

## 2.7. Quantification of surface binding of peptide–AP fusion proteins

Stainless steel rods coated with DLC were placed into microtiter wells containing 0.025–5  $\mu$ M of peptide–AP fusion protein in TBS buffer and incubated for 1 h at room temperature with gentle agitation. The rods were removed from the wells and loosely bound proteins were removed by washing 6 times with TBS. The amount of protein remaining bound to the DLC was quantified by measuring the enzymatic activity of AP. The washed rods were immersed in wells containing the substrate *p*-nitrophenyl phosphate (pNPP) (Sigma–Aldrich, UK) diluted in diethanolamine–MgCl<sub>2</sub> buffer (Reagen, Finland) for 10 min with gentle agitation. The product of the enzymatic reaction, *p*-nitrophenol (pNP), was quantified by measuring absorbance at 405 nm using a Varioskan Flash Multimode Reader. The amount of protein adsorbed to the DLC sticks was determined using a standard curve of AP activity for each protein. The effect of salt and pH on the DLC binding of 0.1  $\mu$ M fusion

protein was determined using TBS buffers at pHs 7, 8, and 9 or NaCl concentrations of 0–300 mM in Tris–buffer at pH 7.5.

## 2.8. Quantification of binding using ellipsometry

Ellipsometric measurements were carried out using a spectroscopic ellipsometer (Nanofilm EP3–SE, Accurion, Germany) operated at a single laser wavelength of 532 nm. The device was set up in a PCSA (polarizer–compensator–sample–analyzer) configuration and the angle of incidence was varied from 45 to 83 degrees to the surface normal during one measurement. The measurement was carried out in air at 21 °C and a relative humidity of 40%, from a DLC coated flat block that had been treated with the peptide–AP fusion proteins. A clean DLC surface was analyzed and used as the substrate material. The ellipsometric angles  $\Delta$  and  $\Psi$  were recorded via the nulling ellipsometry principle in four zones. The complex refractive index of DLC was defined by fitting the measured data to an optical box model containing of an infinitely thick DLC layer in air. The resulting values for  $n$  and  $k$  were 2.233 and 0.373 respectively. The protein film was also modeled by a box model containing of the infinite DLC layer, a protein film (dielectric material,  $n = 1.46$ ) [41,42] and air. The resulting thickness is based on the effective density of the film, thus it averages the density throughout the macroscopic film, which includes protein and the voids between them. The mass of the protein film,  $\Gamma$ , was calculated from the thickness by using the de Fejter’s formula [42]:

$$\Gamma = d_p \frac{n_p - n_a}{dn/dc} \quad (1)$$

where  $d_p$  is the thickness of the protein film,  $n_p$  is the refractive index of the protein (1.46),  $n_a$  is the refractive index of air (1.00) and  $dn/dc$  is the increment of the refractive index due to concentration increase, which can be taken as a constant 0.183 cm<sup>3</sup> g<sup>−1</sup> from the literature [42–44]. By using these values the mass was calculated using the following formula:

$$\Gamma = d_p 2.5137 \text{ g/cm}^3 \quad (2)$$

Error estimation was done based on standard deviation of three repeated measurements.

## 3. Results

### 3.1. Peptide sequences selected from the PhD-12 library

After three rounds of biopanning against DLC, 28 phage clones were randomly picked and their peptide encoding DNAs were sequenced. 18 peptide sequences were novel and were named DLCBP1–18 (Table 1). Eight of the sequenced peptides, were longer than the 12 amino acids that would nominally be expected to be found in the PhD-12 library. However, since they emerged from the selection procedure, they were chosen for further analysis and are indicated by the suffix “L” in their names.

In the pool of sequenced clones, nine of the sequenced peptides were found to have been identified in previous panning experiments using targets unrelated to DLC (Table SM 1). It has frequently been observed that propagation advantages or binding to other components of the screening system (solid phase, contaminants, blocking agents, etc.) causes some peptide sequences to enrich in biopanning [45,46]. Thus it is important to conduct a thorough characterization of the selected peptides using also phage independent methods [25,47,48]. Interestingly, one of the identified peptides had previously been described among others (Table SM 1) as a carbon nanotube binding peptide (CNTB) [23] and thus it was also chosen for further characterization.

Sequence alignment of selected clones did not show any common sequence features (Figure SM 1). The long peptide sequences

**Table 1**

Peptides sequences from a Phd-12 library selected after three rounds of biopanning against DLC surfaces.

Name	Amino acid sequence	Length <sup>a</sup>	GRAVY <sup>b</sup>	Net charge <sup>c</sup>	pI <sup>d</sup>
DLCBP1	YLTQKPSPPYQG	12	-1.367	+1	8.50
DLCBP2	KIHVWPSTPTLT	12	-0.592	+1	8.60
DLCBP3	WTCQKARCVARV	12	0.158	+2	8.96
DLCBP4	FKMPQTMVMRTK	12	-0.508	+3	11.17
DLCBP5	GFNSAYKQPMRD	12	-1.375	+1	8.59
DLCBP6	LPYPQHFGSLGR	12	-0.942	+1	8.75
DLCBP7	FPPSWLAASNRK	12	-0.425	+1	9.75
DLCBP8	LPPQHPWDNSKH	12	-1.958	0	6.92
DLCBP9	HSPVLKTPSTHA	12	-0.558	+1	8.76
DLCBP10	YSWHTDPKTLKR	12	-1.767	+2	9.70
DLCBP11(L)	HFYPGANRSTTQGGGSANLHQTAASAKNSAPQKSENKRVFFYSHSRTRRENNRSIYTA	57	-1.260	+6	10.61
DLCBP12(L)	FHLNSNPLQRSGGGPNLHHAATAASYSTPKSENKRVFFYSHSRPSGVIGKTQP	56	-0.930	+5	10.55
DLCBP13(L)	KYTTDLPNRSRWEVRPNLHQKAMQTTVTSEPKSENKRVFFYSHSKLGGKCGKSDSQ	57	-1.321	+5	9.63
DLCBP14(L)	GNLHHQSKYATNHSQPKSENKRVFFYSHSAPRADKKPKKG	42	-1.833	+6	10.09
DLCBP15(L)	TDQLRPNLHHAATSNASSSSASKSENKRVFFYSHSRHQITPPSIYR	46	-1.172	+4	10.42
DLCBP16(L)	VPLPPLTTSVQGGGSHSTSKYVNPAPKAKSENKRVFFYSHSRSPSNMRSLAYM	53	-0.925	+6	10.21
DLCBP17(L)	AGWSLHNINRSRGGGSANLHHYTSYKSAEYKSENKRVFFYSHSRQTTAASPTKSR	57	-1.282	+4	9.77
DLCBP18(L)	EDATARRIDSRRFGEVVRPNLHHYHQKPEYAAKSENKRVFFYSHSAIPMNTSKNVSL	57	-1.340	+2	9.31
CNTB	LLADTTHRRPWT	12	-0.800	0	6.92

<sup>a</sup> Amino acids.<sup>b</sup> GRAVY – grand average of hydropathicity, calculated based on [49].<sup>c</sup> Net charge at pH 7.<sup>d</sup> pI, isoelectric point. GRAVY and pI value were calculated using ProtParam program <http://web.expasy.org/protparam/>.

have short identical regions arising from mistakes in library generations (see NEB phage display manual and discussion below). All selected peptides were positively charged (except DLCBP8 and CNTB) at neutral pH (Table 1). Most peptides had hydrophilic character based on their GRAVY index [49].

### 3.2. Analysis of the size of the peptide-fused pIII protein displayed on the phage

Since sequencing showed the presence of longer peptides than the expected 12-mers, the pIII protein of the phages were analyzed by SDS-PAGE to verify that displayed peptides were also longer and not for example processed to shorter peptides during phage particle assembly (Fig. 1). The molecular weight of the mature wild-type pIII protein is 42.6 kDa, but the pIII band usually appears larger in SDS-PAGE due to the unusual glycine-rich spacer regions between its protein domains [50]. Our results showed that the pIII-band from phage displaying DLCBP11(L) had a higher molecular weight than the pIII in DLCBP1 (having a 12-mer peptide), and which, as expected, had a higher molecular weight than the wild type pIII verifying that the unexpectedly long peptides are displayed on pIII. The band for the long peptides was however somewhat

smear, suggesting that some proteolytic trimming could have occurred.

### 3.3. Phage binding analysis by titer and ELISA

For phage titer analysis we chose eight 12-mer peptide sequences (DLCBP1–8), four long peptides (DLCBP11(L)–14(L)), and the CNTB. The latter was included since CNTs and DLC are both carbon based materials and their interactions with peptides could have similar characteristics. Phages displaying peptides DLCBP1–8 showed similar or slightly less binding to DLC than the wild-type control phage (Fig. 2). The CNTB peptide displaying phage bound about twice as much as the wild-type to DLC. Interestingly, all phages displaying long peptides showed orders of magnitude more binding to DLC than the wild-type phage.

### 3.4. Peptide binding analysis with AP fusion proteins

Based on the phage particle binding analysis four peptides were chosen for in depth study using peptide–AP fusion proteins, namely DLCBP11(L), DLCBP14(L), DLCBP3, and CNTB. Adsorption isotherms of the peptide–AP fusions on DLC were determined by quantifying bound protein using the enzymatic activity of AP as a means for quantification. The long peptide DLCBP11(L) fused to AP showed highest binding amount on DLC (Fig. 3a). The binding data were fitted to a Langmuir binding model by nonlinear regression analysis using statistical software (Prism software by Graph-Pad CA, USA). A dissociation constant ( $K_d$ ) of  $63 \pm 14$  nM and a binding capacity ( $B_{max}$ ) of  $6.8 \pm 0.4$  pmol/cm<sup>2</sup> was obtained. The non-fused-AP (negative control) bound about 1.9 pmol/cm<sup>2</sup> at the maximum protein concentrations that were possible to apply. However, since it was evident that the maximum binding capacity was not reached, we did not attempt to calculate the  $K_d$ -value. The binding characteristics of the other peptide–AP fusions DLCBP14(L)-AP, DLCBP3-AP, and CNTB-AP did not significantly differ from the AP control (Fig. 3b).

### 3.5. Effect of ionic strength and pH on binding of peptide–AP fusions to DLC

The binding of both DLCBP11(L)-AP and AP decreased as pH is increased from 7 to 9 (Fig. 4b). However, the binding of

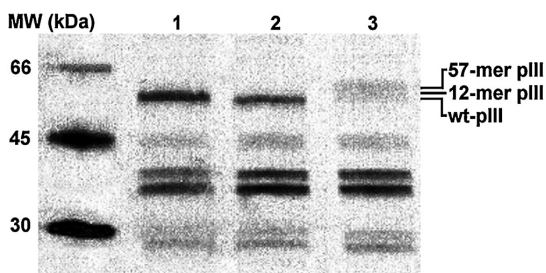


**Fig. 1.** SDS-PAGE analysis of peptide size displayed on phage particles. Phages displaying DLCBP1 (12-mer) (lane 1), no peptide (wild-type phage) (lane 2), and DLCBP11(L) (57-mer) (lane 3) were compared for the size of their pIII-peptide fusions. Protein molecular weight marker is shown in lane MW. Migration of the pIII protein variants is indicated on the right.

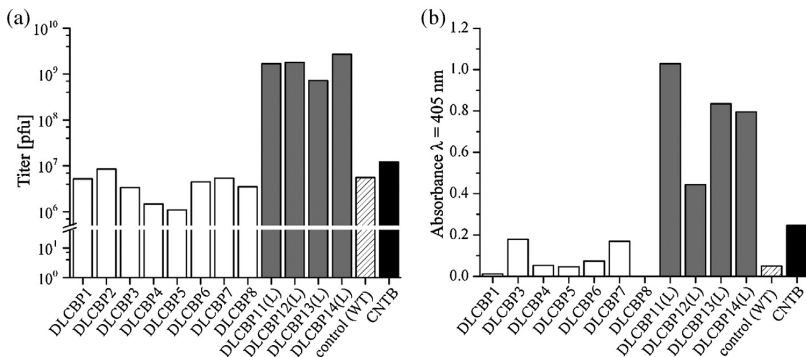


**Fig. 2.** Phage binding to DLC as determined by titer (a) and ELISA (b). When determining the titer, the phages were first eluted from the target surface and then the phages in the eluted sample were analyzed. In the ELISA the phages were analyzed directly from the surface using a phage recognizing antibody conjugated to HRP. Both independent ways of analyzing show that the phages displaying long peptides (DLCBP11(L)–14(L)) bind to the DLC surface significantly more than those displaying 12-mer peptides (DLCBP1–8, CNTB) and the wild-type.

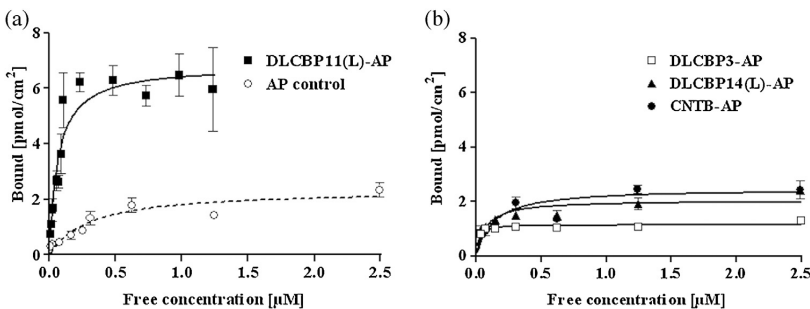


**Fig. 3.** Adsorption isotherms of peptide-AP fusion proteins on DLC. Bound protein was determined by enzymatic activity and comparison to standard activity curves. In panel (a) the adsorption of the best binding peptide-AP fusion, DLCBP11(L)-AP (filled squares), is compared with AP (open circles) and in panel (b) the adsorption of peptides DLCBP3-AP (open squares), DLCBP14(L)-AP (filled triangles), and CNTB-AP (filled circles) are shown. The Langmuir model was fitted to the DLCBP11(L)-AP adsorption data. The Langmuir model was also used to fit the other peptide and AP control data, but because maximum binding was not reached the fitted curve should merely be considered as a guide to the eye. Data are presented as mean values and showing standard deviation ( $N=3$ ).

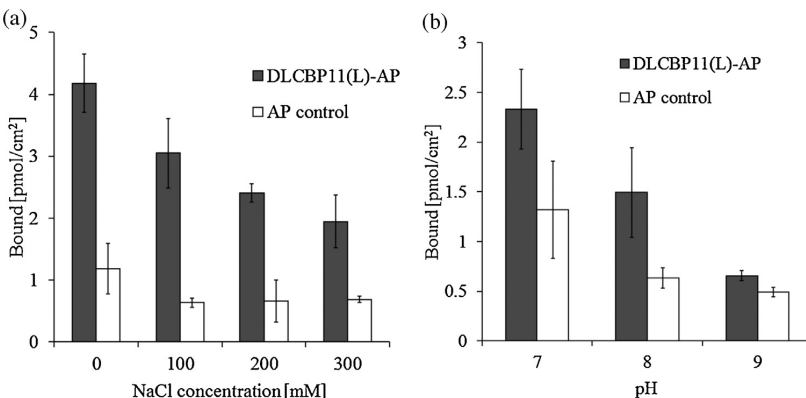


**Fig. 4.** Effect of ionic strength in various NaCl concentrations using Tris buffer at pH 7.5 (a) and pH (b) on DLCBP11(L)-AP (gray) and AP (white) binding to DLC at 0.1 μM protein concentration. The amount of bound protein was determined by the enzymatic activity of the AP. The results are means and error bars indicate standard deviations ( $N=3$ ).

DLCBP11(L)-AP is affected more and at pH 9 the amount of bound protein was almost as low as the amount of AP. Thus we can conclude that the binding of the DLCBP11(L) peptide to DLC is pH dependent. Increasing the ionic strength also reduces the amount of bound DLCBP11(L)-AP but the AP control remains mostly unaffected.

3.6. Analysis of binding to DLC by ellipsometry

Ellipsometry measurements of adsorbed proteins on DLC were carried out to verify the surface binding by a method that was independent of the enzymatic activity of AP. DLC surfaces were treated with DLCBP11(L)-AP or AP control at different concentrations and

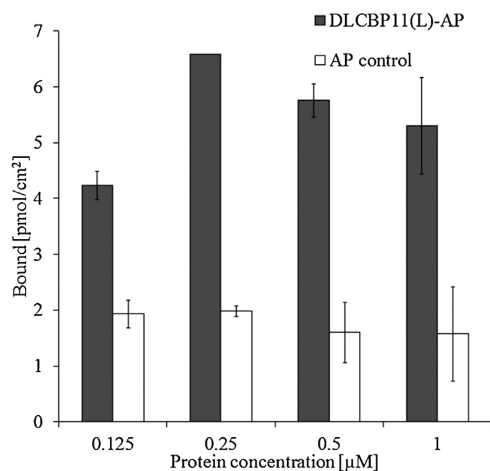


**Fig. 5.** Ellipsometry of bound DLCBP11(L)-AP layer at different applied concentrations. DLCBP11(L)-AP (gray) show higher bound mass than AP control (white). Data are means with indicated standard deviations ( $N=3$ ).

the resulting protein layer thickness was determined. The bound mass of the protein was calculated using equations 1, 2 and presented in Fig. 5. The maximum binding of DLCBP11(L)-AP and AP was  $6.6 \text{ pmol/cm}^2$  and  $2.0 \text{ pmol/cm}^2$ , respectively.

#### 4. Discussion

In this study, peptides binding to DLC were identified from a peptide library using phage display. To eliminate the possibility of false positive results, the quantification of the binding of phages was performed using two unrelated techniques (by ELISA and by titering). Additionally, the peptide function was verified by constructing AP-fusion proteins that also were analyzed in two independent ways (by enzymatic activity and by ellipsometry). A special focus on avoiding false positive results was taken since in previous studies these have been a source of erroneous conclusions [46].

As analyzed by phage particle as well as peptide-AP fusion protein, the peptide DLCBP11(L) showed the best binding to DLC. The dissociation constant of the DLCBP11(L)-AP fusion protein on a DLC surface was determined to be  $63 \text{ nM}$  (Fig. 3a), and its capacity  $6.8 \text{ pmol/cm}^2$ . When comparing the affinity to that determined for other systems it should be recalled that AP is a dimer in its native form. Because the binding entity is dimeric, the affinity of the peptide-AP is not necessarily identical to that of the individual peptide. We can expect that dimers show cooperative binding leading to a higher measured affinity. Nonetheless, the binding affinity determined for DLCBP11(L)-AP was very high, with the constant being in the nanomolar range. Values in the nanomolar range have been described before for peptide surface systems [24,25,32,51,52], most notably for gold-binding peptides. We were not able to measure a reliable value for the binding affinity for the phage particles displaying the peptide. Since it is expected that five peptides be displayed on each particle [37], it is likely that the phage particles would show even higher affinities due to multivalent binding.

It is expected that the measured capacity should ideally correspond to a molecular layer of protein on the DLC surface. Based on the measured capacity, it can be calculated that the surface area occupied by each AP molecule is about  $55 \text{ nm}^2$ . Comparing this value to the molecular dimensions of AP (structure from PDB ID: 1ED9) of  $10 \text{ nm} \times 5.5 \text{ nm}$  as determined by X-ray crystallography,

we can conclude that the binding capacity of the peptide-AP fusion is in the order of magnitude of full coverage of an ideal surface. The values are in good agreement, but should be compared only as approximate since the surface area available for the protein is not exactly known and may be affected by surface irregularities at different length scales. Measurements using ellipsometry showed a capacity value of  $6.6 \text{ pmol/cm}^2$  for DLCBP11(L)-AP, thereby confirming the results obtained by enzyme activity. The ellipsometry experiments do not depend on the enzymatic activity of AP, and therefore the results verified the applicability of using the enzymatic activity of AP for studying the peptide adhesion. However, the measurement errors at very low concentrations using ellipsometry did not allow calculating the value for affinity with sufficient accuracy.

Other peptides that performed well when displayed on the phage particle surface (DLCBP14(L), DLCBP3, and CNTB) did not show DLC binding when fused to AP (Fig. 3b). This context-dependent behavior of peptides has been observed before and one possible explanation is that the avidity effect due to pentavalency of the phage surface display enables good binding of peptides that on their own (or in divalent systems like AP) have a weak binding affinity [48,53,54]. We did not explore the reasons for this context-dependent behavior in more depth. We note however that the binding of phage particles displaying all these peptides was verified by two widely different techniques, the enzyme based ELISA test measuring bound phage particles directly on the surface, without the need of phage elution [55] and titering which relies on the biological function of phages. Analysis of phage particle binding using ELISA qualitatively correlated well with the phage titer analysis. Notably, the phages displaying long peptides bound up to 20-fold better to DLC as the wild-type control phage.

A surprising outcome of the work was that the biopanning resulted in so many phages displaying 42–54-mer peptides (about 30% of clones) along with the nominal 12-mer peptides (Table 1). These long peptides are present only <1% in the starting 12-mer peptide library according to the manufacturer and they are incidentally formed when more than one random peptide encoding DNA inserts are being incorporated into the phage genome during the library ligation process. Although long peptides present in the library are side products, they were enriched in our panning procedure that had been designed to identify DLC-binding peptides. Therefore we considered this as significant and decided to analyze them in depth along with the 12-mer peptides.

Analyzing the DNA sequence at the region of the peptides suggests by which mechanism the long peptides may have appeared in the library. In the DNA sequence of DLCBP11(L) (Fig. 6) there are two KpnI restriction sites (position 35, 170) in between which there is an additional insertion having regions coding the C-terminal end of the pIII leader sequence (VPFYSHS), 12-mer peptide, four amino acid linker (GGGS) in forward and reverse orientation respectively. The forward and reversed part of the extra insert is separated by the residue of an EagI restriction site which is non-functional because it contains a point deletion of a G in the cutting site. The DNA sequence downstream from KpnI (170) to EagI (243) restriction sites is typical for nominal phage clones displaying 12-mer peptide. Due to the extra insertion, pIII leader sequence downstream from KpnI (170) is not complete and most probably is not recognized by pIII peptidase or proteolytic cleavage is less efficient comparison to a non-mutated sequence. However, a full-length pIII leader sequence is present upstream from KpnI (35) restriction site. It is very likely that the extra insertions have occurred due to fortuitous events during the construction of the library.

There may be many reasons why longer peptides have better affinity for DLC than shorter ones. A long peptide does not simply have a higher affinity by virtue of its mass, but in a long peptide there may be more opportunities for advantageous structural

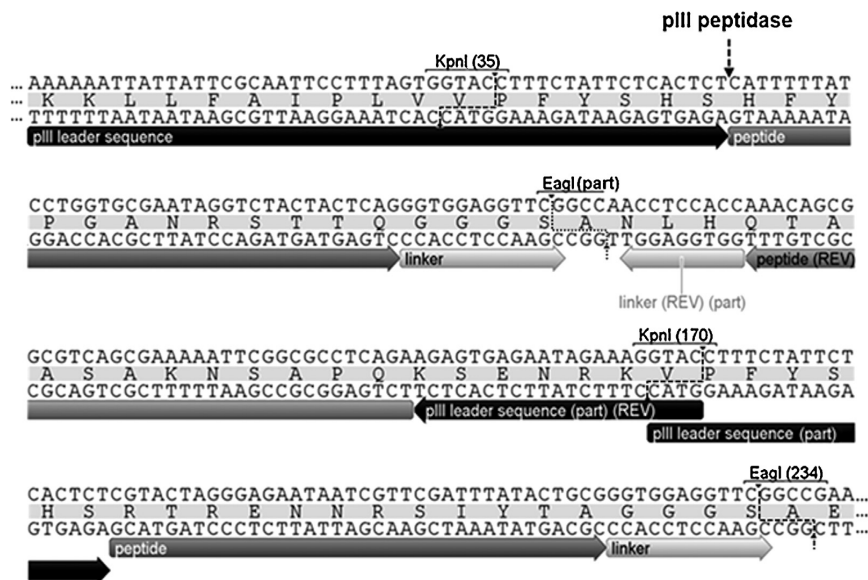


**Fig. 6.** DNA sequence and amino acid translation of the peptide coding part of the phage clone displaying DLCBP11(L). The unintended presence of the long peptide can be understood by observing the structure of the coding region. Multiple inserts in forward and reverse orientation of the randomized region can be identified due to occurrence of additional KpnI restriction site (position 35, overhangs of the inserts are marked with dashed lines). The position of the pIII peptidase cleavage site is marked with the arrow. The amino acid sequence downstream from this point is displayed on the phage.

features or favorable interactions for example hydrogen bonds or ionic interactions to form. These may then lead to higher affinities by cooperative action as observed in some repeat proteins found in nature such as anti-freeze proteins and silaffins [56,57]. Moreover, multivalency is a common strategy found in nature that increases the binding strength by the avidity effect. Engineering multivalency to molecular interaction systems is a useful strategy to increase binding strength for example by making tandem repeats [7,16,25,52] or by using nanosized scaffolds that provide multivalency [48,53,54,58]. On the other hand, in some systems it has been shown that tandem repeats do not increase binding or that there is an optimum for the number of repeats [7,25].

Experiments in which pH and ionic strength were varied were made to investigate the basics features of the interactions for DLC affinity. DLC (a-C:H) consists of amorphous carbon with a mixture of sp<sup>2</sup> and sp<sup>3</sup> C–C bonds and incorporated hydrogen atoms. The surface has a water contact angle of about 53–57° and is thus classified as hydrophilic. The DLCBP11(L) peptide does not reveal any overall feature that could be identified based on its amino acid sequence or composition. The peptide is slightly hydrophilic and its composition does not significantly differ from the average of the library. In a previous computational study [59] it was suggested that increasing the polarity of DLC by introducing polar elements to the surface resulted in decreased peptide adsorption. Therefore non-polar interactions would be the main driving force for binding. Our results do not support these findings as our data suggest that polar interactions play a role in the binding.

The binding of DLCBP11(L) was reduced by increasing the ionic strength and pH as compared to the control protein AP (Fig. 4) which would point toward a dependence of ionic interactions. H-bonding or van der Waals components may have a role in forming the peptide–surface interaction and it is unlikely that binding could simply be explained by the hydrophobic effect. Currently it is unclear what these determinants are, if they involve the formation of a peptide secondary structure or if they are more directly involved in the surface binding.

### 5. Conclusions

In conclusion the DLCBP11(L) peptide identified from a peptide library binds strongly to its target surface DLC. The enrichment of longer peptides than the nominal library peptides indicates that a strong binding to DLC can be achieved by increasing the binding interface size. The developed specific DLC–peptide interaction enables the non-covalent modification and functionalization of DLC surfaces for body implants, mechanical device coatings and other applications. Previously binding of peptides to metals or semi-conductors have been demonstrated, but DLC represents a new type of target for binding peptides. This shows the potential of the phage display technique, but the work also shows that much remains to be understood in terms of what types of peptides function best and how these should be constructed in terms of size and composition. The work also suggests that in general it may be advantageous to design peptide libraries for surface binding so that the displayed peptides are larger than what is currently typically used. Peptide libraries for large peptides can naturally screen a smaller segment of the total possible variation, but this may be compensated by the possible better functionality of long peptides.

### Funding

This work was funded by the VTT Graduate School and the Academy of Finland (project decision # 134256).

### Acknowledgments

We acknowledge the VTT Graduate School and the Academy of Finland for financial support, Timo Hakala, Tiina Ahlroos, and Kenneth Holmberg for help and fruitful discussion on DLC coatings.

## Appendix A. Supplementary data

Supplementary data associated with this article can be found, in the online version, at <http://dx.doi.org/10.1016/j.colsurfb.2013.04.002>.

## References

- [1] G. Luz, J. Mano, *Compos. Sci. Technol.* 70 (2010) 1777.
- [2] C. Tamerler, D. Khatayevich, M. Gungormus, T. Kacar, E.E. Oren, M. Hnilova, M. Sarikaya, *Biopolymers* 94 (2010) 78.
- [3] S.J. Segvich, H.C. Smith, D.H. Kohn, *Biomaterials* 30 (2009) 1287.
- [4] P. Laaksonen, G.R. Szilvay, M.B. Linder, *Trends Biotechnol.* 30 (2012) 191.
- [5] C. Tamerler, M. Sarikaya, *ACS Nano* 3 (2009) 1606.
- [6] A.B. Sanghvi, K.P.-H. Miller, A.M. Belcher, C.E. Schmidt, *Nat. Mater.* 4 (2005) 496.
- [7] U.O.S. Seker, B. Wilson, D. Sahin, C. Tamerler, M. Sarikaya, *Biomacromolecules* 10 (2009) 250.
- [8] S. Wang, E.S. Humphreys, S.-Y. Chung, D.F. Delduco, S.R. Lustig, H. Wang, K.N. Parker, N.W. Rizzo, S. Subramoney, Y.-M. Chiang, A. Jagota, *Nat. Mater.* 2 (2003) 196.
- [9] E.E. Oren, R. Notman, W. Kim, J.S. Evans, T.R. Walsh, R. Samudrala, C. Tamerler, M. Sarikaya, *Langmuir* 26 (2010) 11003.
- [10] C. Li, D.L. Kaplan, *Curr. Opin. Solid State Mater. Sci.* 7 (2003) 265.
- [11] S.R. Whaley, D.S. English, E.L. Hu, P.F. Barbara, A.M. Belcher, *Nature* 405 (2000) 665.
- [12] Y.S. Nam, A.P. Magyar, D. Lee, J.-W. Kim, D.S. Yun, H. Park, T.S. Pollom, D.A. Weitz, A.M. Belcher, *Nat. Nanotechnol.* 5 (2010) 340.
- [13] E. Wang, S.-H. Lee, S.-W. Lee, *Biomacromolecules* 12 (2011) 672.
- [14] E.E. Oren, C. Tamerler, D. Sahin, M. Hnilova, U.O.S. Seker, M. Sarikaya, R. Samudrala, *Bioinformatics* 23 (2007) 2816.
- [15] K.-I. Sano, K. Shiba, *J. Am. Chem. Soc.* 125 (2003) 14234.
- [16] S. Brown, *Nat. Biotechnol.* 15 (1997) 269.
- [17] R.R. Naik, S.J. Stringer, G. Agarwal, S.E. Jones, M.O. Stone, *Nat. Mater.* 1 (2002) 169.
- [18] C.K. Thai, H. Dai, M.S.R. Sastry, M. Sarikaya, D.T. Schwartz, F. Baneyx, *Biotechnol. Bioeng.* 87 (2004) 129.
- [19] C.E. Flynn, C.B. Mao, A. Hayhurst, J.L. Williams, G. Georgiou, B. Iverson, A.M. Belcher, *J. Mater. Chem.* 13 (2003) 2414.
- [20] M. Gungormus, H. Fong, I.W. Kim, J.S. Evans, C. Tamerler, M. Sarikaya, *Biomacromolecules* 9 (2008) 966.
- [21] Y. Morita, T. Ohsugi, Y. Iwasa, E. Tamiya, *J. Mol. Catal. B: Enzym.* 28 (2004) 185.
- [22] C.R. So, Y. Hayamizu, H. Yazici, C. Gresswell, D. Khatayevich, C. Tamerler, M. Sarikaya, *ACS Nano* 6 (2012) 1648.
- [23] Z. Su, T. Leung, J.F. Honek, *J. Phys. Chem. B* 110 (2006) 23623.
- [24] T. Date, J. Sekine, H. Matsuno, T. Serizawa, *ACS Appl. Mater. Interfaces* 3 (2011) 351.
- [25] T. Kacar, M.T. Zin, C. So, B. Wilson, H. Ma, N. Gul-Karaguler, A.K.-Y. Jen, M. Sarikaya, C. Tamerler, *Biotechnol. Bioeng.* 103 (2009) 696.
- [26] A. Erdemir, C. Donnet, *J. Phys. D: Appl. Phys.* 39 (2006) R311.
- [27] R. Hauert, *Diamond Relat. Mater.* 12 (2003) 583.
- [28] R. Hauert, U. Muller, *Diamond Relat. Mater.* 12 (2003) 171.
- [29] A.P. Carapeto, A.P. Serro, B.M.F. Nunes, M.C.L. Martins, S. Todorovic, M.T. Duarte, V. André, R. Colaço, B. Saramago, *Surf. Coat. Technol.* 204 (2010) 3451.
- [30] R. Maalouf, A. Soldatkin, O. Vittori, M. Sigaud, Y. Saikali, H. Chebib, A.S. Loir, F. Garrelie, C. Donnet, N. Jaffrezic-Renault, *Mater. Sci. Eng. C* 26 (2006) 564.
- [31] B. Podgornik, in: C. Donnet, A. Erdemir (Eds.), *Tribology of Diamond-Like Carbon Films SE – 16*, Springer, US, 2008, pp. 410–453.
- [32] M. Hnilova, B.T. Karaca, J. Park, C. Jia, B.R. Wilson, M. Sarikaya, C. Tamerler, *Biotechnol. Bioeng.* 109 (2012) 1120.
- [33] R.K. Roy, K.-R. Lee, *J. Biomed. Mater. Res. B* 83 (2007) 72.
- [34] H. Akasaka, N. Gawazawa, T. Suzuki, M. Nakano, S. Ohshio, H. Saitoh, *Diamond Relat. Mater.* 19 (2010) 1235.
- [35] S. Lousinian, S. Logothetidis, *Microelectron. Eng.* 84 (2007) 479.
- [36] R. Kargl, M. Kahn, S. Köstler, M. Reischl, A. Doliška, K. Stana-Kleinschek, W. Waldhauser, V. Ribitsch, *Thin Solid Films* 520 (2011) 83.
- [37] J.W. Kehoe, B.K. Kay, *Chem. Rev.* 105 (2005) 4056.
- [38] C. Engler, R. Kandzia, S. Marillonnet, *PLoS ONE* 3 (2008) e3647.
- [39] H. Shuttleworth, J. Taylor, N. Minton, *Nucleic Acids Res.* 14 (1986) 8689.
- [40] K. Takkinen, M.L. Laukkanen, D. Sizmann, K. Alfthan, T. Immonen, L. Vanne, M. Kaartinen, J.K. Knowles, T.T. Teeri, *Protein Eng.* 4 (1991) 837.
- [41] H. Arwin, *Thin Solid Films* 313–314 (1998) 764.
- [42] J.A. De Feijter, J. Benjamins, F.A. Veer, *Biopolymers* 17 (1978) 1759.
- [43] V. Ball, J.J. Ramsden, *Biopolymers* 46 (1998) 489.
- [44] H.G. Tompkins, E.A. Irene, *Handbook of Ellipsometry*, William Andrew, 2005.
- [45] L.A. Brammer, B. Bolduc, J.L. Kass, K.M. Felice, C.J. Noren, M.F. Hall, *Anal. Biochem.* 373 (2008) 88.
- [46] M. Vodnik, U. Zager, B. Strukelj, M. Lunder, *Molecules* 16 (2011) 790.
- [47] E. Estephan, C. Larroque, N. Bec, P. Martineau, F.J.G. Cuisinier, T. Cloitre, C. Gergely, *Biotechnol. Bioeng.* 104 (2009) 1121.
- [48] K.-I. Sano, K. Ajima, K. Iwahori, M. Yudasaka, S. Iijima, I. Yamashita, K. Shiba, *Small* 1 (2005) 826.
- [49] J. Kyte, R.F. Doolittle, *J. Mol. Biol.* 157 (1982) 105.
- [50] P. Van Wezenbeek, *Nucleic Acids Res.* 6 (1979) 2799.
- [51] T.M.A. Gronewold, A. Baumgartner, A. Weckmann, J. Knekties, C. Egler, *Acta Biomater.* 5 (2009) 794.
- [52] C. Tamerler, E.E. Oren, M. Duman, E. Venkatasubramanian, M. Sarikaya, *Langmuir* 22 (2006) 7712.
- [53] B.A. Helms, S.W.A. Reulen, S. Nijhuis, P.T.H.M. de Graaf-Heuvelmans, M. Merck, E.W. Meijer, *J. Am. Chem. Soc.* 131 (2009) 11683.
- [54] A.V. Terskikh, J.M. Le Doussal, R. Cramer, I. Fisch, J.P. Mach, A.V. Kajava, *Proc. Natl. Acad. Sci. U.S.A.* 94 (1997) 1663.
- [55] S. Donatan, H. Yazici, H. Bermeck, M. Sarikaya, C. Tamerler, M. Urgen, *Mater. Sci. Eng. C* 29 (2009) 14.
- [56] Z. Jia, P.L. Davies, *Trends Biochem. Sci.* 27 (2002) 101.
- [57] N. Kröger, R. Deutzmann, M. Sumper, *J. Biol. Chem.* 276 (2001) 26066.
- [58] P.O. Craig, V. Alzogaray, F.A. Goldbaum, *Biomacromolecules* 13 (2012) 1112.
- [59] K.B. Borisenko, H.J. Reavy, Q. Zhao, E.W. Abel, *J. Biomed. Mater. Res. A* 86 (2008) 1113.

PUBLICATION II

**The structural basis for function in  
diamond-like carbon binding peptides**

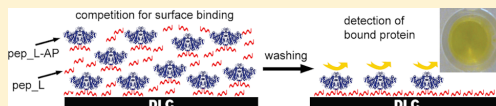
Langmuir 2014, 30 (29): 8798–8802.  
Copyright 2014 American Chemical Society.  
Reprinted with permission from the publisher.

# The Structural Basis for Function in Diamond-like Carbon Binding Peptides

Bartosz Gabryelczyk,<sup>†</sup> Géza R. Szilvay,<sup>†</sup> and Markus B. Linder<sup>\*,†,‡</sup><sup>†</sup>VTT Technical Research Centre of Finland, P.O. Box 1000, 02044 VTT, Finland<sup>‡</sup>Department of Biotechnology and Chemical Technology, Aalto University, P.O. Box 16100, 00076 Aalto, Finland

## Supporting Information

**ABSTRACT:** The molecular structural basis for the function of specific peptides that bind to diamond-like carbon (DLC) surfaces was investigated. For this, a competition assay that provided a robust way of comparing relative affinities of peptide variants was set up. Point mutations of specific residues resulted in significant effects, but it was shown that the chemical composition of the peptide was not sufficient to explain peptide affinity. More significantly, rearrangements in the sequence indicated that the binding is a complex recognition event that is dependent on the overall structure of the peptide. The work demonstrates the unique properties of peptides for creating functionality at interfaces via noncovalent binding for potential applications in, for example, nanomaterials, biomedical materials, and sensors.



## INTRODUCTION

The possibility to use phage display and evolutionary techniques to find peptides or proteins with high selectivity and affinity for solid materials or interfaces is highly interesting for a wide range of materials-related science and technology.<sup>1</sup> The control of interfaces is crucial in, for example, nanotechnology,<sup>2</sup> adhesives,<sup>3</sup> biomimetic composites,<sup>4</sup> colloidal systems,<sup>5</sup> and interfaces in biomedical materials,<sup>6</sup> and for constructing sensors.<sup>7</sup> Although several reports describe the successful use of such peptide systems, an in-depth understanding of their structural basis of function is still largely lacking. Concerns have also been raised about erroneous conclusions drawn from easily occurring artifacts due to inherent problems in both selection and characterization in widely used display systems.<sup>8,9</sup> Some attempts have also been made to create novel target specific peptides using computational based methods and rational design,<sup>10–12</sup> but the ability to design rationally or predict biomolecules with specific function is still very limited.

Given that the selected peptides show a real affinity for the interfaces under study, one can try to understand the function from two different views. One view is that the chemical composition of the peptide is sufficient for understanding the adhesion; that is, that charged residues, sulfhydryl reactivity, and hydrophobicity of side chains lead to solubility characteristics or direct interactions that favor surface adhesion. On the other hand, our understanding of how polypeptides function in nature suggests that the three-dimensional environment provided by peptides as a consequence of their specific primary structure would contribute to the function.

The question of structure–function relations in surface binding peptides has been the focus of several investigations.<sup>13–16</sup> For peptides binding to aqueous silica nanoparticles, it was found that increasing the number of amino groups gave

higher affinity due to the formation of ion-pairs and also that the formation of hydrogen bonds played an important role. On the role of protein conformation, it was concluded that increased conformational flexibility resulted in a higher affinity.<sup>13</sup> In a study on peptides recognizing poly(methyl methacrylate), alanine scanning revealed essential residues but also concluded that a Pro residue was essential, suggesting that it induced structurally important features.<sup>14</sup> For peptides binding to single walled carbon nanotubes, it was suggested that  $\pi$ – $\pi$  interactions were likely driving forces but that steric restriction of peptide conformations had a large impact on binding selectivity.<sup>15</sup> On the other hand, in a study on a conducting polymer (chlorine-doped polypyrrole), the effect of inverting the peptide sequence was small, suggesting that only amino acid composition was important, not conformation.<sup>16</sup> As a general conclusion, many studies identify a limited number of amino acids as critical, but also conclude that conformational properties, typically through altered chain flexibility, have a contributing effect.

It is seldom straightforward to understand structure–function relations in proteins. On one extreme are the intrinsically unstructured proteins that are structurally not defined, but only attain a structure when they bind to their ligand. Often mutations in one part of a protein can result in structural changes in the entire protein or locally in a different part of the protein.<sup>17</sup> These types of structural effects can make structure/function studies difficult to interpret.

In this work, we were interested in the structure–function relationships in a peptide that binds with high affinity to diamond-like carbon (DLC) and that had been selected previously by phage display.<sup>18</sup> Due to its superior phys-

Received: March 5, 2014

Published: July 9, 2014



**Table 1. Peptide Sequences and Their Physicochemical Properties, Used for Studying DLC Binding Specificity**

name	sequence	nt <sup>a</sup>	pI <sup>b</sup>
pep_L	KNSAPQKSENRRKVPFYQHQQGGSTPGGGS	+3	10
pep_L_pep	KNSAPQKSENRRKVPFYQHQQGGSTPGGGSKNSAPQKSENRRKVPFYQHQQ	+6	10.2
pep	KNSAPQKSENRRKVPFYQHQQ	+3	10
(+/-)_pep_L	<u>D</u> N <u>S</u> A <u>P</u> Q <u>D</u> SEN <u>DD</u> VVPFYQHQQGGSTPGGGS	-5	3.7
(+0)_pep_L	<u>N</u> S <u>A</u> P <u>Q</u> SEN <u>Q</u> NVVPFYQHQQGGSTPGGGS	-1	5.2

<sup>a</sup>Estimated net charge at pH 7.5. <sup>b</sup>Isoelectric point. Mutated residues are marked in bold underline and linker in bold italic. pI value was calculated using ProtParam program (<http://web.expasy.org/protparam/>).

icochemical properties, DLC is used widely as a material in biomedical applications.<sup>19</sup> Understanding the molecular basis of the interactions between peptides and DLC can enable creation of functional coatings for implants and biomedical devices. Peptides can serve as nonfouling coatings or molecular linkers for immobilizing biomolecules with desired functionality under ambient conditions overcoming problems of covalent modifications that limit usefulness in some biomedical applications.<sup>3,7,20</sup>

The aim here was to gain a fundamental understanding on how the affinity of the DLC-binding peptide can be understood in terms of its structure. The principal approach was to study the functional effect of variations in the sequence of the peptide.

## EXPERIMENTAL SECTION

**DLC Surfaces.** Stainless steel blocks (disc shape) were coated with the commercial a-C:H DLC coating BALINIT DLC (Oerlikon Balzers, Liechtenstein) and cleaned before each experiment as described previously.<sup>18</sup>

**Synthetic Peptides.** Synthetic peptides (purity > 95%) were obtained from GenScript (HK Limited, Hong Kong). The exact peptide concentration was determined by amino acid analysis (Amino Acid Analysis Center, University of Uppsala, Sweden) and verified by UPLC (Waters, U.K.) using standard curves. All peptides were dissolved in 50 mM Tris buffer pH 7.5.

**Fusion Proteins.** AP-fusion protein peptide (pep\_L) was linked to the alkaline phosphatase (AP) from *Escherichia coli* which was used as a reporter enzyme to quantify the amount of bound protein on the DLC surface. Fusion proteins were prepared by recombinant DNA techniques (golden gate cloning), expressed in *E. coli*, and purified as described previously.<sup>18</sup> Peptide pep\_L (Table 1) is a modified form of a formerly reported DLC binding sequence. Modifications were introduced to remove putative proteolysis sites in the sequence. Because of these modifications, the degree of heterogeneity of the pep\_L-AP fusion protein was reduced to <5%. The purity and homogeneity of the fusion protein was analyzed by SDS-PAGE and MALDI-TOF mass spectrometry. The binding isotherms of pep\_L-AP and the original peptide-AP fusion show that the affinities were very similar (Supporting Information Figure S1).

**Competition Assay.** Competition experiments were carried out to quantify the ability to compete for the binding to target surface between pep\_L-AP fusion protein and synthetic peptides (Tables 1 and 2). Pep\_L-AP fusion protein (concentration 0.2 μM) and the synthetic peptides were mixed together prior to the binding experiments in molar ratios varying from 1 to 250 in 50 mM Tris buffer pH 7.5. The mixture was applied on a clean DLC surface and incubated for 30 min at room temperature. Subsequently, the surfaces were washed five times by immersing the substrate (DLC coated disk) into vessels containing excess of the buffer (50 mM Tris buffer pH 7.5) to remove loosely bound biomolecules. The amount of the fusion protein bound to the DLC was quantified by measuring the enzymatic activity of AP. The AP substrate *p*-nitrophenyl phosphate (pNPP) (Sigma-Aldrich, U.K.) diluted in diethanolamine-MgCl<sub>2</sub> buffer (Reagent, Finland) was applied on the DLC surface and incubated for 10 min. The solution containing the product of the enzymatic

**Table 2. Peptide Sequences Used for Studying the Effect of Sequence Reversion**

name	sequence
pep_L	KNSAPQKSENRRKVPFYQHQQGGSTPGGGS
R_pep_L	<u>SGGGPTSGGGQHQQYFPVKRNEKQPASNK</u>
R_pep_L_1/4	<u>SKQPASNK</u> ENRRKVPFYQHQQGGSTPGGGS
R_pep_L_2/4	KNSAPQK <u>SEFPVKRNEY</u> QHQQGGSTPGGGS
R_pep_L_3/4	KNSAPQKSENRRKVP <u>FGGGHQY</u> TPGGGS
R_pep_L_4/4	KNSAPQKSENRRKVPFYQHQQGG <u>SGGGPT</u>
R_pep_L_1-2/4	<u>FPVKRNEKQPASNK</u> YQHQQGGSTPGGGS
R_pep_L_3-4/4	KNSAPQKSENRRKVP <u>FGGGPTSGGGQHQQ</u>
R_pep_L_1,4/4	<u>SKQPASNK</u> ENRRKVPFYQHQQGG <u>SGGGPT</u>
R_pep_L_2-3/4	KNSAPQK <u>SEFPVKRNEGGQHQQY</u> TPGGGS
R_pep_L_1,3/4	<u>SKQPASNK</u> ENRRKVP <u>FGGGHQY</u> TPGGGS
R_pep_L_2,4/4	KNSAPQK <u>SEFPVKRNEY</u> QHQQGG <u>SGGGPT</u>
R_pep_L_2,4/4	KNSAPQK <u>SSGGPTSGGGQHQQYFPVKRNE</u>
R_pep_L_1,3,4/4	<u>SKQPASNK</u> ENRRKVP <u>FGGGPTSGGGQHQQ</u>
R_pep_L_1-2,4/4	<u>FPVKRNEKQPASNK</u> YQHQQGG <u>SGGGPT</u>
R_pep_L_1-3/4	<u>GGGQHQQYFPVKRNEKQPASNK</u> STPGGGS

Reversed residues are marked in bold italic underline. Mutated residues are marked in bold.

reaction, *p*-nitrophenol (pNP), was transferred to a microtiter plate and quantified by measuring absorbance at 405 nm using a Varioskan Flash Multimode Reader (Thermo Scientific, Tewksbury, MA). The amount of protein adsorbed to the DLC surface was determined using a standard curve of pep\_L-AP activity.

## RESULTS AND DISCUSSION

To obtain a robust comparison of peptides, we set up a competition assay in which variants of peptides were tested for their ability to compete out the peptide pep\_L (Table 1) from a DLC surface. The pep\_L sequence was fused through genetic engineering to alkaline phosphatase (AP) to form the fusion protein pep\_L-AP. The fusion with AP provided a repeatable and robust way of assaying bound protein on the surface. A solution of fusion protein was applied on the DLC surface which was then rinsed and fusion protein remaining bound to the surface was detected by its enzymatic activity. Compared to the original DLC-binding peptide described previously,<sup>18</sup> some mutations were made to reduce heterogeneity of the fused peptide arising from proteolytic processing during protein expression. The changes did not essentially change the binding affinity of the peptide to DLC.

In Figure 1, a curve resulting from a competition experiment between the free pep\_L and pep\_L-AP is shown. The competition curve was obtained by keeping the concentration of pep\_L-AP constant and adding increasing amounts of free peptide. With increasing amounts of free peptide, less pep\_L-AP remained bound which could be detected by assaying the enzymatic activity on the surface. The data were fitted using a simple one-phase exponential decay model. We note that the

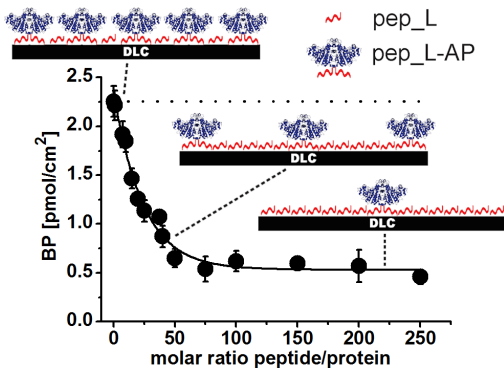


**Figure 1.** Experimental setup for the competition assay. The pep\_L-AP fusion protein and pep\_L synthetic peptide competed for binding to the target surface. The amounts of bound protein were quantified based on enzymatic activity of alkaline phosphatase (AP). Increasing the molar ratio between pep\_L and pep\_L-AP led to a reduction of the binding of fusion protein. One-phase exponential decay model was used for the data fitting. The adsorption of pep\_L-AP at molar ratio = 0 is the baseline signal (a dotted line is shown as a guide for the eye). Data are presented as mean values and showing standard deviation ( $N = 3$ ). BP, bound protein.

free peptide was able to compete out the fusion protein as expected for a specific peptide-dependent binding of the fusion protein. However, the 50% level of reduction in binding did not occur at a one-to-one ratio, but at around 17-fold excess of the peptide. This can be understood since AP naturally forms a dimer, and hence, each AP unit contains two peptides that can function in a cooperative way during binding.<sup>21</sup> To verify the dimer effect, we devised a variant pep\_L\_2 that was essentially a dimer of the initial pep\_L sequence (Table 1). For this dimer-peptide, the 50% level was reached at a ratio of about 4 (Figure 2), which verified the assumption, but showed that the AP fusion protein probably still had a more favorable geometry for synergistic binding.

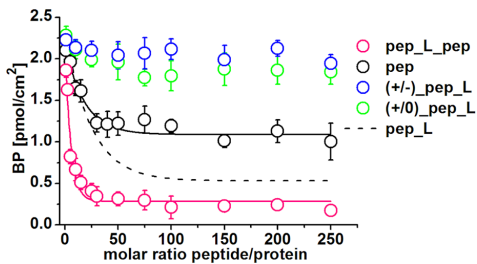


**Figure 2.** Competition experiments. The doubling of the peptide segment in pep\_L\_2 led to significantly better capability to compete with the pep\_L-AP-fusion protein, while removing the linker part in pep variant caused its partial reduction. Mutating positively charged residues to negative ones in (+/-)\_pep\_L and to neutral ones in (+/0)\_pep\_L variants led to complete loss of function. One-phase exponential decay model was used for the data fitting. Data are presented as mean values and showing standard deviation ( $N = 3$ ). BP, bound protein. Pep\_L data (from Figure 1) is shown as a reference curve.

In the peptide, we identified a segment (GGGSTPGGGG) that initially was assigned a role as a linker based on the structure of the phage display construct that was used to obtain the peptide originally. When removing this segment in the variant pep (Table 1), we noted that its ability to compete out AP fusion was decreased (Figure 2) and, therefore, conclude that this segment contributed also to the function and should be treated as a part of the unit, not only as a linker.

To gain a structure-function understanding of how material-specific peptides such as pep\_L function, we investigated the effect of point mutations. The most distinct feature that we noted in the primary structure of the peptide was that it contained an unusually high number of residues with a positive charge. Initially, four residue variants were investigated (Table 1). In the variant (+/-)\_pep\_L, the positive side chains K1, K7, R11, and R12 were changed to negatively charged D side chains. In the variant (+/0)\_pep\_L, the K residues were changed to neutral N residues and the R to Q. The competition experiments (Figure 2) showed that in both peptides targeting the positively charged residues the changes completely eliminated the capability of the peptides to compete out the AP fusion protein.

These data indicate that the positively charged residues are essential for the binding and that Coulombic interactions are the driving force for the affinity of the peptide. However, the experiments did not reveal the possible role of conformational structures in addition to the Coulombic ones. An alternate explanation may even be that the modification of charges altered the conformation of the peptide, disrupting structural features, which led to reduced affinity.

Polypeptides are asymmetrical around the peptide bond, leading to distinct amino and carboxyl termini. Thus, reversing the order of the amino acid residues leads to a structure that has an identical chemical composition with each residue also having the same neighboring residues. However, as a consequence of sequence reversal, the polypeptides do not retain the same overall conformational properties. We therefore constructed and analyzed a variant R\_pep\_L, in which the entire sequence of amino acids had been reversed (Table 2). Remarkably, this peptide showed only a very low capability to compete for binding (Figure 3a).

To investigate if it would be possible to identify a location especially sensitive to structural variations, a set of peptides was made in which varying fractions of the peptides were inverted (Table 2). Peptides with inverted segments restricted to 25% of the sequence in each and scanning throughout the sequence are shown in Table 2. Peptide R\_pep\_L\_1/4 showed approximately half the performance compared to the wild-type (giving the 50% reduction of pep\_L\_2 AP binding at about 40 peptide to fusion protein molar ratio), while peptides R\_pep\_L\_2/4, R\_pep\_L\_3/4, and R\_pep\_L\_4/4 showed almost as efficient performance in the competition experiments as the wild-type (Figure 3a).

Next, peptides were designed where two out of four segments were inverted simultaneously. Peptides R\_pep\_L\_1-2/4 and R\_pep\_L\_3-4/4 were 50% reversed (inverted two adjacent segments) (Figure 3b), and peptides R\_pep\_L\_1,4/4, R\_pep\_L\_2-3/4, R\_pep\_L\_1,3/4, and R\_pep\_L\_2,4/4 had inverted two segments in different locations (Figure 3c).

Inversion of three segments out of four at the same time (Figure 3d) led to significant loss of ability to compete for binding. Peptides R\_pep\_L\_2-4/4, R\_pep\_L\_1,3-4/4, and

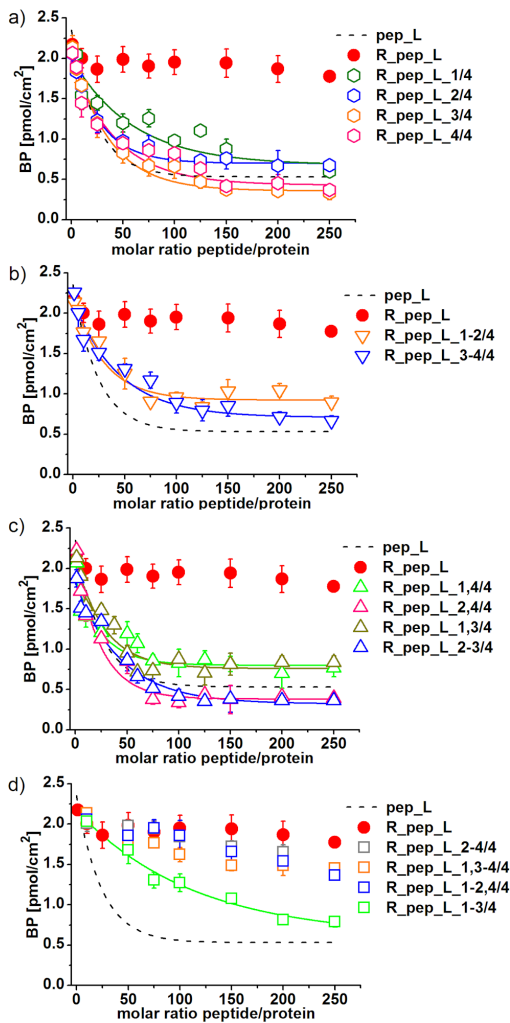


**Figure 3.** Effect of reversing the sequence of the DLC-binding peptide fully or to varying extent: (a) 25% of sequence reversed compared to fully reversed initial sequence, (b) 50% reversed, (c) 50% reversed in nonadjacent segments, and (d) 75% reversed. One-phase exponential decay model was used for the data fitting. Data are presented as mean values and showing standard deviation ( $N = 3$ ). BP, bound protein. Pep\_L data (reused from Figure 1) serve as a reference curve.

R<sub>pep\_L</sub> 1-2,4/4 showed a loss of competing ability comparable to the case of the fully reversed sequence, R<sub>pep\_L</sub>. Only the peptide R<sub>pep\_L</sub> 1-3/4 partially retained its competition ability, reaching half efficiency at a peptide fusion protein ratio of about 78 which is approximately 4.5 times lower than for the wild type peptide.

To study the solution conformation and possible conformational changes, we measured CD spectra for all the peptides (Supporting Information Figure S2). The spectra show that all of the peptides had the same conformation in solution with only minor differences in their spectra. Analysis of the spectra

showed that their shape corresponded to a random coil conformation. To investigate the possibility of formation of dimers or other multimeric forms of peptides, we investigated their retention times in size exclusion chromatography (Supporting Information Figure S3). Comparison of retention times with known standards showed that the peptides were in monomeric form in solution.

We suggest that the insight which can be obtained from this work is that the binding of pep\_L to DLC is a complex recognition event. The interaction cannot be explained by properties such as overall hydrophobicity or charge. Despite the evidence for sequence dependency, our results show that the recognition event allows a significant variation in configuration before it is critically affected (Figure 3b,c). Point mutations showed clearly that the positively charged residues were important for binding, but the collected sequence inversion data showed that the interpretation must be that the positive charges are necessary but not alone sufficient. They must be in their right conformational environment. This means that it may be unfruitful to try to exactly pinpoint critical residues. Rather the interaction is a complex event in which regions of the system are interconnected to each other in a way that is not linearly dependent on each other. As an example, some data (e.g., the 75% inversion) suggest that the C-terminal part of the peptide would have a more significant role in the function, but this conclusion is not supported by all data (e.g., the 25% inversion data). Interestingly, it was also possible to find some sequences where limited inversions led to slightly better functionality.

We showed that a competition assay functioned predictably and was an excellent tool for understanding peptide binding, excluding many problems such as nonspecific binding that typically introduces errors in direct affinity measurements. We could show better binding by the duplicated sequence as well as reduced binding by point mutations, demonstrating that the assay can be used to reliably compare affinities.

## CONCLUSIONS

Peptides provide a unique route toward functionalization of interfaces. We show here that the interactions between peptide and target are highly dependent on the complex environment provided by the peptide. This provides a new insight for understanding the function and use of engineered material-specific peptides. It also serves as a guide for interpreting the role of molecular structural context in the engineering of material architectures at the nanoscale.

## ASSOCIATED CONTENT

### Supporting Information

Additional experimental details, results, figures, and control experiments investigating a possible interaction between AP and peptides. This material is available free of charge via the Internet at <http://pubs.acs.org>.

## AUTHOR INFORMATION

### Corresponding Author

\*E-mail: [markus.linder@aalto.fi](mailto:markus.linder@aalto.fi).

### Notes

The authors declare no competing financial interest.

## ■ ACKNOWLEDGMENTS

We acknowledge the VTT Graduate School and the Academy of Finland for financial support.

## ■ ABBREVIATIONS

DLC, diamond-like carbon; AP, alkaline phosphatase; BP, bound protein

## ■ REFERENCES

- (1) Sarikaya, M.; Tamerler, C.; Jen, A. K.-Y.; Schulten, K.; Baneyx, F. Molecular Biomimetics: Nanotechnology through Biology. *Nat. Mater.* **2003**, *2*, 577–585.
- (2) Lee, Y. J.; Yi, H.; Kim, W.-J.; Kang, K.; Yun, D. S.; Strano, M. S.; Ceder, G.; Belcher, A. M. Fabricating Genetically Engineered High-Power Lithium-Ion Batteries Using Multiple Virus Genes. *Science* **2009**, *324*, 1051–1055.
- (3) Krauland, E. M.; Peelle, B. R.; Wittrup, K. D.; Belcher, A. M. Peptide Tags for Enhanced Cellular and Protein Adhesion to Single-Crystalline Sapphire. *Biotechnol. Bioeng.* **2007**, *97*, 1009–1020.
- (4) Laaksonen, P.; Szilvay, G. R.; Linder, M. B. Genetic Engineering in Biomimetic Composites. *Trends Biotechnol.* **2012**, *30*, 191–197.
- (5) Sheikholeslam, M.; Pritzker, M.; Chen, P. Dispersion of Multiwalled Carbon Nanotubes in Water Using Ionic-Complementary Peptides. *Langmuir* **2012**, *28*, 12550–12556.
- (6) Khatayevich, D.; Gungormus, M.; Yazici, H.; So, C.; Cetinel, S.; Ma, H.; Jen, A.; Tamerler, C.; Sarikaya, M. Biofunctionalization of Materials for Implants Using Engineered Peptides. *Acta Biomater.* **2010**, *6*, 4634–4641.
- (7) Park, T. J.; Lee, S. Y.; Lee, S. J.; Park, J. P.; Yang, K. S.; Lee, K. B.; Ko, S.; Park, J. B.; Kim, T.; Kim, S. K.; et al. Protein Nanopatterns and Biosensors Using Gold Binding Polypeptide as a Fusion Partner. *Anal. Chem.* **2006**, *78*, 7197–7205.
- (8) Vodnik, M.; Zager, U.; Strukelj, B.; Lunder, M. Phage Display: Selecting Straws instead of a Needle from a Haystack. *Molecules* **2011**, *16*, 790–817.
- (9) Huang, J.; Ru, B.; Zhu, P.; Nie, F.; Yang, J.; Wang, X.; Dai, P.; Lin, H.; Guo, F.-B.; Rao, N. MimoDB 2.0: A Mimotope Database and Beyond. *Nucleic Acids Res.* **2012**, *40*, D271–7.
- (10) Oren, E. E.; Tamerler, C.; Sahin, D.; Hnilova, M.; Seker, U. O. S.; Sarikaya, M.; Samudrala, R. A Novel Knowledge-Based Approach to Design Inorganic-Binding Peptides. *Bioinformatics* **2007**, *23*, 2816–2822.
- (11) Schrier, S. B.; Sayeg, M. K.; Gray, J. J. Prediction of Calcite Morphology from Computational and Experimental Studies of Mutations of a de Novo-Designed Peptide. *Langmuir* **2011**, *27*, 11520–11527.
- (12) Masica, D. L.; Schrier, S. B.; Specht, E. A.; Gray, J. J. De Novo Design of Peptide-Calcite Biomineralization Systems. *J. Am. Chem. Soc.* **2010**, *132*, 12252–12262.
- (13) Patwardhan, S. V.; Emami, F. S.; Berry, R. J.; Jones, S. E.; Naik, R. R.; Deschaume, O.; Heinz, H.; Perry, C. C. Chemistry of Aqueous Silica Nanoparticle Surfaces and the Mechanism of Selective Peptide Adsorption. *J. Am. Chem. Soc.* **2012**, *134*, 6244–6256.
- (14) Serizawa, T.; Sawada, T.; Matsuno, H. Highly Specific Affinities of Short Peptides against Synthetic Polymers. *Langmuir* **2007**, *23*, 11127–11133.
- (15) Su, Z.; Mui, K.; Daub, E.; Leung, T.; Honek, J. Single-Walled Carbon Nanotube Binding Peptides: Probing Tryptophan's Importance by Unnatural Amino Acid Substitution. *J. Phys. Chem. B* **2007**, *111*, 14411–14417.
- (16) Sanghvi, A. B.; Miller, K. P.-H.; Belcher, A. M.; Schmidt, C. E. Biomaterials Functionalization Using a Novel Peptide That Selectively Binds to a Conducting Polymer. *Nat. Mater.* **2005**, *4*, 496–502.
- (17) Dyson, H. J.; Wright, P. E. Intrinsically Unstructured Proteins and Their Functions. *Nat. Rev. Mol. Cell Biol.* **2005**, *6*, 197–208.
- (18) Gabryelczyk, B.; Szilvay, G. R.; Salomäki, M.; Laaksonen, P.; Linder, M. B. Selection and Characterization of Peptides Binding to Diamond-like Carbon. *Colloids Surf, B* **2013**, *110C*, 66–73.

(19) Roy, R. K.; Lee, K. Biomedical Applications of Diamond-Like Carbon Coatings: A Review. *J. Biomed. Mater. Res., Part B* **2007**, *72*–84.

(20) Khoo, X.; Hamilton, P.; O'Toole, G. A.; Snyder, B. D.; Kenan, D. J.; Grinstaff, M. W. Directed Assembly of PEGylated-Peptide Coatings for Infection-Resistant Titanium Metal. *J. Am. Chem. Soc.* **2009**, *131*, 10992–10997.

(21) Cantor, C.; Schimmel, P. *Biophysical Chemistry, Part III*; W. H. Freeman & Co.: New York, 1980; pp 874–1018.

PUBLICATION III

**Engineering of the function of diamond-  
like carbon binding peptides through  
structural design**

Biomacromolecules 2015, in press.  
Copyright 2015 American Chemical Society.  
Reprinted with permission from the publisher.

# Engineering of the Function of Diamond-like Carbon Binding Peptides through Structural Design

Bartosz Gabryelczyk,<sup>†,‡</sup> Géza R. Szilvay,<sup>‡</sup> Vivek K. Singh,<sup>§</sup> Joonas Mikkilä,<sup>†</sup> Mauri A. Kostianen,<sup>†</sup> Jari Koskinen,<sup>§</sup> and Markus B. Linder<sup>\*,†</sup>

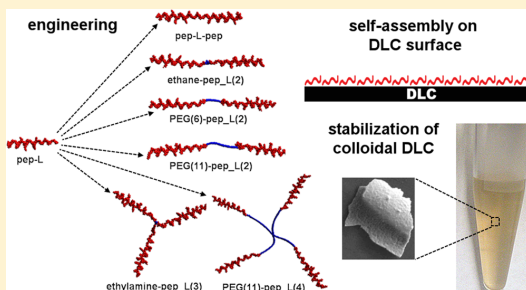
<sup>†</sup>Department of Biotechnology and Chemical Technology, Aalto University, P.O. Box 16100, 00076 Aalto, Finland

<sup>‡</sup>VTT Technical Research Centre of Finland, P.O. Box 1000, 02044 VTT, Finland

<sup>§</sup>Department of Materials Science, Aalto University, P.O. Box 11000, 00076 Aalto, Finland

**S** Supporting Information

**ABSTRACT:** The use of phage display to select material-specific peptides provides a general route towards modification and functionalization of surfaces and interfaces. However, a rational structural engineering of the peptides for optimal affinity is typically not feasible because of insufficient structure–function understanding. Here, we investigate the influence of multivalency of diamond-like carbon (DLC) binding peptides on binding characteristics. We show that facile linking of peptides together using different lengths of spacers and multivalency leads to a tuning of affinity and kinetics. Notably, increased length of spacers in divalent systems led to significantly increased affinities. Making multimers influenced also kinetic aspects of surface competition. Additionally, the multivalent peptides were applied as surface functionalization components for a colloidal form of DLC. The work suggests the use of a set of linking systems to screen parameters for functional optimization of selected material-specific peptides.



## INTRODUCTION

Biology shows an impressive diversity in functional materials based on a relatively limited set of basic building blocks. The virtually endless variation that proteins exhibit at interfaces inspires researchers to harness some of these possibilities for development of practical applications. Examples of how the functionality of even relatively short peptides can be used to control assembly and ultrastructure in devices such as batteries,<sup>1</sup> photovoltaic systems,<sup>2</sup> or tools for cancer imaging and detection<sup>3,4</sup> show the wide application range of this technology.

Sophisticated biotechnological techniques such as phage display allow the use of evolutionary approaches for the identification of interactions that are not found in nature. This access to new types of molecules has the potential to change many aspects of materials science.<sup>5–7</sup> The understanding of how peptides interact with surfaces and how these interactions can be engineered at different levels offers research challenges that will lead to a toolbox for building nanostructured materials, adhesives, biosensors, and nonfouling and biomineralization agents.<sup>7</sup>

Many native biological systems, such as antifreeze proteins,<sup>8</sup> receptors, antibodies or viruses contain multimeric binding sites that function in a cooperative way and by this mechanism increase the strength of interactions with their targets due to a

cooperative effect, also referred to as avidity<sup>9</sup> or multivalency.<sup>10</sup> The concept of enhanced binding due to display of multiple functional units could be also potentially used in surface science to create very stable, high affinity binding peptide coatings.

Multivalency in peptide systems can be achieved by either combining binding units in tandem repeats<sup>11</sup> or displaying them as separate units using nanosized scaffolds such as multimeric proteins or dendrimers.<sup>12–15</sup> Both types of multivalent peptides can be created by fusing them to proteins using genetic engineering or by chemical synthesis and cross-linking together individual peptide units. The binding strength toward solid materials (affinity) of multivalent peptides systems has very often been found to positively correlate with the number of peptide repeats.<sup>13,14,16–18</sup> For instance, in a study with a titanium binding peptide, an increase in the number of binding units from one to four resulted in a 10-fold improvement in binding affinity.<sup>17</sup> In another study, a hundredfold increase in affinity was observed for a tetravalent hydroxyapatite binding peptide as compared to its monovalent form.<sup>18</sup> A similar effect was achieved when a collagen binding peptide was engineered to pentavalent form using a dendrimer

**Received:** October 15, 2014

**Revised:** December 18, 2014

scaffold.<sup>13</sup> An even larger increase in binding affinity (four orders of magnitude) was measured for another titanium binding sequence (minTBP-1) when it was linked to ferritin, which resulted in display of 24 binding units.<sup>14</sup> On the other hand, in some studies, increasing the number of binding units did not result in enhanced binding as, for example, with three-repeat tandem silica or platinum binding peptides.<sup>11</sup> The authors suggested that one of the possible explanations for this behavior is conformational changes between single and multiple repeat polypeptides. It was also found that for some peptides there is an optimum number of binding units, for instance,  $n = 5$  for gold binding peptide, and further multimerization leads to decrease in binding.<sup>19</sup>

These differences in behavior of various multivalent peptide systems show that the binding affinity is not always enhanced by simply increasing the number of the binding units but also other factors, such as overall three-dimensional structure of the multimer, way of connecting individual peptides, or length and chemical nature of a linker used to fuse the binding units, are important and might contribute to the binding. Thus, detailed understanding of the structure–function relationship of multivalent peptides systems is essential for generating conjugates that can be successfully utilized in practical applications.

We have previously identified peptides binding to diamond-like carbon (DLC) from a phage display library and characterized their binding properties to the target surface.<sup>20</sup> One of the selected DLC binding peptides (pep\_L) was further engineered and studied in detail in terms of structure–function relationship.<sup>21</sup> It was shown that the affinity of the peptide is dependent on both the chemical composition of the amino acid sequence and the overall three-dimensional structure. However, CD spectroscopy did not reveal any specific folded conformation of the peptide. We also demonstrated better binding by duplication of the peptide sequence (tandem repeat).

Here we describe the engineering of the pep\_L peptide to di-, tri-, and tetravalent forms using different linkers and compare their functionality in relation to their molecular architecture. We investigate the use of repeated DLC binding domains to increase its affinity and the peptide coating stability on the target surface. We also present the use of the multivalent DLC binding peptides for the stabilization of colloidal DLC dispersions. Flakes of the DLC film represent a new approach for the utilization of DLC materials.<sup>22</sup> The flakes possess the superior physicochemical material properties of DLC,<sup>23</sup> and their interaction with DLC-specific peptides offers a straightforward route for their functionalization for various applications.

## MATERIALS AND METHODS

**Materials.** DLC surfaces were obtained by coating stainless steel discs with the commercial amorphous hydrogenated DLC (a-C:H DLC) coating, BALINIT DLC (Oerlikon Balzers, Liechtenstein). The discs were cleaned before each experiment as described previously.<sup>20</sup> Synthetic peptides (pep\_L, pep\_L\_pep, pep\_L-Cys), purity >95%, were purchased from a commercial supplier (GenScript, USA). Exact peptide concentrations and purities were verified by ultra-performance liquid chromatography (UPLC) (Acquity, Waters, USA) using a C18 (1.7  $\mu\text{m}$ ) column (2.1 mm  $\times$  50 mm) (Waters, USA) and a water/acetonitrile mobile phase with 0.1% trifluoroacetic acid. For concentration determination, UPLC standards were made from aliquots for which concentration had been determined by amino acid analysis. All peptides were dissolved in Milli-Q water. Maleimide functionalized cross-linker bis(maleimido)ethane (BMOE) was

obtained from Thermo Fisher Scientific (USA), PEG(11)-bis-maleimide from Conju-Probe (USA), Tris-[2-maleimidoethyl]amine (TMEA) from Thermo Fisher Scientific (USA), and the four-arm branched PEG(11) with maleimide end-groups based on a pentaerythritol core (4-Arm PEG-MAL) from Creative PEGWorks (USA). The details of the PEG(6)-bis-maleimide synthesis as well as <sup>1</sup>H, <sup>13</sup>C, and <sup>1</sup>H–<sup>1</sup>H COSY NMR spectra are presented in the Supporting Information.

**Conjugation of Peptides Using Maleimide Functionalized Cross-Linkers.** Maleimide-functionalized cross-linkers were conjugated to the sulfhydryl group of the C-terminal cysteine of peptide pep\_L-Cys in 40 mM MOPS buffer pH 6.6 containing 5 mM EDTA at room temperature for 1 h with occasional mixing. The cross-linking reaction was carried out using following protocol: 250  $\mu\text{L}$  of pep\_L-Cys (1.87  $\mu\text{mol}$ , 5.82 mg) solution was mixed with 50  $\mu\text{L}$  of 10X MOPS buffer and one of the cross-linkers; final reaction volume (500  $\mu\text{L}$ ) was adjusted with water. Stock solutions of the cross-linkers were prepared in DMSO, volumes added to the reaction mix were as follows: 17.5  $\mu\text{L}$  of BMOE (0.7  $\mu\text{mol}$ , 0.15 mg), 10  $\mu\text{L}$  of TMEA (0.38  $\mu\text{mol}$ , 0.15 mg), 15  $\mu\text{L}$  of PEG(11)-bis-maleimide (0.69  $\mu\text{mol}$ , 0.58 mg), 10  $\mu\text{L}$  of PEG(6)-bis-maleimide (0.85  $\mu\text{mol}$ , 0.5 mg), and 15  $\mu\text{L}$  of 4-Arm PEG-MAL (0.3  $\mu\text{mol}$ , 0.6 mg). The peptide conjugates were purified using reversed-phase HPLC (GE Healthcare, Sweden) on a semipreparative Vydac C4 column (1 cm  $\times$  25 cm) (Grace, USA). Peptide containing fractions were pooled and lyophilized. The purity of peptide samples was analyzed by UPLC as described above (UPLC chromatograms are presented in the Supporting Information).

The molecular masses of the purified peptide conjugates were analyzed using MALDI-TOF Autoflex II (Bruker Daltonics, Germany) mass spectrometer equipped with UV/N2-laser (337 nm/100  $\mu\text{J}$ ) (MALDI-TOF spectra are presented in the Supporting Information). Alpha-cyano-4-hydroxycinnamic acid (Sigma-Aldrich, USA) dissolved in water containing 50% acetonitrile and 0.1% trifluoroacetic acid was used as a matrix. Protein Calibration Standard I from Bruker Daltonics (Germany) was used for calibration of the instrument.

The solubility of the peptide conjugates was examined by UPLC by analyzing aliquots containing different concentrations of the conjugates and comparing the results with peptide concentration standard curves. All of the peptide conjugates were fully soluble at the concentrations used in the experiments.

**Peptide Binding Experiments.** Peptide binding was analyzed using simulations and sequential competition assays. In both types of experiments, the alkaline phosphatase (AP) enzyme fused to pep\_L peptide (giving pep\_L-AP) was used as a reporter for quantitation of bound protein on the surface. Gene cloning, expression, and protein purification have been described earlier.<sup>20</sup>

In simultaneous competition experiments (Figure 2), solutions of peptide and pep\_L-AP reporter were mixed prior to surface binding. The concentration of pep\_L-AP was kept constant (0.2  $\mu\text{M}$ ), while the peptide concentration varied from 0.2–4  $\mu\text{M}$ . The mixture was applied on a cleaned DLC surface and incubated for 30 min at room temperature. The surface was washed five times with 50 mM Tris buffer pH 7.5 to remove loosely bound biomolecules. The amount of the pep\_L-AP that remained bound to the surface was quantified by measuring the enzymatic activity of AP as described previously.<sup>20</sup>

In sequential displacement experiments, solutions of peptides and pep\_L-AP reporter were applied on the DLC surface sequentially. The DLC surface was first incubated either with peptide solution (concentration 4  $\mu\text{M}$ ) (Figure 3a) or fusion protein (concentration 1  $\mu\text{M}$ ) (Figure 3b) and incubated for 30 min at room temperature. Next, the DLC surface was washed with an excess of 50 mM Tris buffer pH 7.5. The wash was repeated three times when the DLC was coated with peptide (Figure 3a) and four times when it was coated with fusion protein (Figure 3b). After the washing step, the fusion protein (concentration 1  $\mu\text{M}$ ) was applied on the DLC surface coated previously with peptides (concentration 4  $\mu\text{M}$ ) (Figure 3a), and peptides were applied on the surfaces coated previously with the fusion proteins (Figure 3b). Biomolecules were incubated on the DLC surface for an additional 30 min (at room temperature) and washed again with Tris buffer following the procedure of the first washing step.

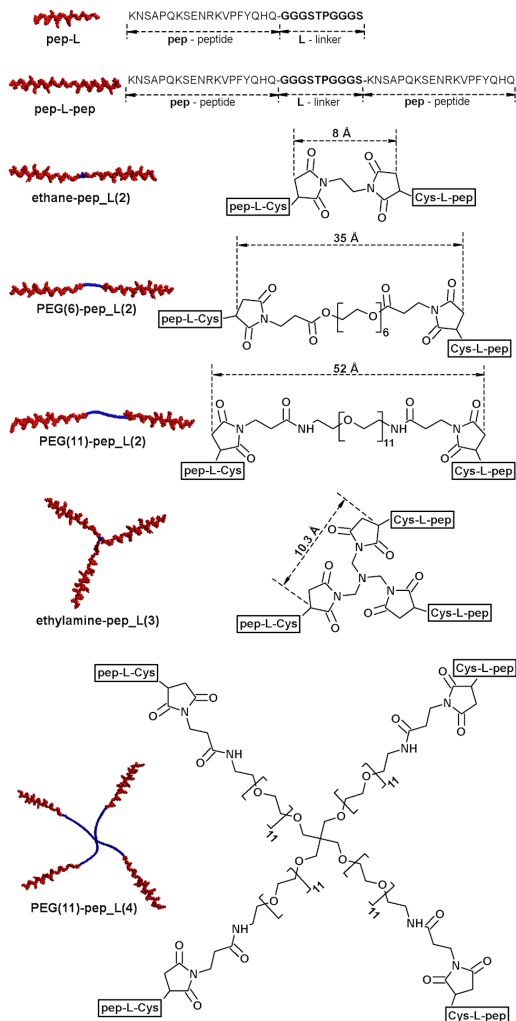


**Figure 1.** Schematic presentations of the peptide conjugates showing peptides (red) and linkers (blue) as well as amino acid sequences of pep<sub>L</sub> and pep<sub>L</sub>-pep, and chemical structures of the linkers.

The amount of the fusion protein that remained bound to the surface was quantified by measuring the enzymatic activity of alkaline phosphatase as described previously.<sup>20</sup> The maximum binding (100% displacement) of the fusion protein was measured for the sample where only fusion protein was applied on the surface (buffer was used instead of peptide).

**Preparation of DLC Flakes.** DLC flakes were produced by deposition of about 100 nm thick films using pulsed vacuum cathodic arc from a graphitic electrode. Each pulse yielded on average 0.5 monolayers of DLC on the substrate.<sup>24</sup> A thin film (around 1 μm) of NaCl on a glass slide was used as the substrate. It was prepared by a spray coating method using 1 M NaCl solution.

After deposition, the glass slides with DLC coated NaCl crystals were placed in plastic tubes containing Milli-Q water. The tubes were gently mixed to aid in dissolving the salt and to release the DLC as thin flakes. The glass slides were then removed, and the suspension of DLC flakes was centrifuged for 5 min at 4000 rpm. Subsequently, the pellet was washed three times with Milli-Q water to remove salt. The

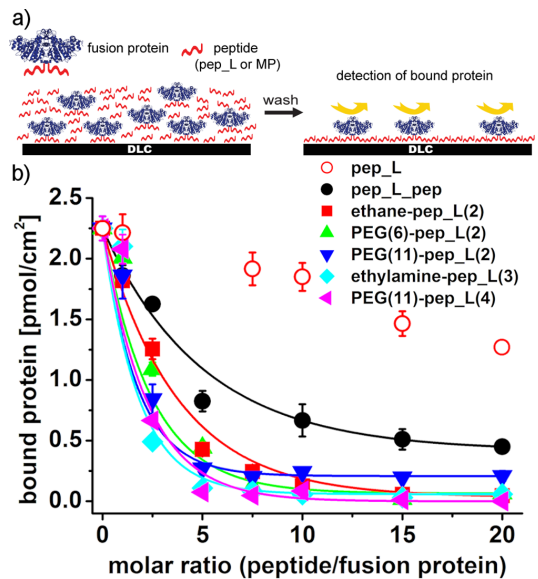


**Figure 2.** Comparison of peptide binding in a simultaneous competition assay. (a) Scheme of the simultaneous competition assay. (b) Competition curves for the peptides with increasing molar ratio of peptide to reporter. Mean values with standard deviations are shown ( $N = 3$ ).

suspension was then sonicated with a tip sonicator (amplitude 40%, energy 10 kJ, 2 mm tip) to reduce the size of the DLC flakes. After sonication, the suspension was allowed to stabilize for 20 min. The suspended fraction was then collected for binding studies, while the sediment was discarded.

**Scanning Electron Microscopy.** SEM images were obtained using SIGMA VP Field Emission-SEM microscope (ZEISS, Germany). Highly ordered pyrolytic graphite (HOPG) (NT-MDT, Russia) served as a substrate. A sample of the water suspension of the DLC flakes was pipetted onto a freshly cleaned HOPG substrate and let dry for 2 h prior to imaging.

**Zeta ( $\zeta$ ) Potential and Dynamic Light Scattering (DLS).** Zeta potential and dynamic light scattering measurements of the DLC flakes (and the DLC flakes modified with peptides) were carried out using Nano ZS Zetasizer (Malvern Instruments, UK) at 25 °C using the disposable capillary cells (Zeta potential) and small volume disposable cuvettes (DLS). Fresh samples were prepared before each measurement. The concentration of peptide was 0.25 mg/mL, DLC flakes 0.1 mg/mL, respectively. The pH of the samples was adjusted to the desired value using small amounts (<1% of total) of 1 M NaOH or 1 M HCl. In the DLS experiments, the back-scattered light intensities of the samples were collected at an angle of 173°. The size distribution of the colloidal dispersions was obtained based on the intensity data.

## RESULTS AND DISCUSSION

**Construction of Multivalent Peptides (MPs).** A set of MPs of the DLC binding peptide (pep<sub>L</sub>) was constructed by its chemical conjugation to a series of maleimide-functionalized cross-linkers (that reacted with sulfhydryl group of a cysteine residue that was introduced to the C-terminus of pep<sub>L</sub> peptide). The schematic structures of prepared MPs as well as the chemical structures of the linkers are shown in Figure 1. Three of the MPs were divalent with two identical pep<sub>L</sub> units connected by linkers of different length. One MP contained three copies of pep<sub>L</sub> units, and one MP contained four copies.

C

DOI: 10.1021/bm501522j  
Biomacromolecules XXXX, XXX, XXX–XXX



As an additional variation, we used a MP that was synthesized as one long peptide chain, which had a duplicated DLC binding sequence following directly an initial one.

**Determining the Effect of MP Design for Affinity.** The effect of MP structure for affinity was analyzed using a simultaneous competition assay.<sup>21</sup> In the assay, a fusion protein (pep\_L-AP) was used in which pep\_L peptide had been linked to the enzyme AP. Since AP naturally is a dimer,<sup>25</sup> each AP complex displayed two pep\_L peptides (see scheme in Figure 2a). The advantage of using pep\_L-AP was that very low amounts of enzyme bound to surfaces could be accurately determined, which gives a highly reproducible and sensitive binding assay. The dissociation constant,  $K_d$ , of pep\_L-AP was previously determined to be 63 nM.<sup>20,21</sup> For comparison of the affinities of the MPs in a competition assay, a fixed concentration of pep\_L-AP was mixed with different concentrations of peptide (pep\_L or MP) (Figure 2a). Plotting the amount of MP versus the amount of bound pep\_L-AP gave a measure of the ability of the peptide to compete with pep\_L-AP for binding. By this method, the different peptide constructs could be ranked by relative affinity visually from the graph (Figure 2b) and as determined from the molar ratio at which pep\_L-AP binding was reduced by 50% (Table S1, Supporting Information).

A clear trend in the efficiency of competing out pep\_L-AP was shown for MPs as seen by the steep competition curves. The monovalent pep\_L showed a significantly lower ability to compete out pep\_L-AP than any of the MPs. For the divalent peptides, there was a clear trend that an increase in linker length led to better affinities. The increase in binding affinity is expected to be based on a cooperative effect, that is, when one peptide binds, the effective concentration of its pair becomes high closer to the surface, and therefore it binds with a higher probability.<sup>9,26</sup> The effect of the linker on the affinity depends additionally on how well the distance between binding sites corresponds to the dimensions of the linker. If the binding sites are very close to each other, the effective concentration should increase with decreased linker length. Since the affinity increased with increased linker length, the results suggest that binding sites on the surface are relatively far apart.

Increasing the number of peptides in the MPs to three in ethylamine-pep\_L(3) and four in PEG(11)-pep\_L(4) led to an increased affinity. In the MP ethylamine-pep\_L(3), the linker lengths were as in the MP ethane-pep\_L(2), and in PEG(11)-pep\_L(4), linker lengths were longer as in PEG(11)-pep\_L(2). The effect of multivalency was clearly seen in both sets, for example, a 2.5 excess of MP gave a 44% reduction in reporter (pep\_L-AP) binding for ethane-pep\_L(2) compared to a 78% reduction for ethylamine-pep\_L(3), while PEG(11)-pep\_L(2) gave 63% and PEG(11)-pep\_L(4) gave a 70% reduction. Therefore, in relative terms, the multivalency caused a greater effect in the smaller, more restrained system compared to the larger one, even when the larger system had a higher valency of peptide. The effect of the tandem repeat peptide pep\_L-pep on reporter binding was much lower, 28%.<sup>21</sup> This construct was synthesized as a single peptide and contained a partly duplicated sequence in a head-to-tail arrangement.

The MP variants also showed different behavior in the way they were able to reduce pep\_L-AP binding. For example, the divalent PEG(11)-pep\_L(2), trivalent, and tetravalent peptide leveled out competition curves at similar concentrations (molar excess approximately between 5 and 7.5). However, they differed in the level of reducing the pep\_L-AP binding at higher

concentrations. At the highest applied concentration, the PEG(11)-pep\_L(2) reduced the reporter adsorption to 11% and the trivalent MP to approximately 1%, while the tetravalent MP limited its binding completely. The finding that for certain constructs (even having high binding affinity), the competition curves do not reach zero can be explained by the existence of multiple binding sites with slightly different properties or that there are structural restraints in the way MPs are linked that do not allow full coverage.

To estimate the extent of synergy in the binding of individual peptides in the MPs, the data from the Figure 2, panel b were plotted so that the values for the  $x$ -axis were multiplied with the number of peptides that each MP contained (Figure S3, Supporting Information). This way of plotting gives an estimate of the extent of synergy between peptides in the MPs. The values for 50% inhibition (Tables S1 and S2) show that in all MPs, there is a clear synergistic effect so that peptides in divalent MPs become more efficient with increasing linker length. However, for the trivalent MP (ethylamine-pep\_L(3)), the contribution of a single peptide was in the range of the PEG(6)-pep\_L-AP, and the contribution of a single peptide in the tetravalent MP (PEG(11)-pep\_L(4)) was at the level of pep\_L-pep. We conclude that synergy was evident in all constructs, but the level was highly dependent on structural features of linking.

**Effect of MP-Structure for Sequential Competition and Kinetics.** Next we investigated the competition between pep\_L-AP fusion protein and the different peptides by studying how well they could compete out each other when one had already been bound to the surface. In this way, we investigated the potential role of kinetic effects in the binding. First, the displacement of surface bound peptide by the reporter protein, pep\_L-AP, was investigated (Figure 3a). The assay was performed by initially saturating the surface with peptide. The surface was then rinsed with buffer to remove any free peptide. The surface was then incubated with pep\_L-AP or plain buffer, and finally the remaining pep\_L-AP was assayed. In a second variation, the experiment was performed in the reversed way, which first allowed pep\_L-AP to bind and then added peptide (Figure 3b). In neither case did the buffer alone remove bound peptide/protein from the surface (Figure 3c).

These sequential competition experiments followed the same general trend as in the case of simultaneous competition experiments described above. The monovalent peptide showed again the weakest displacement with 85% reporter binding after competition. Displacement with the divalent peptide pep\_L-pep the surface left 75% of bound pep\_L-AP protein on the surface. The chemically conjugated divalent peptides showed very similar properties with about 22% bound reporter left after competition. Again, increased linker length had a positive effect on the peptide binding both in the forward and reverse versions of the experiment.

Surprisingly, the tri- and tetravalent MP showed a distinct behavior in the competition experiments. In both sets of experiments, there was a clear difference in the forward and reverse versions. Most notably, only 0.2% of the pep\_L-AP remained bound in the experiment where ethylamine-pep\_L(3) was used to compete out pep\_L-AP. In the case of the tetravalent PEG(11)-pep\_L(4), the MP resisted very well being competed out by pep\_L-AP, with only 1% of pep\_L-AP being able to bind. The results were highly repeatable and indicate that the dynamics of surface interactions are distinctly different for the different arrangements of peptide linking.

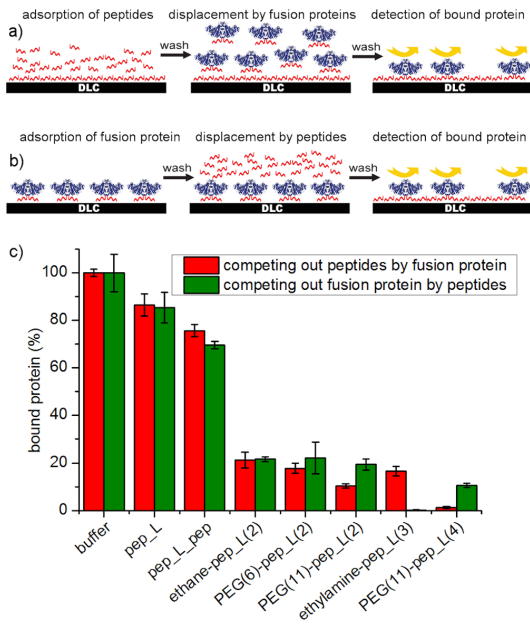


**Figure 3.** Peptide binding in sequential competition assays with reporter protein (pep\_L-AP). Schematic presentations of the assays (a) peptide displacement by reporter and (b) reporter displacement by peptide. (c) Amount of bound reporter protein after the competition. Data are presented as mean values with standard deviations ( $N = 3$ ).

In this assay, the linker length seems to have a less significant role in peptide binding. We note that the behavior of the trivalent peptide is different in the two sequential binding assays and thus dependent on the order of binding. The difference in performance between tri- and tetravalent peptides can be explained by the difference in size of the molecules. The tetravalent peptide was not able to displace all bound reporters perhaps because of its large size. The trivalent peptide is more compact and has less conformational freedom due to its small and star-shaped linker as compared to the tetravalent peptide that is linked through PEG units. This architecture is probably more optimal and aids the trivalent peptide for easier penetration through protein layer.

**Utilization of the MPs for Functionalization of the Colloidal Form of DLC.** To investigate the function of MPs at interfaces, we prepared a powder form of DLC. The effects of MPs on the properties of colloidal dispersions of the DLC were then studied. DLC powders were prepared by depositing an about 100 nm thick DLC film on a layer of NaCl crystals and subsequent delamination. Because of the internal stress of the DLC coating, dissolving the salt substrate in water resulted in a spontaneous delamination of the DLC film into a powder consisting of flake-like particles of approximately 10–100  $\mu\text{m}$  size (Figure 4a). Application of mechanical energy by ultrasonication was able to break the flakes into smaller particles with diameters below 5  $\mu\text{m}$  (Figure 4b).

We then investigated how the DLC binding peptides affect the Zeta potential and colloidal stability of the DLC dispersion. The Zeta potential of the plain DLC particles was very negative at basic pHs and became less charged as the pH was lowered (Figure 4c). The addition of DLC binding peptides to the DLC

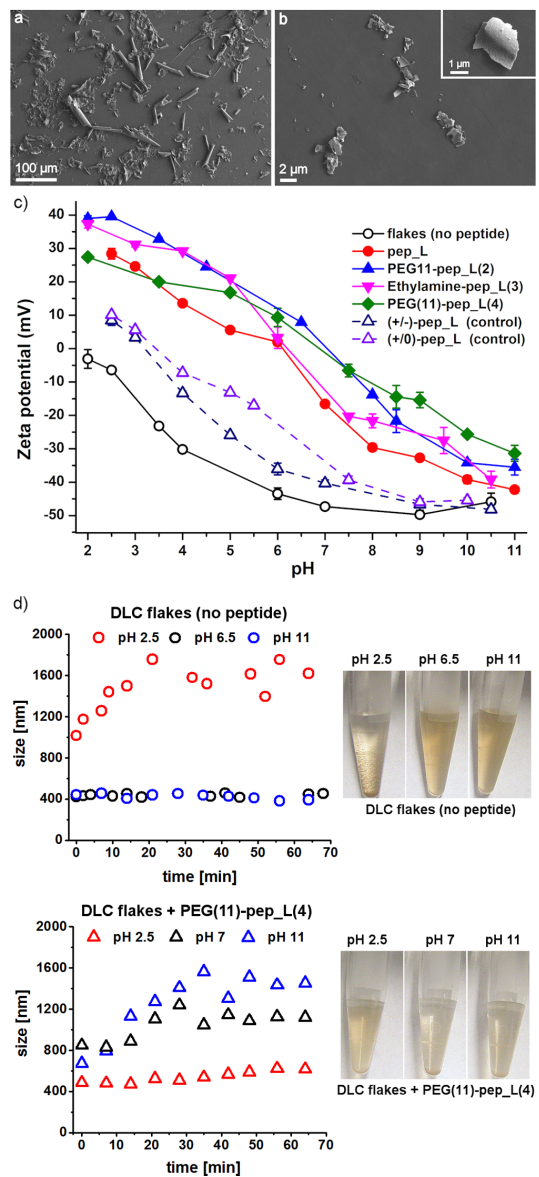


**Figure 4.** Modifying DLC flakes by DLC binding peptides. Scanning electron microscopy image of DLC powder: (a) flakes after delamination from salt crystals and (b) after sonication. (c) Zeta potential of particles treated with different variants of peptide and as a function of pH ( $N = 3$ ). (d) Effect of peptides on the stability of colloidal dispersions of DLC flakes at different pH values: plots present the changes of the colloidal size of the dispersions in time with and without peptides, pictures the sedimentation rate of the suspensions after 1 h.

flakes increased the Zeta potential across the whole pH range. The DLC binding peptides contain a high number of positively charged residues. Our previous structure–function studies on the DLC binding peptides showed that the positive charge is

one of the factors that affects the binding of peptides to DLC.<sup>21</sup> In line with this, peptide binding to the negatively charged DLC flakes increased the Zeta potential. Weakly binding control peptides ( $\pm$ )\_pep\_L (pI 3.7) and (+/0)\_pep\_L (pI 5.2), where the positively charged lysine residues were mutated to negatively charged or neutral residues, respectively (see Figure S4, Supporting Information), showed only a small change in Zeta potential of the DLC flakes.

Subsequently, we measured the changes of the colloidal size of the dispersions as a function of time at different pH values using DLS (Figure 4d). In line with the Zeta potential data, the colloidal size of the suspensions of DLC flakes without peptides was stable in time at pH values of 6.5 and 11 (colloidal size 400–500 nm, Zeta potential  $-40$  mV), while at pH 2.5, it rapidly increased to 1800 nm due to sedimentation (Zeta potential  $-6$  mV). Coating the DLC flakes with PEG(11)-pep\_L(4) reversed their stability pattern. The flakes were stable in solution at pH 2.5 (colloidal size 400–600 nm) but sediment at pH 7 and 11, which is indicated by the increase of their colloidal size. These results are confirmed in the photographic images of the suspensions obtained at different pH values after 1 h incubation that are presented in Figure 4, panel d. Changing the Zeta potential and colloidal stability of the DLC flakes by the peptide coating shows that the developed peptides can be used for the surface modification of colloidal DLC flakes and to control their stability in solution.

## CONCLUSIONS

Engineering the multivalency of surface-binding peptides can greatly modify the function of these and should be seen as an essential stage in the development of peptides for applications. We showed that the interaction between DLC surface and the DLC binding peptide pep\_L is affected in multiple ways when peptides are linked together. The structure of the linkers by which peptides were linked to each other in dimers resulted in significant affinity differences. Dimers lead to increased affinity with the affinity being adjustable by changing the length of the linker. This result suggested that binding sites on DLC are relatively far apart since long linkers showed better complementarity with binding sites. Overall, the most substantial functional difference came from how peptides are linked, not only their number. Making trimers or tetramers increased affinity somewhat further but showed more significant functional differences in kinetic aspects, that is, how they were able to compete out other molecules or resist being competed out by other molecules. These kinetic aspects did not directly correlate to affinity.

We also demonstrated that the developed multivalent peptides were able to control the surface properties of a colloidal form of DLC and accordingly control its colloidal stability. We suggest that surface functionalization of DLC using peptides will expand the functional properties of DLC materials for applications.

## ASSOCIATED CONTENT

### Supporting Information

Information about synthesis and  $^1\text{H}$ ,  $^{13}\text{C}$ , and  $^1\text{H}-^1\text{H}$  COSY NMR spectra of PEG(6)-bis-maleimide. UPLC chromatograms and MALDI-TOF spectra of purified multivalent peptides. Fitting parameters and a plot that shows an alternative presentation of the competition curves. Amino acid sequences of control peptides. This material is available free of charge via the Internet at <http://pubs.acs.org>.

## AUTHOR INFORMATION

### Corresponding Author

\*E-mail: markus.linder@aalto.fi. Phone: +358 50 4315525.

### Notes

The authors declare no competing financial interest.

## ACKNOWLEDGMENTS

We acknowledge the Academy of Finland and VTT Graduate School for financial support. Riitta Suihkonen is thanked for the technical assistance and Dorothee Barth for help with the binding data analysis. This work was supported by the Academy of Finland through its Centers of Excellence Program (2014–2019) and under Project No. 259034 as well as the VTT Graduate School.

## ABBREVIATIONS

DLC, diamond-like carbon; a-C:H DLC, amorphous hydrogenated DLC; UPLC, ultra-performance liquid chromatography; MOPS, 3-(N-morpholino)propanesulfonic acid; EDTA, ethylenediaminetetraacetic acid; DMSO, dimethyl sulfoxide; MALDI-TOF, matrix-assisted laser desorption/ionization-time-of-flight mass spectrometer; BMOE, bis(maleimido)ethane; TMEA, Tris-[2-maleimidoethyl]amine; 4-Arm PEG-MAL, four-arm branched PEG(11) with maleimide end-groups based on a pentaerythritol core; AP, alkaline phosphatase; HOPG, highly ordered pyrolytic graphite; MP, multivalent peptide; DLS, dynamic light scattering

## REFERENCES

- (1) Oh, D.; Qi, J.; Lu, Y.; Zhang, Y.; Shao-Horn, Y.; Belcher, A. M. *Nat. Commun.* **2013**, *4*, 2756.
- (2) Dang, X.; Yi, H.; Ham, M.-H.; Qi, J.; Yun, D. S.; Ladewski, R.; Strano, M. S.; Hammond, P. T.; Belcher, A. M. *Nat. Nanotechnol.* **2011**, *6*, 377–384.
- (3) Ghosh, D.; Lee, Y.; Thomas, S.; Kohli, A. G.; Yun, D. S.; Belcher, A. M.; Kelly, K. A. *Nat. Nanotechnol.* **2012**, *7*, 677–682.
- (4) Ghosh, D.; Bagley, A. F.; Na, Y. J.; Birrer, M. J.; Bhatia, S. N.; Belcher, A. M. *Proc. Natl. Acad. Sci. U. S. A.* **2014**, *111*, 13948–13953.
- (5) Sarikaya, M.; Tamerler, C.; Jen, A. K.-Y.; Schulten, K.; Baneyx, F. *Nat. Mater.* **2003**, *2*, 577–585.
- (6) Shiba, K. *Curr. Opin. Biotechnol.* **2010**, *21*, 412–425.
- (7) Tamerler, C.; Sarikaya, M. *ACS Nano* **2009**, *3*, 1606–1615.
- (8) Garnham, C. P.; Campbell, R. L.; Davies, P. L. *Proc. Natl. Acad. Sci. U. S. A.* **2011**, *108*, 7363–7367.
- (9) Mammen, M.; Choi, S.-K.; Whitesides, G. M. *Angew. Chem., Int. Ed.* **1998**, *37*, 2754–2794.
- (10) Fasting, C.; Schallge, C. A.; Weber, M.; Seitz, O.; Hecht, S.; Koksche, B.; Dervedde, J.; Graf, C.; Knapp, E. W.; Haag, R. *Angew. Chem., Int. Ed.* **2012**, *51*, 10472–10498.
- (11) Seker, U. O. S.; Wilson, B.; Sahin, D.; Tamerler, C.; Sarikaya, M. *Biomacromolecules* **2009**, *10*, 250–257.
- (12) Craig, P. O.; Alzogaray, V.; Goldbaum, F. A. *Biomacromolecules* **2012**, *13*, 1112–1121.
- (13) Helms, B. A.; Reulen, S. W. A.; Nijhuis, S.; de Graaf-Heuvelmans, P. T. H. M.; Merckx, M.; Meijer, E. W. *J. Am. Chem. Soc.* **2009**, *131*, 11683–11685.
- (14) Sano, K.-I.; Ajima, K.; Iwahori, K.; Yudasaka, M.; Iijima, S.; Yamashita, I.; Shiba, K. *Small* **2005**, *1*, 826–832.
- (15) Terskikh, A. V.; Le Doussal, J. M.; Cramer, R.; Fisch, I.; Mach, J. P.; Kajava, A. V. *Proc. Natl. Acad. Sci. U. S. A.* **1997**, *94*, 1663–1668.
- (16) Brown, S. *Nat. Biotechnol.* **1997**, *15*, 269–272.
- (17) Khoo, X.; O'Toole, G. A.; Nair, S. A.; Snyder, B. D.; Kenan, D. J.; Grinstaff, M. W. *Biomaterials* **2010**, *31*, 9285–9292.

- (18) Tang, W.; Ma, Y.; Xie, S.; Guo, K.; Katzenmeyer, B.; Wesdemiotis, C.; Becker, M. L. *Biomacromolecules* **2013**, *14*, 3304–3313.
- (19) Kacar, T.; Zin, M. T.; So, C.; Wilson, B.; Ma, H.; Gul-Karaguler, N.; Jen, A. K.-Y.; Sarikaya, M.; Tamerler, C. *Biotechnol. Bioeng.* **2009**, *103*, 696–705.
- (20) Gabryelczyk, B.; Szilvay, G. R.; Salomäki, M.; Laaksonen, P.; Linder, M. B. *Colloids Surf., B* **2013**, *110C*, 66–73.
- (21) Gabryelczyk, B.; Szilvay, G. R.; Linder, M. B. *Langmuir* **2014**, *30*, 8798–8802.
- (22) Ohana, T.; Nakamura, T.; Tanaka, A. *Diamond Relat. Mater.* **2010**, *19*, 894–898.
- (23) Erdemir, A.; Donnet, C. *J. Phys. D.: Appl. Phys.* **2006**, *39*, R311–R327.
- (24) Laurila, T.; Rautiainen, A.; Sintonen, S.; Jiang, H.; Kaivosoja, E.; Koskinen, J. *Mater. Sci. Eng., C* **2014**, *34*, 446–454.
- (25) Torriani, A. *J. Bacteriol.* **1968**, *96*, 1200–1207.
- (26) Cantor, C.; Schimmel, P. *Biophysical Chemistry*, Part III; W. H. Freeman & Co.: New York, 1980; pp 874–1018.

Title	<b>Diamond-like carbon binding peptides – evolutionary selection, characterization, and engineering</b>
Author(s)	Bartosz Gabryelczyk
Abstract	<p>The possibility of controlling interactions at interfaces and surfaces of solid materials is highly interesting for a wide range of nanotechnological applications. In Nature, evolution has developed a wide range of proteins and peptides that possess the ability to recognize, specifically bind, and modify the surfaces of solid materials. The natural evolution processes can be mimicked in the laboratory scale with the use of a directed evolution approach, for instance, based on the selection of short material-specific peptides from combinatorial libraries displayed on the surface of bacteriophages or bacterial cells. Selected from billions of different variants, material-specific peptides can be studied to define their sequence, structure, binding properties, and subsequently engineered to tailor their function for practical applications.</p> <p>In this work, a phage display was used to identify peptides binding to diamond-like carbon (DLC). DLC is an amorphous form of carbon, with chemical and physical properties resembling natural diamond. It is used as a coating material in many industrial and biomedical applications. Peptides binding to DLC were selected from the commercial phage display library (Ph.D.-12). During the selection process phages displaying longer than the expected 12-mer peptides (generally present in Ph.D.-12 library) were enriched. Binding studies by phage ELISA and titer analysis indicated that enriched phages displaying long (42–57-mer) peptides bind more efficiently to DLC surface compared to the clones displaying standard 12-mer sequences. Selected DLC binding peptides (DLCBP) were fused to the alkaline phosphatase (AP), which was used as a reporter enzyme in order to determinate their binding properties in a different molecular context. The adsorption of the DLCBP-AP fusions on DLC was quantified using the AP enzymatic activity, and verified by ellipsometry. A 57-mer peptide, DLCBP11(L)-AP, showed the highest binding to DLC with a binding <math>K_d</math> value of 63 nM. Studies of different variants of the peptide demonstrated that its shorter form (pep_L), composed of 29 amino acids, had very similar binding properties. The structural basis of the function of the pep_L peptide was investigated by mutagenesis approach. The influence of mutations was measured using a competition assay in which peptide variants in free, soluble form competed for binding to DLC with the pep_L-AP fusion protein. Analysis of point mutations demonstrated that a positive charge is important for peptide function. Rearrangement of the order of amino acid residues in the primary sequence showed that the peptide's function is dependent on its chemical composition and likely the overall three-dimensional structure. Engineering of the peptide to different multivalent forms showed that binding affinity and kinetics of the multimers can be tailored by specific structural design. Finally, it was demonstrated that the peptides can be successfully utilized in nanotechnological applications, i.e., for self-assembling coatings on the DLC surface, and for controlling properties of a colloidal form of DLC.</p> <p>Besides finding and characterizing peptides binding to DLC, the work also highlights various challenges of the directed evolution techniques, for example, selection of target unrelated peptides during biopanning, and the necessity of multiple independent ways of analyzing the functionality of selected peptides. Moreover, the most frequent mistakes that are found in the literature when analyzing results of the biopanning are discussed.</p>
ISBN, ISSN	ISBN 978-951-38-8216-7 (Soft back ed.) ISBN 978-951-38-8217-4 (URL: <a href="http://www.vtt.fi/publications/index.jsp">http://www.vtt.fi/publications/index.jsp</a> ) ISSN-L 2242-119X ISSN 2242-119X (Print) ISSN 2242-1203 (Online)
Date	February 2015
Language	English
Pages	84 p. + app. 27 p.
Name of the project	
Commissioned by	
Keywords	inorganic-binding peptides, material specific peptides, diamond-like carbon (DLC), phage display, molecular recognition, structure-function relationship, multivalent peptides, colloidal DLC
Publisher	VTT Technical Research Centre of Finland Ltd P.O. Box 1000, FI-02044 VTT, Finland, Tel. 020 722 111

## **Diamond-like carbon binding peptides – evolutionary selection, characterization, and engineering**

The possibility of controlling interactions at interfaces and surfaces of solid materials is highly interesting for a wide range of materials-related nanotechnological applications. In Nature, evolution processes through successive cycles of random mutations and selection led to development of biomolecules that specifically interact and modify surfaces of solid materials. These biological mechanisms can be mimicked in the laboratory scale with the use of a directed evolution approach, for instance, based on the selection of short material-specific peptides from the combinatorial libraries. Selected from billions of different variants, material-specific peptides can be studied by experimental and computational methods to define their sequence, structure, binding properties, and engineered for practical applications.

The studies presented in the thesis show how directed evolution approach was applied to identify peptides that bind to diamond-like carbon (DLC). DLC is used as a coating in many industrial and biomedical applications. Peptides binding to DLC were selected from a combinatorial phage display library. Their binding and molecular basis of the function were investigated in different molecular contexts by multiple independent methods. It was also demonstrated that the peptides can be used in nanotechnological applications, i.e., as a self-assembling coating on the DLC surface, and for controlling properties of a colloidal form of DLC.

Besides finding and characterizing peptides binding to DLC, the thesis also highlights different challenges of the directed evolution techniques based on various examples from the literature.

ISBN 978-951-38-8216-7 (Soft back ed.)  
ISBN 978-951-38-8217-4 (URL: <http://www.vtt.fi/publications/index.jsp>)  
ISSN-L 2242-119X  
ISSN 2242-119X (Print)  
ISSN 2242-1203 (Online)

